Effective dynamics of two-dimensional Bloch electrons in external fields derived from symmetry

E. A. Fajardo and R. Winkler

Phys. Rev. B **100**, 125301 — Published 3 September 2019

DOI: 10.1103/PhysRevB.100.125301

Effective Dynamics of 2D Bloch Electrons in External Fields Derived From Symmetry

E. A. Fajardo*
Department of Physics, Northern Illinois University, DeKalb, IL 60115, USA

R. Winkler
Department of Physics, Northern Illinois University, DeKalb, IL 60115, USA and
Materials Science Division, Argonne National Laboratory, Argonne, IL 60439, USA
(Dated: August 12, 2019)

We develop a comprehensive theory for the effective dynamics of Bloch electrons based on symmetry. We begin with a scheme to systematically derive the irreducible representations (IRs) characterizing the Bloch eigenstates in a crystal. Starting from a tight-binding (TB) approach, we decompose the TB basis functions into localized symmetry-adapted atomic orbitals and crystal-periodic symmetry-adapted plane waves. Each of these two subproblems is independent of the details of a particular crystal structure and it is largely independent of the relevant aspects of the other subproblem, hence permitting for each subproblem an independent universal solution. Taking monolayer MoS_2 and few-layer graphene as examples, we tabulate the symmetrized p and d orbitals as well as the symmetrized plane wave spinors relevant for these crystal structures. The symmetry-adapted basis functions block-diagonalize the TB Hamiltonian such that each block yields eigenstates transforming according to one of the IRs of the group of the wave vector $\mathcal{G}_{\mathbf{k}}$.

For many crystal structures, it is possible to define multiple distinct coordinate systems such that for wave vectors $\mathbf{k}$ at the border of the Brillouin zone the IRs characterizing the Bloch states depend on the coordinate system, i.e., these IRs of $\mathcal{G}_{\mathbf{k}}$ are not uniquely determined by the symmetry of a crystal structure. The different coordinate systems are related by a coordinate shift that results in a rearrangement of the IRs of $\mathcal{G}_{\mathbf{k}}$ characterizing the Bloch states. We illustrate this rearrangement with three coordinate systems for MoS_2 and tri-layer graphene.

The freedom to choose different distinct coordinate systems can simplify the symmetry analysis of the Bloch states. Given the IRs of the Bloch states in one coordinate system, a rearrangement lemma yields immediately the IRs of the Bloch states in the other coordinate systems. The rearrangement of the IRs in different coordinate systems does not affect observable physics such as selection rules or the effective Hamiltonians for the dynamics of Bloch states in external fields.

Using monolayer MoS_2 as an example, we combine the symmetry analysis of its bulk Bloch states with the theory of invariants to construct a generic multiband Hamiltonian for electrons near the $\mathbf{K}$ point of the Brillouin zone. The Hamiltonian includes the effect of spin-orbit coupling, strain and external electric and magnetic fields. Invariance of the Hamiltonian under time reversal yields additional constraints for the allowed terms in the Hamiltonian and it determines the phase (real or imaginary) of the prefactors.

I. INTRODUCTION

Near a band extremum, the electron dynamics in a crystalline solid resembles the dynamics of free electrons in the absence of the periodic crystal potential. In the multi-band envelope-function approximation (EFA) the electrons are characterized by an $N \times N$ Hamiltonian $\mathscr{H}$ for N-component spinors conceptually similar to relativistic electrons described by the Dirac equation [1–5]. The simplest approach within the EFA is the effective-mass approximation (EMA) that represents the electron dynamics by a Schrödinger equation with effective mass m^* reflecting the curvature of the band dispersion $E(\mathbf{k})$. External electric and magnetic fields $\mathscr{E}$ and $\mathscr{B}$ break the lattice periodicity of the crystal structure. It is an important advantage of EFA and EMA that they allow one to incorporate the field $\mathscr{E}$ by adding the corresponding scalar potential Φ to the diagonal of the Hamiltonian, and the operator of crystal momentum $\hbar\mathbf{k} = -i\hbar\nabla$ is replaced by $-i\hbar\nabla + e\mathbf{A}$, where $\mathbf{A}$ is the vector potential for the magnetic field $\mathscr{B}$. Other perturbations such as spin-orbit coupling, strain and electron-phonon coupling can likewise be included in the Hamiltonian [3]. This is a major reason why EFA and EMA are very popular for theoretical studies of both bulk semiconductors (e.g., Refs. [3, 6–11]) and semiconductor quantum structures (e.g., Refs. [4, 5, 12–16]).

The form of the Hamiltonian $\mathscr{H}$ depends on the symmetry of the crystal structure and more specifically on the symmetry of the bulk electronic states that are included in $\mathscr{H}$ [3, 17, 18]. The relevant symmetry group for states with wave vector $\mathbf{k}$ is the point group $\mathcal{G}_{\mathbf{k}}$ which includes those symmetry elements of the crystallographic point group $\mathcal{G}_0$ (crystal class) which either leave $\mathbf{k}$ unchanged or map $\mathbf{k}$ onto an equivalent wave vector. The symmetry of individual states at $\mathbf{k}$ is characterized by the respective irreducible representations (IRs) of $\mathcal{G}_{\mathbf{k}}$ accord-

* On leave from Department of Physics, Mindanao State University–Main Campus, Marawi City, Lanao del Sur, Philippines 9700

ing to which these states transform. The general form of the Hamiltonian $\mathscr{H}$ including its dependence on, e.g., spin-orbit coupling, strain and external fields can then be derived from its invariance under $\mathscr{G}_{\mathbf{k}}$ [3, 17]. Here we develop a general theory to determine the IRs of Bloch functions for a given wave vector $\mathbf{k}$, focusing for clarity on symmorphic space groups. Using a tight-binding (TB) approach along with the fact that the atomic orbitals are localized in the vicinity of the atomic sites we demonstrate that the TB basis functions can be factorized into localized symmetry-adapted atomic orbitals and crystal-periodic symmetry-adapted plane waves. Each of these two subproblems permits a universal classification, independent of the details of a particular crystal structure and also largely independent of the other subproblem. The symmetrized atomic orbitals depend only on the angular momentum of the atomic orbitals and the point group $\mathscr{G}_{\mathbf{k}}$ of the wave vector $\mathbf{k}$; but these orbitals are independent of the specific type of atom and the details of the crystal structure. The symmetrized plane waves form discrete Bloch functions that depend on the wave vector $\mathbf{k}$ and the Wyckoff positions of the atoms in a crystal structure; but they are independent of the type of atoms occupying these positions. The symmetry-adapted basis functions block-diagonalize the TB Hamiltonian such that each block yields eigenstates transforming according to one of the IRs of the group of the wave vector $\mathscr{G}_{\mathbf{k}}$.

Given the symmetry group G of a quantum system, the IRs of G are generally assumed to provide a distinct label for the eigenstates of the Hamiltonian, as noted by Wigner: "*The representation of the group of the Schrödinger equation which belongs to a particular eigenvalue is uniquely determined up to a similarity transformation.*" (Ref. [19], p. 110, highlighting adopted from Ref. [19]). This uniqueness of the IRs is immediately relevant for many physical properties of a physical system that depend on the symmetry of its electronic states. For example, the Wigner-Eckart theorem allows one to express the selection rules for optical transitions in terms of the IRs of the initial and final states between which a transition occurs [19]. Similarly, the EFA Hamiltonians $\mathscr{H}$ depend on the IRs of the bands described by $\mathscr{H}$, as noted above. We demonstrate that the IRs characterizing the Bloch eigenstates in certain crystals including transition metal dichalcogenides (TMDCs) are *not unique*, but they depend on the coordinate system used to describe the space group symmetries of these materials [20–23]. We show that distinct valid coordinate systems are related by a coordinate shift that defines a rearrangement representation. The IRs of the electronic states in the different coordinate systems are then related via a rearrangement lemma that facilitates the symmetry analysis of Bloch states. Also, we show how important physics including optical selection rules and EFA Hamiltonians $\mathscr{H}$, despite the rearrangement of band IRs, does not depend on the coordinate system being used.

Our general theory applies to any crystalline material. For a detailed example, we focus on a monolayer of the TMDC MoS_2. TMDCs are of the general form TX_2, where T is a transition-metal such as Mo or W and X is a chalcogen which can be S, Se, or Te. 3D bulk TX_2 consists of covalently bonded 2D monolayers coupled vertically by weak van-der-Waals forces [24] making it possible to obtain monolayers via, e.g., mechanical exfoliation [25]. Electronic band structure calculations for several TMDCs have shown that bulk 2H-MoS_2 is a semiconductor [24]. More recently, optical spectroscopy [25] and theoretical studies [26–28] found that decreasing the number of layers changes the fundamental gap from indirect to direct in the limit of a single monolayer. The spin-dependent dispersion of monolayer TMDCs has been studied using TB [29, 30] and $\mathbf{k}\cdot\mathbf{p}$ methods [16, 31]. See Refs. [32–35] for general reviews of 2D TMDCs. In this paper, we combine our symmetry analysis for the bulk Bloch states in monolayer MoS_2 with the theory of invariants [3] to derive a generic multiband EFA Hamiltonian for electrons near the **K** point of the Brillouin zone (BZ). The Hamiltonian includes the effect of strain, external electric and magnetic fields, spin and valley degrees of freedom. For comparison, we also perform a symmetry analysis for few-layer graphene [14] which confirms earlier work [36, 37]. We note that our work expands on the theory of IRs for point and space groups [3, 38, 39]. It is conceptually rather different from recent work on band representations [40–42].

In Sec. II, we develop the general theory of the symmetry of TB Bloch functions. The decomposition of TB wave functions is discussed in Sec. II C followed by detailed discussions of the symmetrized atomic orbitals (Sec. II E) and symmetrized plane waves (Sec. II F). The rearrangement of the IRs of Bloch states under a change of the coordinate system is discussed in Sec. II G. We use the general formalism of Sec. II to derive the symmetry of bulk Bloch states in monolayer TMDCs (Sec. III) such as MoS_2 and to few-layer graphene (Sec. IV). We show in Sec. V how optical selection rules are not affected by the rearrangement of IRs under a change of coordinate system. In Sec. VI we derive the generic invariant expansion of the EFA Hamiltonian $\mathscr{H}$ for MoS_2. Section VII contains our conclusions.

II. SYMMETRY OF BLOCH FUNCTIONS

Very generally, the eigenstates of a Hamiltonian transform according to an IR of the symmetry group of the Hamiltonian. In band theory it is thus an important goal to determine the IRs of the energy bands $E_n(\mathbf{k})$ and corresponding Bloch functions $\Psi_{n\mathbf{k}}(\mathbf{r})$, where the symmetry group $\mathscr{G}_{\mathbf{k}}$ at a given wave vector $\mathbf{k}$ is called the point group of the wave vector $\mathbf{k}$. In this section we discuss a general method for determining the transformation properties of Bloch functions with a certain wave vector $\mathbf{k}$, which allows us to determine the corresponding IRs of $\mathscr{G}_{\mathbf{k}}$. We also discuss a rearrangement lemma for the IRs characterizing the Bloch functions in a crystal. Applica-

tions to specific materials such as monolayer MoS_2 will be discussed in subsequent sections.

A. The group of the wave vector

In the following, we will repeatedly need to evaluate the action of a point symmetry operation g on a plane wave $\exp(i\mathbf{k}\cdot\mathbf{r})$. Here, g can be represented via an orthogonal 3×3 matrix $\mathbf{g}$. (In the context of quasi-2D materials discussed below $\mathbf{g}$ becomes a 2×2 matrix.) Thus we have

$$g\,\exp(i\mathbf{k}\cdot\mathbf{r}) = \exp(i\mathbf{k}\cdot\mathbf{g}\cdot\mathbf{r}) \equiv \exp(i\mathbf{k}\cdot\mathbf{r}') \tag{1a}$$

with

$$\mathbf{r}' = \mathbf{g}\cdot\mathbf{r}. \tag{1b}$$

Note that when transforming the position vector $\mathbf{r}$, the wave vector $\mathbf{k}$ is a fixed parameter characterizing the plane wave $\exp(i\mathbf{k}\cdot\mathbf{r})$ that does not change under g. Nonetheless, since g is an orthogonal transformation, we can also write Eq. (1a) as

$$g\,\exp(i\mathbf{k}\cdot\mathbf{r}) = \exp[i(\mathbf{g}^{-1}\cdot\mathbf{k})\cdot\mathbf{r}] \tag{2a}$$
$$= \exp(i\mathbf{k}'\cdot\mathbf{r}) \tag{2b}$$

with

$$\mathbf{k}' = \mathbf{g}^{-1}\cdot\mathbf{k}. \tag{2c}$$

Thus we can evaluate g either by transforming the position vector $\mathbf{r}$ or by inversely transforming the wave vector $\mathbf{k}$.

In the group theory of crystallographic space groups, the point-group symmetries g of Bloch functions $\Psi_{\mathbf{k}}(\mathbf{r})$ with wave vector $\mathbf{k}$ form the point group $\mathcal{G}_{\mathbf{k}}$ of the wave vector $\mathbf{k}$ [3, 38, 39]. Given the point group $\mathcal{G}_0$ of a crystal structure, the group $\mathcal{G}_{\mathbf{k}}$ is defined by the condition that it contains the symmetry elements of $\mathcal{G}_0$ that map $\mathbf{k}$ onto a vector $\mathbf{k}'$ such that

$$\mathbf{k}' = \mathbf{g}^{-1}\cdot\mathbf{k} = \mathbf{k} + \mathbf{b}_g, \tag{3}$$

where $\mathbf{b}_g$ is a reciprocal lattice vector with the possibility $\mathbf{b}_g = 0$. Indeed, since g represents point group operations, we can have $\mathbf{b}_g \neq 0$ only if $\mathbf{k}$ is from the border of the BZ. For positions $\mathbf{r} = \mathbf{a}$ that are lattice vectors we have

$$g\,\exp(i\mathbf{k}\cdot\mathbf{a}) = \exp(i\mathbf{k}'\cdot\mathbf{a}) = \exp(i\mathbf{k}\cdot\mathbf{a}) \tag{4}$$

by definition of $\mathcal{G}_{\mathbf{k}}$.

B. Tight-binding Hamiltonian

We denote the tight-binding (TB) basis functions (that are Bloch functions) as

$$\Phi^{W\mu}_{\nu\mathbf{k}}(\mathbf{r}) = \frac{e^{i\mathbf{k}\cdot\mathbf{r}}}{\sqrt{N}}\sum_j e^{-i\mathbf{k}\cdot(\mathbf{r}-\mathbf{R}_j^{W\mu})}\,\phi^W_\nu(\mathbf{r}-\mathbf{R}_j^{W\mu}), \tag{5}$$

where $\phi^W_\nu(\mathbf{r}-\mathbf{R}_j^{W\mu})$ are the atomic orbitals of type ν centered about the positions $\mathbf{R}_j^{W\mu}$ of the atoms. The label W denotes the Wyckoff letter of the atomic positions of the crystal structure [43]. The label μ has values $\mu = 1,\ldots,m$ where m is the multiplicity of W. The index j labels the unit cells of the crystal structure; it runs through the positions in a Bravais lattice. The matrix elements of the TB Hamiltonian can then be written as

$$H(\mathbf{k})^{W\mu W'\mu'}_{\nu\nu'} = \int \Phi^{W\mu *}_{\nu\mathbf{k}}(\mathbf{r})\,H\,\Phi^{W'\mu'}_{\nu'\mathbf{k}}(\mathbf{r})\,d^3r \tag{6a}$$
$$= \epsilon^W_\nu\,\delta_{\nu\nu'}\,\delta_{WW'}\,\delta_{\mu\mu'} + {\sum_{jj'}}' t^{WW'\mu\mu'}_{\nu\nu' jj'}, \tag{6b}$$

where

$$\epsilon^W_\nu \equiv \int \phi^{W*}_\nu(\mathbf{r}-\mathbf{R}_j^{W\mu})\,H\,\phi^W_\nu(\mathbf{r}-\mathbf{R}_j^{W\mu})\,d^3r \tag{7a}$$
$$= \int \phi^{W*}_\nu(\mathbf{r})\,H\,\phi^W_\nu(\mathbf{r})\,d^3r \tag{7b}$$

denotes the on-site energies for the atomic orbitals (that do not depend on the indices μ and j) and

$$t^{WW'\mu\mu'}_{\nu\nu' jj'} \equiv\; e^{-i\mathbf{k}\cdot(\mathbf{R}_j^{W\mu}-\mathbf{R}_{j'}^{W'\mu'})} \times \int \phi^{W*}_\nu(\mathbf{r}-\mathbf{R}_j^{W\mu})\,H\,\phi^{W'}_{\nu'}(\mathbf{r}-\mathbf{R}_{j'}^{W'\mu'})\,d^3r \tag{8}$$

are the hopping integrals. The prime on the summation sign in Eq. (6b) indicates that the sum excludes the on-site term ϵ^W_ν. The TB approximation implies that this sum is restricted to nth-nearest neighbors with a small value of n. The hopping integrals can be written in terms of the Slater-Koster parameters [44] for hopping integrals between atomic orbitals at positions $\mathbf{R}_j^{W\mu}$ and $\mathbf{R}_{j'}^{W'\mu'}$.

C. Decomposition of TB wave functions

Generally, the basis functions (5) for a given wave vector $\mathbf{k}$ transform according to a representation $\Gamma^\Phi_{\mathbf{k}W}$ of the group of the wave vector $\mathcal{G}_{\mathbf{k}}$ that need not be irreducible. (Here the generic superscript Φ accounts for the fact that multiple atomic orbitals with different indices ν may transform jointly according to the same representation. By definition of Wyckoff letters W, orbitals at different positions μ of a given Wyckoff letter W transform jointly according to one representation.) As a consequence of the Wigner-Eckart theorem [19, 45] and the fact that H transforms according to the identity representation Γ_1 of $\mathcal{G}_{\mathbf{k}}$, the hopping integrals (8) vanish when the product of the representations $\Gamma^\Phi_{\mathbf{k}W}$ and $\Gamma^{\Phi'}_{\mathbf{k}W'}$ does not contain the identity representation. In the following, we present a general scheme for transforming the set of basis functions (5) into a symmetry-adapted set of basis functions, where each function transforms irreducibly under $\mathcal{G}_{\mathbf{k}}$, so that two such basis functions only

couple when they both transform according to the same IR of $\mathcal{G}_{\mathbf{k}}$. This scheme is based on a decomposition of the basis functions into symmetry-adapted plane waves and symmetry-adapted atomic orbitals.

We denote

$$\tilde{\phi}^{W}_{\nu\mathbf{k}}(\mathbf{r}-\mathbf{R}_j^{W\mu}) \equiv e^{-i\mathbf{k}\cdot(\mathbf{r}-\mathbf{R}_j^{W\mu})}\,\phi^{W}_{\nu}(\mathbf{r}-\mathbf{R}_j^{W\mu}), \tag{9}$$

so that Eq. (5) becomes

$$\Phi^{W\mu}_{\nu\mathbf{k}}(\mathbf{r}) = \frac{e^{i\mathbf{k}\cdot\mathbf{r}}}{\sqrt{N}}\sum_j \tilde{\phi}^{W}_{\nu\mathbf{k}}(\mathbf{r}-\mathbf{R}_j^{W\mu}). \tag{10}$$

Assuming for conceptual simplicity that the atomic orbitals ϕ^W_ν are localized over a region much smaller than the nearest-neighbor distance [46], the functions $\tilde{\phi}^{W}_{\nu\mathbf{k}}(\mathbf{r}-\mathbf{R}_j^{W\mu})$ are only nonzero for $\mathbf{r}$ close to $\mathbf{R}_j^{W\mu}$. Hence, in the vicinity of any atomic position $\mathbf{R}_j^{W\mu}$, i.e., for $\mathbf{r}\equiv\mathbf{R}_j^{W\mu}+\delta\mathbf{r}$ with small $\delta\mathbf{r}$, we have

$$\tilde{\phi}^{W}_{\nu\mathbf{k}}(\mathbf{r}-\mathbf{R}_j^{W\mu}) \approx \phi^{W}_{\nu}(\mathbf{r}-\mathbf{R}_j^{W\mu}). \tag{11}$$

Therefore, the TB basis function $\Phi^{W\mu}_{\nu\mathbf{k}}(\mathbf{r})$ can be approximated as

$$\Phi^{W\mu}_{\nu\mathbf{k}}(\mathbf{r}) \approx \frac{e^{i\mathbf{k}\cdot\mathbf{r}}}{\sqrt{N}}\sum_j \phi^{W}_{\nu}(\mathbf{r}-\mathbf{R}_j^{W\mu}) \tag{12a}$$

$$= e^{i\mathbf{k}\cdot\mathbf{r}}\,\mathcal{A}^{W\mu}_{\nu}(\mathbf{r}) \tag{12b}$$

with atomic functions

$$\mathcal{A}^{W\mu}_{\nu}(\mathbf{r}) = \frac{1}{\sqrt{N}}\sum_j \phi^{W}_{\nu}(\mathbf{r}-\mathbf{R}_j^{W\mu}) \tag{13}$$

independent of the wave vector $\mathbf{k}$. For strongly localized atomic orbitals and positions $\mathbf{r}=\mathbf{R}_j^{W\mu}+\delta\mathbf{r}$ we have

$$\mathcal{A}^{W\mu}_{\nu}(\mathbf{r}=\mathbf{R}_j^{W\mu}+\delta\mathbf{r}) = \frac{1}{\sqrt{N}}\sum_j \phi^{W}_{\nu}(\delta\mathbf{r}) \propto \phi^{W}_{\nu}(\delta\mathbf{r}), \tag{14}$$

that is, near an atomic site $\mathbf{R}_j^{W\mu}$, the atomic functions $\mathcal{A}^{W\mu}_{\nu}(\mathbf{r})$ are simply proportional to $\phi^W_\nu(\delta\mathbf{r})$, independent of the index μ. Therefore, the atomic functions $\mathcal{A}^{W\mu}_{\nu}(\mathbf{r}=\mathbf{R}_j^{W\mu}+\delta\mathbf{r})$ have the same symmetry properties as the atomic orbitals $\phi^W_\nu(\delta\mathbf{r})$.

The plane wave $e^{i\mathbf{k}\cdot\mathbf{r}}$ for positions $\mathbf{r}=\mathbf{R}_j^{W\mu}+\delta\mathbf{r}$ near an atomic site $\mathbf{R}_j^{W\mu}$ is approximately given by

$$\exp[i\mathbf{k}\cdot(\mathbf{R}_j^{W\mu}+\delta\mathbf{r})] \approx \exp(i\mathbf{k}\cdot\mathbf{R}_j^{W\mu}) \equiv q_{\mathbf{k}}(\mathbf{R}_j^{W\mu}), \tag{15}$$

where $q_{\mathbf{k}}(\mathbf{R}_j^{W\mu})$ denotes the plane wave with wave vector $\mathbf{k}$ associated with the Wyckoff position $\mathbf{R}_j^{W\mu}$ for fixed W and μ, but j runs over all positions in a Bravais lattice. These discrete quantities $q_{\mathbf{k}}(\mathbf{R}_j^{W\mu})$ will be discussed in more detail in Sec. II F. The TB basis function thus can be factorized (ignoring normalization)

$$\Phi^{W\mu}_{\nu\mathbf{k}}(\mathbf{r}=\mathbf{R}_j^{W\mu}+\delta\mathbf{r}) \approx q_{\mathbf{k}}(\mathbf{R}_j^{W\mu})\,\phi^{W}_{\nu}(\delta\mathbf{r}). \tag{16}$$

This expression will be analyzed further in the following sections.

As a side remark, we note that the eigenfunctions of the TB Hamiltonian (6) for the band n and wave vector $\mathbf{k}$ expressed in terms of the basis functions (5) take the form

$$\Psi_{n\mathbf{k}}(\mathbf{r}) = \sum_{W\mu\nu}\psi^{W\mu}_{\nu n\mathbf{k}}\,\Phi^{W\mu}_{\nu\mathbf{k}}(\mathbf{r}) \tag{17}$$

with expansion coefficients $\psi^{W\mu}_{\nu n\mathbf{k}}$. These eigenfunctions permit a factorization similar to Eq. (16)

$$\Psi_{n\mathbf{k}}(\mathbf{r}=\mathbf{R}_j^{W\mu}+\delta\mathbf{r}) \approx \sum_{W\mu} q_{\mathbf{k}}(\mathbf{R}_j^{W\mu})\sum_\nu \psi^{W\mu}_{\nu n\mathbf{k}}\,\phi^{W}_{\nu}(\delta\mathbf{r}). \tag{18}$$

However, the discussion of the TB wave functions $\Psi_{n\mathbf{k}}(\mathbf{r})$ is greatly simplified if instead of the basis functions (5) we use symmetry-adapted basis functions to be discussed in the following.

D. Symmetry-adapted basis functions

The main advantage of the approximate expression (16) lies in the fact that the function (16) has the same symmetry properties as the TB basis function (5). Yet the factorization in Eq. (16) allows one to discuss the symmetry of the plane waves $q_{\mathbf{k}}(\mathbf{R}_j^{W\mu})$ (characterized by a representation $\Gamma^q_{\mathbf{k}W}$ of $\mathcal{G}_{\mathbf{k}}$, see Sec. II F) separate from the symmetry of the atomic orbitals $\phi^W_\nu(\delta\mathbf{r})$ (characterized by a representation $\Gamma^\phi_{\mathbf{k}W}$ of $\mathcal{G}_{\mathbf{k}}$, see Sec. II E). Often, these representations are irreducible, though generally they can be reducible. The TB basis functions (5) at one Wyckoff letter W then transform according to the product representation

$$\Gamma^\Phi_{\mathbf{k}W} \equiv \Gamma^q_{\mathbf{k}W}\times\Gamma^\phi_{\mathbf{k}W}. \tag{19}$$

The representation $\Gamma^\Phi_{\mathbf{k}W}$ may be reducible (even if $\Gamma^q_{\mathbf{k}W}$ and $\Gamma^\phi_{\mathbf{k}W}$ are irreducible), giving the decomposition

$$\Gamma^\Phi_{\mathbf{k}W} = \sum_I a_I\Gamma_I, \tag{20}$$

where $a_I\geq 0$ are the multiplicities with which the IRs Γ_I of $\mathcal{G}_{\mathbf{k}}$ appear in $\Gamma^\Phi_{\mathbf{k}W}$. Generally, the IRs Γ_I contained in $\Gamma^\Phi_{\mathbf{k}W}$ give symmetry-adapted basis functions

$$\Phi^{WI\alpha\beta}_{\mathbf{k}}(\mathbf{r}) = \sum_{\mu\nu}\mathcal{C}^{W\mu\nu\mathbf{k}}_{I\alpha\beta}\,\Phi^{W\mu}_{\nu\mathbf{k}}(\mathbf{r}), \tag{21}$$

where $\alpha=1,2,\ldots,a_I$ and β labels the different functions transforming jointly according to Γ_I. The coefficients

$\mathscr{C}^{W\mu\nu\mathbf{k}}_{I\alpha\beta}$ represent the weights with which the functions $\Phi^{W\mu}_{\nu\mathbf{k}}(\mathbf{r})$ contribute to the symmetry-adapted basis functions $\Phi^{WI\alpha\beta}_{\mathbf{k}}(\mathbf{r})$. Given symmetry-adapted plane waves transforming according to the IR Γ_J and atomic orbitals transforming according to the IR $\Gamma_{J'}$ (see discussion below), the expansion coefficients $\mathscr{C}^{W\mu\nu\mathbf{k}}_{I\alpha\beta}$ are given by the Clebsch-Gordan coefficients for coupling Γ_J and $\Gamma_{J'}$ to obtain Γ_I.

For the symmetry-adapted basis functions (21), the matrix elements (6) of the TB Hamiltonian become block-diagonal with respect to different IRs Γ_I

$$H(\mathbf{k})^{WW'II'}_{\alpha\alpha'\beta\beta'} = \delta_{II'}\Big[\epsilon^{W}_{I\alpha}\,\delta_{WW'}\,\delta_{\alpha\alpha'}\,\delta_{\beta\beta'} + {\sum_{jj'}}' t^{WW'I\,\alpha\alpha'}_{\beta\beta'\,jj'}\Big]. \tag{22}$$

Here

$$\epsilon^{W}_{I\alpha} \equiv \int \Phi^{WI\alpha\beta *}_{\mathbf{k}}(\mathbf{r})\, H\, \Phi^{WI\alpha\beta}_{\mathbf{k}}(\mathbf{r})\, d^3r \tag{23}$$

denotes the on-site energies. These can always be made diagonal in the index α by a suitable definition of the a_I sets of basis functions (21) transforming according to Γ_I. The hopping matrix elements become

$$t^{WW'I\,\alpha\alpha'}_{\beta\beta'\,jj'} \equiv \int \Phi^{WI\alpha\beta *}_{\mathbf{k}}(\mathbf{r})\, H\, \Phi^{W'I\alpha'\beta'}_{\mathbf{k}}(\mathbf{r}')\, d^3r \tag{24}$$

with $\mathbf{r} = \mathbf{R}^{W\mu}_{j} + \delta\mathbf{r}$ and $\mathbf{r}' = \mathbf{R}^{W'\mu'}_{j'} + \delta\mathbf{r}$. We remark that in actual TB models it may happen that a block (22) can be further decomposed into subblocks if symmetry-allowed couplings between distant neighbors are ignored within the TB approximation.

Each block (22) of the TB Hamiltonian yields eigenfunctions

$$\Psi^{I\beta}_{n\mathbf{k}}(\mathbf{r}) = \sum_{W,\alpha} C^{WI\alpha}_{n\mathbf{k}} \Phi^{WI\alpha\beta}_{\mathbf{k}}(\mathbf{r}) \tag{25}$$

with expansion coefficients $C^{WI\alpha\beta}_{n\mathbf{k}}$ that transform irreducibly according to the βth component of the IR Γ_I of $\mathscr{G}_{\mathbf{k}}$. To proceed, we discuss first the symmetry of the atomic orbitals $\phi^{W}_{\nu}(\delta\mathbf{r})$, followed by a discussion of the symmetry of the plane waves $q_{\mathbf{k}}(\mathbf{R}^{W\mu}_{j})$.

E. Transformation of atomic orbitals $\phi^{W}_{\nu}(\delta\mathbf{r})$

We can study the symmetry of the atomic function $\mathscr{A}^{W\mu}_{\nu}(\mathbf{r})$ in the vicinity of the atomic positions $\mathbf{R}^{W\mu}_{j}$ by only looking at the orbitals $\phi^{W}_{\nu}(\delta\mathbf{r})$. Obviously, this problem is independent of the index μ, the band index n, and the wave vector $\mathbf{k}$ though, of course, we are generally interested in the transformational behavior of these orbitals with respect to the group $\mathscr{G}_{\mathbf{k}}$ of the wave vector $\mathbf{k}$. For symmetry operations $g \in \mathscr{G}_{\mathbf{k}}$ we have

$$g\,\phi^{W}_{\nu}(\delta\mathbf{r}) = \phi^{W}_{\nu}(g\,\delta\mathbf{r}) = \sum_{\nu'} \mathscr{D}^{\phi}_{\mathbf{k}W}(g)_{\nu\nu'}\phi^{W}_{\nu'}(\delta\mathbf{r}), \tag{26}$$

where $\Gamma^{\phi}_{\mathbf{k}W} = \{\mathscr{D}^{\phi}_{\mathbf{k}W}(g) : g \in \mathscr{G}_{\mathbf{k}}\}$ is the representation describing the transformation of the atomic orbitals ϕ^{W}_{ν}. As usual, we assume that the atomic orbitals are characterized by some orbital angular momentum $l = 0, 1, 2, \ldots$, so that the matrices $\mathscr{D}^{\phi}_{\mathbf{k}W}(g)$ acquire a block structure corresponding to different values of l, indicating that there exists no mixing between atomic orbitals with different angular momenta under symmetry transformations $g \in \mathscr{G}_{\mathbf{k}}$.

In general, the representation $\Gamma^{\phi}_{\mathbf{k}W}$ is reducible [47]. The projection operators (A1) yield symmetry-adapted atomic orbitals $\phi^{W}_{I\beta}(\delta\mathbf{r})$ transforming like component β of the IR Γ_I of $\mathscr{G}_{\mathbf{k}}$,

$$\phi^{W}_{I\beta}(\delta\mathbf{r}) \equiv \Pi_{I\beta}\,\phi^{W}_{\nu}(\delta\mathbf{r}) \tag{27a}$$

$$= \frac{n_I}{h}\sum_{g} \mathscr{D}_I(g)^{*}_{\beta\beta}\, g\,\phi^{W}_{\nu}(\delta\mathbf{r}) \tag{27b}$$

$$= \sum_{\nu'} c^{W\nu'}_{I\beta}\phi^{W}_{\nu'}(\delta\mathbf{r}) \tag{27c}$$

with expansion coefficients

$$c^{W\nu'}_{I\beta} = \frac{n_I}{h}\sum_{g} \mathscr{D}_I(g)^{*}_{\beta\beta}\,\mathscr{D}^{\phi}_{\mathbf{k}W}(g)_{\nu\nu'}. \tag{27d}$$

We note that this analysis applies to the spinless case when the angular part of the atomic orbitals is given by the usual spherical harmonics Y^{m}_{l}. It can likewise be used in the spin-dependent case when the angular part of the atomic orbitals is given by spin-angular functions and the projection operators $\Pi_{I\beta}$ project on the double-group representations of $\mathscr{G}_{\mathbf{k}}$.

F. Transformation of plane waves $q_{\mathbf{k}}(\mathbf{R}^{W\mu}_{j})$

While the IRs of TB eigenfunctions (17) depend on the band index n, the symmetry of the plane waves $q_{\mathbf{k}}(\mathbf{R}^{W\mu}_{j})$ can be discussed independent of the index n. Very generally, for a given Wyckoff letter W, the positions $\mathbf{R}^{W\mu}_{j}$ transform among themselves under the operations of the space group. Hence, using the matrix $\mathbf{g}$ defined in Eq. (1), we have

$$g\,\mathbf{R}^{W\mu}_{j} = \mathbf{g}\cdot\mathbf{R}^{W\mu}_{j} \equiv \mathbf{R}^{W\mu'}_{j'}, \tag{28}$$

i.e., a symmetry transformation $g \in \mathscr{G}_{\mathbf{k}}$ generally changes both μ and j. We rewrite this as

$$\mathbf{g}\cdot\mathbf{R}^{W\mu}_{j} = \mathbf{R}^{W\mu'}_{j} + \left[\mathbf{R}^{W\mu'}_{j'} - \mathbf{R}^{W\mu'}_{j}\right], \tag{29}$$

where the term in square brackets is a lattice vector. Applying the operation g to the plane wave $q_{\mathbf{k}}(\mathbf{R}^{W\mu}_{j})$ yields

$$g\,q_{\mathbf{k}}(\mathbf{R}^{W\mu}_{j}) = \exp(i\mathbf{k}\cdot\mathbf{R}^{W\mu'}_{j'}) \tag{30a}$$

$$= q_{\mathbf{k}}(\mathbf{R}^{W\mu'}_{j})\exp[i\mathbf{k}\cdot(\mathbf{R}^{W\mu'}_{j'} - \mathbf{R}^{W\mu'}_{j})]. \tag{30b}$$

Hence, the symmetry operation g generally maps the plane wave $q_{\mathbf{k}}(\mathbf{R}_j^{W\mu})$ onto $q_{\mathbf{k}}(\mathbf{R}_j^{W\mu'})$ multiplied by a phase factor.

To analyze the mappings (30) further, we interpret the discrete plane waves $\{q_{\mathbf{k}}(\mathbf{R}_j^{W\mu}) : \mu = 1,\ldots,m\}$ as basis vectors in an m-dimensional vector space. Relative to this basis, we can express arbitrary points as m-component spinors. It facilitates this analysis to introduce m-component base spinors $\{\boldsymbol{q}_{\mathbf{k}}(\mathbf{R}_j^{W\mu}) : \mu = 1,\ldots,m\}$ with components ν equal to $\delta_{\mu\nu}$. Using these base spinors, a plane wave at positions $\boldsymbol{\mathcal{R}}_j^W \equiv \{\mathbf{R}_j^{W\mu} : \mu = 1,\ldots,m\}$ becomes

$$Q_{\mathbf{k}}(\boldsymbol{\mathcal{R}}_j^W) = \sum_\mu \boldsymbol{q}_{\mathbf{k}}(\mathbf{R}_j^{W\mu}) = \begin{pmatrix} 1 \\ \vdots \\ 1 \end{pmatrix}. \tag{31}$$

Applying a symmetry transformation g to $Q_{\mathbf{k}}(\boldsymbol{\mathcal{R}}_j^W)$ gives

$$g\, Q_{\mathbf{k}}(\boldsymbol{\mathcal{R}}_j^W) = \mathcal{D}^q_{\mathbf{k}W}(g)\, Q_{\mathbf{k}}(\boldsymbol{\mathcal{R}}_j^W), \tag{32}$$

where $\mathcal{D}^q_{\mathbf{k}W}(g)$ is an $m \times m$ matrix corresponding to the group element g. Each row and each column of $\mathcal{D}^q_{\mathbf{k}W}(g)$ has only one nonzero matrix element which, according to Eq. (30), is given by

$$\mathcal{D}^q_{\mathbf{k}W}(g)_{\mu'\mu} = \exp[i\mathbf{k}\cdot(\mathbf{R}_{j'}^{W\mu'} - \mathbf{R}_j^{W\mu'})], \tag{33}$$

where the g dependence on the RHS is given by Eq. (29).

We show in the following that $\Gamma^q_{\mathbf{k}W} \equiv \{\mathcal{D}^q_{\mathbf{k}W}(g) : g \in \mathcal{G}_{\mathbf{k}}\}$ defines an m-dimensional representation of $\mathcal{G}_{\mathbf{k}}$, i.e., for any two group elements $g_1, g_2 \in \mathcal{G}_{\mathbf{k}}$ we have

$$\mathcal{D}^q_{\mathbf{k}W}(g_2)\mathcal{D}^q_{\mathbf{k}W}(g_1) = \mathcal{D}^q_{\mathbf{k}W}(g_2 g_1). \tag{34}$$

Given a position $\mathbf{R}_{j_0}^{W\mu_0}$ and using Eq. (29), we have

$$\begin{aligned} g_1\mathbf{R}_{j_0}^{W\mu_0} &= \mathbf{g}_1\cdot\mathbf{R}_{j_0}^{W\mu_0} \\ &\equiv \mathbf{R}_{j_1}^{W\mu_1} = \mathbf{R}_{j_0}^{W\mu_1} + \left[\mathbf{R}_{j_1}^{W\mu_1} - \mathbf{R}_{j_0}^{W\mu_1}\right], \quad (35a) \\ g_2\mathbf{R}_{j_0}^{W\mu_1} &= \mathbf{g}_2\cdot\mathbf{R}_{j_0}^{W\mu_1} \\ &\equiv \mathbf{R}_{j_2}^{W\mu_2} = \mathbf{R}_{j_0}^{W\mu_2} + \left[\mathbf{R}_{j_2}^{W\mu_2} - \mathbf{R}_{j_0}^{W\mu_2}\right], \quad (35b) \end{aligned}$$

so that the phase (33) for the group elements g_1 and g_2 becomes

$$\mathcal{D}^q_{\mathbf{k}W}(g_1)_{\mu_1\mu_0} = \exp[i\mathbf{k}\cdot(\mathbf{R}_{j_1}^{W\mu_1} - \mathbf{R}_{j_0}^{W\mu_1})], \tag{36a}$$
$$\mathcal{D}^q_{\mathbf{k}W}(g_2)_{\mu_2\mu_1} = \exp[i\mathbf{k}\cdot(\mathbf{R}_{j_2}^{W\mu_2} - \mathbf{R}_{j_0}^{W\mu_2})]. \tag{36b}$$

The product $g_2\, g_1$, i.e., the transformation g_1 followed by g_2, is also an element of $\mathcal{G}_{\mathbf{k}}$, giving

$$\begin{aligned} g_2\, g_1\, q_{\mathbf{k}}(\mathbf{R}_{j_0}^{W\mu_0}) &= \exp(i\mathbf{k}\cdot g_2\mathbf{R}_{j_1}^{W\mu_1}) \quad (37a) \\ &= \exp(i\mathbf{k}\cdot g_2\mathbf{R}_{j_0}^{W\mu_1})\exp[i\mathbf{k}\cdot g_2(\mathbf{R}_{j_1}^{W\mu_1} - \mathbf{R}_{j_0}^{W\mu_1})] \quad (37b) \\ &= \exp(i\mathbf{k}\cdot\mathbf{R}_{j_0}^{W\mu_2})\exp[i\mathbf{k}\cdot(\mathbf{R}_{j_2}^{W\mu_2} - \mathbf{R}_{j_0}^{W\mu_2})]\,\exp[i\mathbf{k}\cdot g_2(\mathbf{R}_{j_1}^{W\mu_1} - \mathbf{R}_{j_0}^{W\mu_1})]. \quad (37c) \end{aligned}$$

As $\mathbf{R}_{j_1}^{W\mu_1} - \mathbf{R}_{j_0}^{W\mu_1}$ is a lattice vector, it follows from Eq. (4)

$$g_2\, g_1\, q_{\mathbf{k}}(\mathbf{R}_{j_0}^{W\mu_0}) = q_{\mathbf{k}}(\mathbf{R}_{j_0}^{W\mu_2})\,\mathcal{D}^q_{\mathbf{k}W}(g_2\, g_1)_{\mu_2\mu_0} \tag{38}$$

with

$$\mathcal{D}^q_{\mathbf{k}W}(g_2\, g_1)_{\mu_2\mu_0} = \exp[i\mathbf{k}\cdot(\mathbf{R}_{j_2}^{W\mu_2} - \mathbf{R}_{j_0}^{W\mu_2} + \mathbf{R}_{j_1}^{W\mu_1} - \mathbf{R}_{j_0}^{W\mu_1})]. \tag{39}$$

This confirms Eq. (34).

We remark that for $\mathbf{k} = 0$ the representation $\Gamma^q_{\mathbf{k}W}$ is known as permutation representation [48] or equivalence representation [39], where it characterizes the permutations of m objects under the symmetry operations $g \in \mathcal{G}_0$.

Using the fact that g is an orthogonal transformation, we can also write Eq. (33) as

$$\begin{aligned} \mathcal{D}^q_{\mathbf{k}W}(g)_{\mu'\mu} &= \exp[i\mathbf{k}\cdot(\mathbf{R}_{j'}^{W\mu'} - \mathbf{R}_j^{W\mu'})] \quad (40a) \\ &= \exp[i\mathbf{k}\cdot(\mathbf{g}\cdot\mathbf{R}_j^{W\mu} - \mathbf{R}_j^{W\mu'})] \quad (40b) \\ &= \exp\{i[(\mathbf{g}^{-1}\cdot\mathbf{k})\cdot\mathbf{R}_j^{W\mu} - \mathbf{k}\cdot\mathbf{R}_j^{W\mu'}]\}. \quad (40c) \end{aligned}$$

For $\mathbf{k}$ inside the Brillouin zone, where $\mathbf{g}^{-1}\cdot\mathbf{k} = \mathbf{k}$ by definition of $\mathcal{G}_{\mathbf{k}}$, the nonzero matrix elements of $\mathcal{D}^q_{\mathbf{k}W}(g)$ therefore become

$$\mathcal{D}^q_{\mathbf{k}W}(g)_{\mu'\mu} \equiv \exp[i\mathbf{k}\cdot(\mathbf{R}_j^{W\mu} - \mathbf{R}_j^{W\mu'})]. \tag{41}$$

We see that the representation is generally non-trivial for $m > 1$. However, for $m = 1$, we have $\mathbf{R}_j^{W\mu} = \mathbf{R}_j^{W\mu'}$, so that $q_{\mathbf{k}}(\mathbf{R}_j^{W\mu})$ transforms according to the identity representation Γ_1.

1. *Wyckoff positions with multiplicity $m = 1$*

We consider first the special case of Wyckoff positions with multiplicity $m = 1$. Here we drop the index μ,

denoting atomic positions as $\mathbf{R}_j^W$. This case is equivalent to atomic positions $\mathbf{R}_j^W$ forming a Bravais lattice. Note also that multiplicities $m = 1$ occur only for symmorphic space groups [43]. Here, plane waves $Q_\mathbf{k}(\mathbf{R}_j^W) = q_\mathbf{k}(\mathbf{R}_j^W)$ transform according to the one-dimensional IR

$$\mathscr{D}^q_{\mathbf{k}W}(g) = \exp[i\,\mathbf{k}\cdot(\mathbf{R}^W_{j'} - \mathbf{R}^W_j)]. \tag{42}$$

We saw in Eq. (41) that for wave vectors $\mathbf{k}$ inside the BZ this becomes the identity representation Γ_1. It is illuminating to rederive this result by writing Eq. (42) as

$$\mathscr{D}^q_{\mathbf{k}W}(g) = \exp[i\,(\mathbf{k}\cdot\mathbf{g} - \mathbf{k})\cdot\mathbf{R}^W_j] \tag{43a}$$
$$= \exp[i\,(\mathbf{g}^{-1}\cdot\mathbf{k} - \mathbf{k})\cdot\mathbf{R}^W_j]. \tag{43b}$$

It follows from Eq. (3) that $\mathbf{k}' = \mathbf{g}^{-1}\cdot\mathbf{k} = \mathbf{k} + \mathbf{b}_g$ with a reciprocal lattice vector $\mathbf{b}_g$. Thus Eq. (42) describing the effect of g in real space is equivalent to

$$\mathscr{D}^q_{\mathbf{k}W}(g) = \exp[i\,\mathbf{b}_g\cdot\mathbf{R}^W_j] \tag{44}$$

describing the effect of g in reciprocal space. Hence, for $m = 1$ plane waves $Q_\mathbf{k}(\mathbf{R}_j^W)$ transform under $\mathcal{G}_\mathbf{k}$ in a non-trivial way only if the vector $\mathbf{k}$ is from the border of the BZ when $\mathbf{k}' = \mathbf{g}^{-1}\cdot\mathbf{k}$ and $\mathbf{k}$ can differ by a reciprocal lattice vector $\mathbf{b}_g \neq 0$. Otherwise, $\mathbf{k}' = \mathbf{k}$ implies that $Q^W_\mathbf{k}(\mathbf{R}_j^W)$ transforms according to Γ_1 of $\mathcal{G}_\mathbf{k}$.

If a space group has Wyckoff positions $W \neq W'$ each with multiplicity $m = 1$, we can compare the IRs of the plane waves at the positions $\mathbf{R}_j^W$ and $\mathbf{R}_j^{W'}$. We have

$$\mathscr{D}^q_{\mathbf{k}W}(g) = \exp(i\mathbf{b}_g\cdot\mathbf{R}^W_j), \tag{45a}$$
$$\mathscr{D}^q_{\mathbf{k}W'}(g) = \exp(i\mathbf{b}_g\cdot\mathbf{R}^{W'}_j). \tag{45b}$$

Hence

$$\mathscr{D}^q_{\mathbf{k}W}(g) = \mathscr{D}^q_{\mathbf{k}W'}(g)\exp[i\mathbf{b}_g\cdot(\mathbf{R}^W_j - \mathbf{R}^{W'}_j)]. \tag{46}$$

For $W \neq W'$, the vector $\mathbf{R}_j^W - \mathbf{R}_j^{W'}$ is not equal to a lattice vector, so that for nonzero $\mathbf{b}_g$ (i.e., for $\mathbf{k}$ on the boundary of the Brillouin zone) we generally have

$$\Gamma^q_{\mathbf{k}W} \neq \Gamma^q_{\mathbf{k}W'}. \tag{47}$$

This implies that a nontrivial change of the coordinate system which requires a relabeling of the Wyckoff letters associated with atomic positions changes the IRs of the plane waves at these positions. This relabeling of IR assignments will be discussed in Sec. II F 2.

As a simple example for Eq. (47), consider the case where the positions $\mathbf{R}_j^W$ are equal to lattice vectors, i.e., one of the positions $\mathbf{R}_j^W$ is at the origin of the coordinate system. Hence, Eq. (44) gives $\Gamma^q_{\mathbf{k}W} = \{\mathscr{D}^q_{\mathbf{k}W}(g) = 1 : g \in \mathcal{G}_\mathbf{k}\}$, i.e., the plane wave $Q_\mathbf{k}(\mathbf{R}_j^W)$ transforms according to the identity representation. On the other hand, the IR $\Gamma^q_{\mathbf{k}W'}$ at a different Wyckoff position W' can never be the identity representation.

Examples of Wyckoff positions with multiplicity $m = 1$ are the positions occupied by the Mo atoms and the center of the hexagon in monolayer MoS_2. The plane wave at these positions transforms according to different IRs. In a certain coordinate system where one of these two inequivalent positions are located at the origin, the plane waves at that Wyckoff position transform as the identity representation, while the plane waves at the other Wyckoff position transform according to a different IR. Another example is given by the inequivalent IRs of the plane waves at the positions of C atoms in the central layer of graphene with odd number of layers such as the trilayer graphene discussed in Sec. IV A 3.

2. *Wyckoff positions with multiplicity $m > 1$*

For Wyckoff positions with multiplicity $m > 1$ the simple analysis based on Eq. (3) is not valid as it does not keep track of how positions $\mathbf{R}_j^{W\mu}$ are mapped onto each other by symmetry operations $g \in \mathcal{G}_\mathbf{k}$. Instead we need to use the plane-wave spinors (31). For multiplicity $m > 1$, the representation $\Gamma^q_{\mathbf{k}W}$ characterizing the plane-wave spinors $Q_\mathbf{k}(\boldsymbol{\mathscr{R}}_j^W)$ is generally reducible. Using the projection operator (A1), we can construct linear combinations $\mathbb{Q}^{I\beta}_\mathbf{k}(\boldsymbol{\mathscr{R}}_j^W)$ of the base spinors $q_\mathbf{k}(\mathbf{R}_j^{W\mu})$ transforming like component β of the IR Γ_I of $\mathcal{G}_\mathbf{k}$ contained in $\Gamma^q_{\mathbf{k}W}$

$$\mathbb{Q}^{I\beta}_\mathbf{k}(\boldsymbol{\mathscr{R}}_j^W) \equiv \Pi^{I\beta}_\mathbf{k}\, Q_\mathbf{k}(\boldsymbol{\mathscr{R}}_j^W) \tag{48a}$$
$$= \frac{n_I}{h}\sum_g \mathscr{D}_I(g)^*_{\beta\beta}\, g\, Q_\mathbf{k}(\boldsymbol{\mathscr{R}}_j^W) \tag{48b}$$
$$= \frac{n_I}{h}\sum_g \mathscr{D}_I(g)^*_{\beta\beta}\, \mathscr{D}^q_{\mathbf{k}W}(g)\, Q_\mathbf{k}(\boldsymbol{\mathscr{R}}_j^W), \tag{48c}$$

where we used Eq. (32). This yields

$$\mathbb{Q}^{I\beta}_\mathbf{k}(\boldsymbol{\mathscr{R}}_j^W) = \sum_m u^{I\beta}_{\mathbf{k}W\mu}\, q_\mathbf{k}(\mathbf{R}_j^{W\mu}) = \begin{pmatrix} u^{I\beta}_{\mathbf{k}W1} \\ \vdots \\ u^{I\beta}_{\mathbf{k}Wm} \end{pmatrix} \tag{49}$$

with expansion coefficients

$$u^{I\beta}_{\mathbf{k}W\mu} = \frac{n_I}{h}\sum_g \mathscr{D}_I(g)^*_{\beta\beta}\sum_{\tilde\mu}\mathscr{D}^q_{\mathbf{k}W}(g)_{\mu\tilde\mu} \tag{50}$$

that completely characterize each symmetrized spinor $\mathbb{Q}^{I\beta}_\mathbf{k}(\boldsymbol{\mathscr{R}}_j^W)$.

Upon translation by a lattice vector $\mathbf{a}$, the plane waves $q_\mathbf{k}(\mathbf{R}_j^{W\mu})$ acquire a phase $\exp(i\mathbf{k}\cdot\mathbf{a})$

$$q_\mathbf{k}(\mathbf{R}_j^{W\mu} + \mathbf{a}) = \exp(i\mathbf{k}\cdot\mathbf{a})\, q_\mathbf{k}(\mathbf{R}_j^{W\mu}). \tag{51}$$

This implies that $q_\mathbf{k}(\mathbf{R}_j^{W\mu})$ represents (for each μ) a discrete Bloch function for wave vector $\mathbf{k}$. Similarly, linear

combinations of these base spinors including the spinors $Q_{\mathbf{k}}(\boldsymbol{\mathcal{R}}_j^W)$ and $\mathbb{Q}_{\mathbf{k}}^{I\beta}(\boldsymbol{\mathcal{R}}_j^W)$ are thus discrete Bloch functions for wave vector $\mathbf{k}$. The expansion coefficients $u_{\mathbf{k}W\mu}^{I\beta}$ take the role of lattice-periodic functions for these discrete Bloch functions.

The projection (48) is valid for all wave vectors $\mathbf{k}$ in the Brillouin zone (though trivial for $m = 1$ when $\mathbf{k}$ is inside the Brillouin zone, as noted above). In general, the projectors $\Pi_{\mathbf{k}}^{I\beta}$ decompose a plane wave spinor $Q_{\mathbf{k}}(\boldsymbol{\mathcal{R}}_j^W)$ into multiple Bloch functions $\mathbb{Q}_{\mathbf{k}}^{I\beta}(\boldsymbol{\mathcal{R}}_j^W)$ corresponding to different IRs Γ_I of $\mathcal{G}_{\mathbf{k}}$. Yet we often have sets of special positions $\boldsymbol{\mathcal{R}}_{Wj}^{I\mathbf{k}} = \{\mathbf{R}_{W\mu j}^{I\mathbf{k}} : \mu = 1, \ldots, m\}$ within the unit cell where only the Bloch functions $\mathbb{Q}_{\mathbf{k}}^{I\beta}(\boldsymbol{\mathcal{R}}_j^W)$ for one IR Γ_I are nonzero, but all other projections vanish. This greatly simplifies further discussion of TB Bloch functions at positions $\boldsymbol{\mathcal{R}}_{Wj}^{I\mathbf{k}}$. The positions $\boldsymbol{\mathcal{R}}_{Wj}^{I\mathbf{k}}$ are characterized by two different groups, the group describing the site symmetry [43] denoted as $\mathcal{G}_W$ and the group of the wave vector $\mathcal{G}_{\mathbf{k}}$. Often the positions $\boldsymbol{\mathcal{R}}_{Wj}^{I\mathbf{k}}$ with nontrivial $\mathcal{G}_{\mathbf{k}}$ coincide with Wyckoff positions with a non-trivial $\mathcal{G}_W$. For Wyckoff positions with multiplicity $m = 1$, we always have $\mathcal{G}_W = \mathcal{G}_0$, so that $\mathcal{G}_{\mathbf{k}} \subseteq \mathcal{G}_W$. However, for $m > 1$ we will find below that in general there is no simple relation between the group $\mathcal{G}_W$ characterizing such special positions $\boldsymbol{\mathcal{R}}_{Wj}^{I\mathbf{k}}$ and the group of the wave vector $\mathcal{G}_{\mathbf{k}}$ for which this happens [49].

The *symmetrized plane waves* $\mathbb{Q}_{\mathbf{k}}^{I\beta}(\boldsymbol{\mathcal{R}}_j^W)$ including the positions $\boldsymbol{\mathcal{R}}_{Wj}^{I\mathbf{k}}$ are universal features of each space group, independent of the "atomistic realization" of a space group in different crystal structures (e.g., the number and positions of atoms in a unit cell). They apply both to spinless models and models that include the spin degree of freedom. We note that the symmetrized plane waves $\mathbb{Q}_{\mathbf{k}}^{I\beta}(\boldsymbol{\mathcal{R}}_j^W)$ introduced here in the context of the TB approximation for Wyckoff positions $\boldsymbol{\mathcal{R}}_j^W$ are conceptually different from the symmetrized plane waves discussed previously in the context of the nearly-free electron approximation, see, e.g., Refs. [38, 39, 50].

G. Rearrangement of IRs of Bloch states under a change of the coordinate system

The Bloch states in certain crystal structures are characterized by IRs of the group $\mathcal{G}_{\mathbf{k}}$ that depend in a nontrivial way on the location of the origin or the orientation of the coordinate system relative to the position of the atoms [20–23]. Cornwell [22] has given a general discussion of the origin dependence of the symmetry labeling of electron states in such systems. Here we review and extend these findings, focusing on symmorphic space groups and adopting a notation matching other parts of this study. We show that for different choices of the origin we get a rearrangement of the IRs of Bloch states. We exploit this rearrangement lemma when discussing band symmetries for specific materials further below.

We consider a crystal structure with space group $\mathcal{G}$. For the coordinate system $\mathbf{r} = (x, y, z)$, the lattice-periodic (single-electron) Hamiltonian is $H(\mathbf{r})$. The eigenfunctions of $H(\mathbf{r})$ are Bloch functions $\Psi_{n\mathbf{k}}^{I\beta}(\mathbf{r})$, obeying the eigenvalue equation

$$H(\mathbf{r})\,\Psi_{n\mathbf{k}}^{I\beta}(\mathbf{r}) = E_n(\mathbf{k})\,\Psi_{n\mathbf{k}}^{I\beta}(\mathbf{r}) \tag{52}$$

with energy $E_n(\mathbf{k})$. For a given wave vector $\mathbf{k}$, the index I denotes the IR Γ_I of the point group $\mathcal{G}_{\mathbf{k}}$ of the wave vector, to be discussed in more detail below. The eigenfunction $\Psi_{n\mathbf{k}}^{I\beta}(\mathbf{r})$ transforms according to the βth component of the IR Γ_I. For brevity, we drop in this section the band index n.

We denote coordinate transformations using the Seitz notation as $\{g|\boldsymbol{\tau}\}$, where g is a (proper or improper) rotation that is followed by a translation $\boldsymbol{\tau}$. We seek to identify a pure translation $T \equiv \{\mathbb{1}|\boldsymbol{\tau}\}$ of the coordinate system $\mathbf{r}$, where $\boldsymbol{\tau}$ equals a fraction of a lattice vector such that for the shifted, primed coordinated system $\mathbf{r}' = (x', y', z')$ the crystal structure has the same space group symmetry $\mathcal{G}$ as for the unprimed coordinate system $\mathbf{r} = (x, y, z)$. The translation T transforms the Bloch function $\Psi_{\mathbf{k}}^{I\beta}(\mathbf{r})$ into

$$\Psi_{\mathbf{k}}^{I'\beta}(\mathbf{r}') \equiv T\,\Psi_{\mathbf{k}}^{I\beta}(\mathbf{r}). \tag{53}$$

The index $I' \neq I$ will be justified below. As $T = \{\mathbb{1}|\boldsymbol{\tau}\}$ commutes with primitive translations $\{\mathbb{1}|\mathbf{a}\}$ we get

$$\{\mathbb{1}|\mathbf{a}\}\,\Psi_{\mathbf{k}}^{I'\beta}(\mathbf{r}') = \exp(-i\mathbf{k}\cdot\mathbf{a})\,\Psi_{\mathbf{k}}^{I'\beta}(\mathbf{r}'), \tag{54}$$

so that the transformed Bloch function $\Psi_{\mathbf{k}}^{I'\beta}(\mathbf{r}')$ has, indeed, the same wave vector $\mathbf{k}$ as $\Psi_{\mathbf{k}}^{I\beta}(\mathbf{r})$. Furthermore, the Hamiltonian in the primed coordinate system becomes

$$H(\mathbf{r}') = T\,H(\mathbf{r})\,T^{-1}. \tag{55}$$

Thus

$$H(\mathbf{r}')\,\Psi_{\mathbf{k}}^{I'\beta}(\mathbf{r}') = T\,H(\mathbf{r})\,\Psi_{\mathbf{k}}^{I\beta}(\mathbf{r}) \tag{56a}$$

$$= E(\mathbf{k})\,\Psi_{\mathbf{k}}^{I'\beta}(\mathbf{r}'), \tag{56b}$$

so that the transformed function $\Psi_{\mathbf{k}}^{I'\beta}(\mathbf{r}')$ is an eigenfunction of $H(\mathbf{r}')$ with the same eigenvalue $E(\mathbf{k})$ as $\Psi_{\mathbf{k}}^{I\beta}(\mathbf{r})$.

Given the space group $\mathcal{G}$ of the crystal, the invariance of $H(\mathbf{r})$ under the symmetry operations $\mathcal{T} \equiv \{g|\mathbf{a}\} \in \mathcal{G}$ reads

$$\mathcal{T}\,H(\mathbf{r})\,\mathcal{T}^{-1} = H(\mathbf{r}) \quad \forall \mathcal{T} \in \mathcal{G}. \tag{57}$$

For the Hamiltonian $H(\mathbf{r}')$ in the primed coordinate system we get

$$\mathcal{T}\,H(\mathbf{r}')\,\mathcal{T}^{-1} = T\left(T^{-1}\,\mathcal{T}\,T\right)H(\mathbf{r})\left(T^{-1}\,\mathcal{T}\,T\right)^{-1}T^{-1}. \tag{58}$$

Hence the primed Hamiltonian $H(\mathbf{r}')$ obeys an invariance condition analogous to Eq. (57) if $(T^{-1}\,\mathcal{T}\,T)$ commutes with $H(\mathbf{r})$

$$[T^{-1}\,\mathcal{T}\,T, H(\mathbf{r})] = 0. \tag{59}$$

This requires in turn, given Eq. (57), that for all $\mathcal{T} \in \mathcal{G}$

$$T^{-1}\,\mathcal{T}\,T = \{\mathbb{1}|-\boldsymbol{\tau}\}\,\{g|\mathbf{a}\}\,\{\mathbb{1}|\boldsymbol{\tau}\} \tag{60a}$$
$$= \{g|g\,\boldsymbol{\tau} - \boldsymbol{\tau} + \mathbf{a}\} \tag{60b}$$

is an element of the space group $\mathcal{G}$, so that $g\,\boldsymbol{\tau} - \boldsymbol{\tau}$ must be equal to a lattice vector $\mathbf{a}'$ of the crystal

$$g\,\boldsymbol{\tau} - \boldsymbol{\tau} = \mathbf{a}' \quad \forall\, g \equiv \{g|0\} \in \mathcal{G}_0, \tag{61}$$

where $\mathcal{G}_0$ is the point group corresponding to the space group $\mathcal{G}$. A nontrivial solution to this problem is a vector $\boldsymbol{\tau}$ that is not equal to a lattice vector $\mathbf{a}$. Equation (61) defines the allowed shifts $\boldsymbol{\tau}$ (up to a lattice vector) that provide alternative descriptions of a crystal structure with space group $\mathcal{G}$.

We obtain nontrivial solutions to Eq. (61), for example, if a crystal consists of atoms at Wyckoff positions $W = A, B, \ldots$ each with multiplicity $m = 1$ [51]. We denote these positions in the unit cell as $\mathbf{t}_\mathrm{A}$, $\mathbf{t}_\mathrm{B}$, $\mathbf{t}_\mathrm{C}$, …, respectively. By definition of the space group $\mathcal{G}$, these positions $\mathbf{t}_W$ obey the condition

$$g\,\mathbf{t}_W - \mathbf{t}_W = \mathbf{a}' \qquad \forall\, g \in \mathcal{G}_0, \quad W = \mathrm{A}, \mathrm{B}, \mathrm{C}, \ldots \tag{62}$$

with lattice vectors $\mathbf{a}'$. Hence, any linear combination of these position vectors $\{\mathbf{t}_W\}$ with integer prefactors (e.g., $\boldsymbol{\tau} = \mathbf{t}_W - \mathbf{t}_{W'}$ with $W \neq W'$) yields a translation $\boldsymbol{\tau}$ consistent with Eq. (61).

In the unprimed coordinate system the eigenfunctions $\Psi_\mathbf{k}^{I\beta}(\mathbf{r})$ transform according to the βth component of an IR Γ_I of the point group $\mathcal{G}_\mathbf{k}$ of the wave vector $\mathbf{k}$

$$\{g|0\}\,\Psi_\mathbf{k}^{I\beta}(\mathbf{r}) = \sum_{\beta'} \mathcal{D}_I(g)_{\beta'\beta}\,\Psi_\mathbf{k}^{I\beta'}(\mathbf{r}) \tag{63}$$

with representation matrices $\mathcal{D}_I(g)_{\beta'\beta}$. We can evaluate the action of a symmetry operation $g \in \mathcal{G}_\mathbf{k}$ on primed Bloch functions $\Psi_\mathbf{k}^{I'\beta}(\mathbf{r}')$ as follows

$$\{g|0\}\,\Psi_\mathbf{k}^{I'\beta}(\mathbf{r}')$$
$$= \{g|0\}\,\{\mathbb{1}|\boldsymbol{\tau}\}\,\Psi_\mathbf{k}^{I\beta}(\mathbf{r}) \tag{64a}$$
$$= \{\mathbb{1}|\boldsymbol{\tau}\}\,\{\mathbb{1}|g\,\boldsymbol{\tau} - \boldsymbol{\tau}\}\,\{g|0\}\,\Psi_\mathbf{k}^{I\beta}(\mathbf{r}) \tag{64b}$$
$$= \sum_{\beta'} \mathcal{D}_I(g)_{\beta'\beta}\,\{\mathbb{1}|\boldsymbol{\tau}\}\,\{\mathbb{1}|g\,\boldsymbol{\tau} - \boldsymbol{\tau}\}\,\Psi_\mathbf{k}^{I\beta'}(\mathbf{r}) \tag{64c}$$
$$= \sum_{\beta'} \mathcal{D}_I(g)_{\beta'\beta}\,\exp[-i\mathbf{k}\cdot(g\,\boldsymbol{\tau} - \boldsymbol{\tau})]\,\{\mathbb{1}|\boldsymbol{\tau}\}\,\Psi_\mathbf{k}^{I\beta'}(\mathbf{r}) \tag{64d}$$
$$= \sum_{\beta'} \mathcal{D}_{I'}(g)_{\beta'\beta}\,\Psi_\mathbf{k}^{I'\beta'}(\mathbf{r}), \tag{64e}$$

where the primed representation matrices $\mathcal{D}_{I'}(g)_{\beta'\beta}$ become

$$\mathcal{D}_{I'}(g)_{\beta'\beta} = \mathcal{D}_I(g)_{\beta'\beta}\,\exp[-i\mathbf{k}\cdot(g\,\boldsymbol{\tau} - \boldsymbol{\tau})]. \tag{65}$$

We denote the phase factors in Eq. (65) by

$$\mathcal{D}_{\boldsymbol{\tau}}^{\mathbf{k}}(g) = \exp[-i\mathbf{k}\cdot(g\,\boldsymbol{\tau} - \boldsymbol{\tau})]. \tag{66}$$

Using Eq. (3), this becomes

$$\mathcal{D}_{\boldsymbol{\tau}}^{\mathbf{k}}(g) = \exp(-i\mathbf{b}_g\cdot\boldsymbol{\tau}) \tag{67a}$$

with a reciprocal lattice vector

$$\mathbf{b}_g = g^{-1}\mathbf{k} - \mathbf{k}. \tag{67b}$$

The phase $\mathcal{D}_{\boldsymbol{\tau}}^{\mathbf{k}}(g)$ is therefore nontrivial when $\mathbf{b}_g \neq 0$, which can only happen at the border of the Brillouin zone.

We show in the next paragraph that $\Gamma_{\boldsymbol{\tau}} \equiv \{\mathcal{D}_{\boldsymbol{\tau}}^{\mathbf{k}}(g) : g \in \mathcal{G}_\mathbf{k}\}$ defines a one-dimensional IR of $\mathcal{G}_\mathbf{k}$ (for every wave vector $\mathbf{k}$ in the Brillouin zone). Therefore, the IR $\Gamma_{I'}$ of a Bloch function in the primed coordinate system is given by $\Gamma_{\boldsymbol{\tau}}$ times the IR Γ_I of the Bloch function in the unprimed coordinate system, so that Eq. (65) becomes

$$\Gamma_{I'} = \Gamma_{\boldsymbol{\tau}} \times \Gamma_I. \tag{68}$$

The rearrangement lemma for IRs discussed in Appendix B applied to Eq. (68) shows that, unless we have the trivial case that $\Gamma_{\boldsymbol{\tau}}$ is the identity representation, each IR Γ_I of $\mathcal{G}_\mathbf{k}$ in the unprimed coordinate system is mapped on an IR $\Gamma_{I'} \neq \Gamma_I$ in the primed coordinate system. Hence we call Eq. (68) the rearrangement lemma for the IRs of Bloch states and $\Gamma_{\boldsymbol{\tau}}$ the *rearrangement representation* (RAR) for the coordinate shift $\boldsymbol{\tau}$. Examples for this rearrangement of IRs of Bloch states will be given below when we study the symmetries of the Bloch functions in monolayer MoS_2 (Sec. III B) and trilayer graphene (Sec. IV A 3). It follows from Eq. (67) that only at the border of the Brillouin zone the IR labeling of Bloch states can depend on the origin of the coordinate system [22]. Also, Eq. (67) implies $\Gamma_{-\boldsymbol{\tau}} = \Gamma_{\boldsymbol{\tau}}^*$. Generally, the shift $\boldsymbol{\tau}$ is defined up to a lattice vector $\mathbf{a}$. It follows immediately from Eq. (67) that $\boldsymbol{\tau}$ and $\tilde{\boldsymbol{\tau}} \equiv \boldsymbol{\tau} + \mathbf{a}$ define the same RAR $\Gamma_{\boldsymbol{\tau}}$.

To show that $\Gamma_{\boldsymbol{\tau}} = \{\mathcal{D}_{\boldsymbol{\tau}}^{\mathbf{k}}(g) : g \in \mathcal{G}_\mathbf{k}\}$ defines a one-dimensional IR of $\mathcal{G}_\mathbf{k}$ we consider two group elements $g_i \in \mathcal{G}_\mathbf{k}$ $(i = 1, 2)$. According to Eq. (61), the transformations $g_i\,\boldsymbol{\tau}$ differ from $\boldsymbol{\tau}$ by lattice vectors $\mathbf{a}_i$

$$g_i\,\boldsymbol{\tau} = \boldsymbol{\tau} + \mathbf{a}_i, \tag{69}$$

so that

$$\mathcal{D}_{\boldsymbol{\tau}}^{\mathbf{k}}(g_i) = \exp[-i\mathbf{k}\cdot(g_i\,\boldsymbol{\tau} - \boldsymbol{\tau})] = \exp(-i\mathbf{k}\cdot\mathbf{a}_i) \tag{70}$$

and

$$\mathcal{D}_{\boldsymbol{\tau}}^{\mathbf{k}}(g_1)\mathcal{D}_{\boldsymbol{\tau}}^{\mathbf{k}}(g_2) = \exp[-i\mathbf{k}\cdot(\mathbf{a}_1 + \mathbf{a}_2)]. \tag{71}$$

We can also write $g_1 g_2\,\boldsymbol{\tau}$ as

$$g_1 g_2\,\boldsymbol{\tau} = g_1\,\boldsymbol{\tau} + g_1\,\mathbf{a}_2 \tag{72a}$$
$$= \boldsymbol{\tau} + \mathbf{a}_1 + \mathbf{a}_2 + g_1\,\mathbf{a}_2 - \mathbf{a}_2. \tag{72b}$$

Hence

$$\mathcal{D}^{\mathbf{k}}_{\boldsymbol{\tau}}(g_1 g_2) = \exp[-i\mathbf{k}\cdot(g_1 g_2\,\boldsymbol{\tau} - \boldsymbol{\tau})] \tag{73a}$$
$$= \exp[-i\mathbf{k}\cdot(\mathbf{a}_1 + \mathbf{a}_2 + g_1\,\mathbf{a}_2 - \mathbf{a}_2)] \tag{73b}$$
$$= \mathcal{D}^{\mathbf{k}}_{\boldsymbol{\tau}}(g_1)\mathcal{D}^{\mathbf{k}}_{\boldsymbol{\tau}}(g_2)\exp[-i\mathbf{k}\cdot(g_1\,\mathbf{a}_2 - \mathbf{a}_2)]. \tag{73c}$$

We get similar to Eq. (2) and using Eq. (3)

$$\exp[-i\mathbf{k}\cdot(g_1\mathbf{a}_2 - \mathbf{a}_2)] = \exp[-i(g_1^{-1}\mathbf{k} - \mathbf{k})\cdot\mathbf{a}_2)] \tag{74a}$$
$$= \exp[-i\mathbf{b}_{g_1}\cdot\mathbf{a}_2] = 1. \tag{74b}$$

This gives us finally

$$\mathcal{D}^{\mathbf{k}}_{\boldsymbol{\tau}}(g_1 g_2) = \mathcal{D}^{\mathbf{k}}_{\boldsymbol{\tau}}(g_1)\mathcal{D}^{\mathbf{k}}_{\boldsymbol{\tau}}(g_2), \tag{75}$$

so that, indeed, $\Gamma_{\boldsymbol{\tau}} = \{\mathcal{D}^{\mathbf{k}}_{\boldsymbol{\tau}}(g) : g \in \mathcal{G}_{\mathbf{k}}\}$ is a one-dimensional IR of the group $\mathcal{G}_{\mathbf{k}}$.

The above argument [22] is based on the full Bloch functions $\Psi_{\mathbf{k}}(\mathbf{r})$. We showed in Eq. (16) that in a TB description, these Bloch functions can be factorized as $\Phi^{W\mu}_{\nu\mathbf{k}}(\mathbf{r}) = q_{\mathbf{k}}(\mathbf{R}^{W\mu}_j)\,\phi^W_\nu(\delta\mathbf{r})$, so that the symmetry of the plane waves $q_{\mathbf{k}}(\mathbf{R}^{W\mu}_j)$ can be discussed separately from the symmetry of the atomic orbitals $\phi^W_\nu(\delta\mathbf{r})$. The orbitals $\phi^W_\nu(\delta\mathbf{r})$ only depend on $\delta\mathbf{r}$ but not on the actual positions $\mathbf{R}^{W\mu}_j$. Hence it follows immediately that the symmetry of the orbitals $\phi^W_\nu(\delta\mathbf{r})$ is independent of the coordinate system used, see also Eq. (26). Only the representation $\Gamma^q_{\mathbf{k}W}$ of the plane waves $q_{\mathbf{k}}(\mathbf{R}^{W\mu}_j)$ depends, in general, on the coordinate system. A translation of the coordinate system by $\boldsymbol{\tau}$ maps the positions $\mathbf{R}^{W\mu}_j$ onto the atomic position $\mathbf{R}^{W'\mu}_j = \mathbf{R}^{W\mu}_j - \boldsymbol{\tau}$. The new coordinate system is valid if and only if $g\,\boldsymbol{\tau} - \boldsymbol{\tau}$ are lattice vectors for all $g \in \mathcal{G}_{\mathbf{k}}$ [see Eq. (61)], so that the plane waves transform as $\Gamma^q_{\mathbf{k}W'}$. We have

$$\mathbf{R}^{W'\mu'}_{j'} \equiv g\,\mathbf{R}^{W'\mu}_j = g\,(\mathbf{R}^{W\mu}_j - \boldsymbol{\tau}) \tag{76a}$$
$$= g\,\mathbf{R}^{W\mu}_j - g\,\boldsymbol{\tau} \tag{76b}$$
$$= \mathbf{R}^{W\mu'}_{j'} - g\,\boldsymbol{\tau}, \tag{76c}$$

so that for the transformed Wyckoff letter W', Eq. (33) becomes

$$\mathcal{D}^{W'}_{\mathbf{k}}(g)_{\mu'\mu} = \exp[i\mathbf{k}\cdot(\mathbf{R}^{W'\mu'}_{j'} - \mathbf{R}^{W'\mu'}_j)] \tag{77a}$$
$$= \exp[i\mathbf{k}\cdot(\mathbf{R}^{W\mu'}_{j'} - g\,\boldsymbol{\tau} - \mathbf{R}^{W\mu}_j + \boldsymbol{\tau})] \tag{77b}$$
$$= \exp[i\mathbf{k}\cdot(\mathbf{R}^{W\mu'}_{j'} - \mathbf{R}^{W\mu}_j)]\exp[-i\mathbf{k}\cdot(g\,\boldsymbol{\tau} - \boldsymbol{\tau})] \tag{77c}$$
$$= \mathcal{D}^q_{\mathbf{k}W}(g)_{\mu'\mu}\,\mathcal{D}^{\mathbf{k}}_{\boldsymbol{\tau}}(g) \tag{77d}$$

with $\mathcal{D}^{\mathbf{k}}_{\boldsymbol{\tau}}(g)$ given by Eq. (66). This gives us the rearrangement lemma for the representations of plane waves

$$\Gamma^q_{\mathbf{k}W'} = \Gamma_{\boldsymbol{\tau}} \times \Gamma^q_{\mathbf{k}W}. \tag{78}$$

Hence we confirm that the nontrivial case $\Gamma^q_{\mathbf{k}W'} \neq \Gamma^q_{\mathbf{k}W}$ requires that $\Gamma_{\boldsymbol{\tau}} = \{\mathcal{D}^{\mathbf{k}}_{\boldsymbol{\tau}}(g) : g \in \mathcal{G}_{\mathbf{k}}\}$ is not the identity representation. As mentioned above, the symmetry of plane waves $q_{\mathbf{k}}(\mathbf{R}^{W\mu}_j)$ is a universal problem for each space group $\mathcal{G}$, independent of the detailed realization of a crystal structure. This holds, in particular, if the atoms are located at positions $\mathbf{R}^{I\mathbf{k}}_{W\mu j}$ where the $q^{I\beta}_{\mathbf{k}}(\mathbf{R}^{I\mathbf{k}}_{W\mu j})$ transforms according to only one IR Γ_I. Hence it is possible to discuss the rearrangement lemma for the IRs of Bloch states independent of a particular crystal structure, but it depends only on the space group $\mathcal{G}$. Among all 230 space groups, 159 contain Wyckoff sites with origin-dependent site symmetries [52]. Though a necessary criterion, it is however not a sufficient criterion for a rearrangement of the IRs of Bloch states under a change of the coordinate system [22].

H. Effect of time reversal

In the absence of an external magnetic field, the eigenfunctions of the TB Hamiltonian obey time-reversal symmetry Θ. This implies that if an eigenfunction $\Psi^{I\beta}_{\mathbf{k}}(\mathbf{r})$ with energy $E(\mathbf{k})$ transforms according to the βth component of the IR Γ_I of $\mathcal{G}_{\mathbf{k}}$, the time-reversed wave function $\Theta\,\Psi^{I\beta}_{\mathbf{k}}(\mathbf{r}) = \Psi^{I\beta}_{\mathbf{k}}(\mathbf{r})^* = \Psi^{\tilde{I},\beta'}_{-\mathbf{k}}(\mathbf{r})$ [which is likewise an eigenfunction of the Hamiltonian with energy $E(-\mathbf{k}) = E(\mathbf{k})$] transforms according to the β'th component of the complex conjugate IR Γ^*_I of $\mathcal{G}_{-\mathbf{k}} = \mathcal{G}_{\mathbf{k}}$. Therefore, if the eigenfunctions of the TB Hamiltonian for some energy $E(\mathbf{k})$ contain atomic orbitals transforming according to an IR Γ^ϕ_J of $\mathcal{G}_{\mathbf{k}}$ and symmetry-adapted plane waves transforming according to $\Gamma^q_{J'}$, the eigenfunctions for wave vector $-\mathbf{k}$ with energy $E(-\mathbf{k}) = E(\mathbf{k})$ contain atomic orbitals transforming according to the complex conjugate IR $\Gamma^{\phi*}_J$ and plane waves transforming according to $\Gamma^{q*}_{J'}$. Here, the symmetry-adapted atomic orbitals at $-\mathbf{k}$ are the complex conjugates of the corresponding atomic orbitals at $\mathbf{k}$. We obtain the symmetry-adapted plane waves at $-\mathbf{k}$ from the corresponding plane waves at $\mathbf{k}$ by replacing $\mathbf{k} \to -\mathbf{k}$.

Degeneracies of Bloch states due to time-reversal symmetry are discussed in Refs. [3, 38, 53]. In general, three cases must be distinguished [54]. In case (a), eigenfunctions Ψ and $\Theta\,\Psi$ of the crystal Hamiltonian $H(\mathbf{r})$ are linearly dependent. In case (b), eigenfunctions Ψ and $\Theta\,\Psi$ of $H(\mathbf{r})$ are linearly independent and transform according to inequivalent representations Γ_I and Γ^*_I, i.e., $\chi_I(g) \neq \chi^*_I(g)$ for some $g \in \mathcal{G}_{\mathbf{k}}$. Finally, in case (c), eigenfunctions Ψ and $\Theta\,\Psi$ of $H(\mathbf{r})$ are linearly independent and transform according to equivalent representations Γ_I and Γ^*_I, i.e., $\chi_I(g) = \chi^*_I(g)$ for all $g \in \mathcal{G}_{\mathbf{k}}$. In cases (b) and (c) invariance under time reversal causes

additional degeneracy. We have for symmorphic space groups [3, 38, 53]

$$\frac{f}{h}\sum_{g\in\mathcal{G}_0}\chi_I(g^2)\,\delta_{g\mathbf{k}+\mathbf{k},\mathbf{b}} = \begin{cases} \Theta^2 & \text{case (a)} \\ 0 & \text{case (b)} \\ -\Theta^2 & \text{case (c)} \end{cases}, \qquad (79)$$

where f is the number of points of the star of $\mathbf{k}$, h is the order of the crystallographic point group $\mathcal{G}_0$ of the crystal, $\chi_I(g)$ are the characters of the IR Γ_I of the point group $\mathcal{G}_\mathbf{k}$ of the wave vector $\mathbf{k}$, and $g\mathbf{k}+\mathbf{k}$ may be zero or a reciprocal lattice vector $\mathbf{b}$. We have $\Theta^2 = +1$ for single-group representations and $\Theta^2 = -1$ for double-group representations. The criterion (79) applies to the IRs Γ_I of $\mathcal{G}_\mathbf{k}$ independent of the origin of the coordinate system. If a crystal structure permits a change of the coordinate system characterized by a vector $\boldsymbol{\tau}$ with RAR $\Gamma_{\boldsymbol{\tau}}$, a Bloch function transforming according to the IR Γ_I of $\mathcal{G}_\mathbf{k}$ in the old coordinate system transforms according to $\Gamma_{I'} = \Gamma_{\boldsymbol{\tau}} \times \Gamma_I$ in the new coordinate, see Eq. (68). Therefore, the IRs Γ_I and $\Gamma_{I'}$ of $\mathcal{G}_\mathbf{k}$ must fall into the same category according to Eq. (79).

In a more detailed analysis [3, 38, 55], for each of the cases (a), (b), and (c) three possibilities must be distinguished: (1) the points $\mathbf{k}$ and $-\mathbf{k}$ are equivalent, i.e., $\mathbf{k} = -\mathbf{k}+\mathbf{b}$; (2) $\mathbf{k}$ is not equivalent to $-\mathbf{k}$, but the space group contains an element R which maps $\mathbf{k}$ onto $-\mathbf{k}$

$$R\mathbf{k} = -\mathbf{k}; \qquad (80)$$

(3) the points $\mathbf{k}$ and $-\mathbf{k}$ are in different stars. For the systems discussed below, case (1) applies to the $\mathbf{\Gamma}$ and $\mathbf{M}$ points of the BZ, whereas case (2) applies to the $\mathbf{K}$ points.

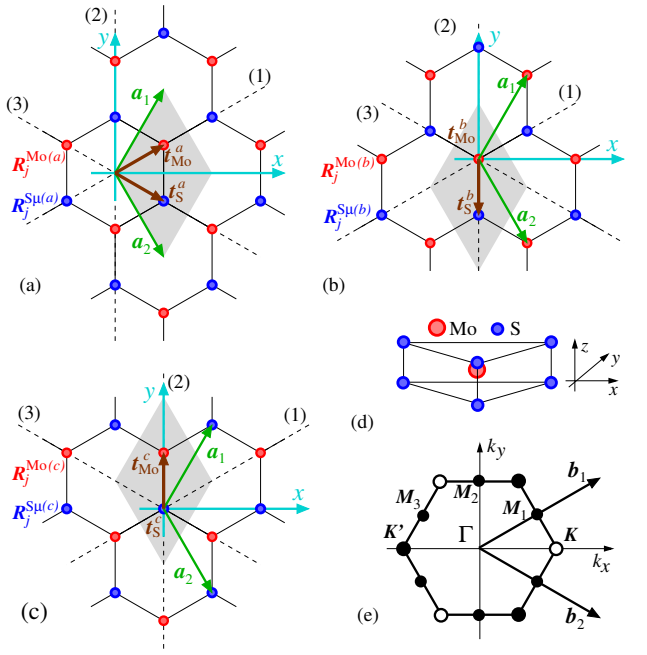

FIG. 1. Crystal structure of single-layer MoS_2. Three coordinate systems $\alpha = a, b, c$ are considered with (a) the origin located at the center of a hexagon, (b) origin at an Mo atom, and (c) origin at the midpoint between top and bottom S atoms. The atomic positions of Mo and S in unit cell j are denoted by $\mathbf{R}_j^{\mathrm{Mo}(\alpha)}$ and $\mathbf{R}_j^{\mathrm{S}\mu(\alpha)}$, respectively. For the S atom, the top (bottom) atoms are labeled $\mu = 1$ ($\mu = 2$). The primitive lattice vectors are denoted $\mathbf{a}_1$ and $\mathbf{a}_2$. The shaded region shows a unit cell ($j = 1$). The vectors $\mathbf{t}^\alpha_{\mathrm{Mo}}$ and $\mathbf{t}^\alpha_{\mathrm{S}}$ give the positions of the Mo and S atoms within a unit cell. The dashed axes (1), (2) and (3) are the two-fold rotation axes of the point group D_{3h}. (d) Three-dimensional illustration of single-layer MoS_2. (e) The first Brillouin zone.

III. BAND SYMMETRIES IN MoS_2

Having derived a systematic theory for the symmetry of TB Bloch functions, we now apply this theory to several quasi-2D materials. Our main focus is on monolayer MoS_2. For comparison, we also discuss single-layer (SLG), bilayer (BLG), and trilayer (TLG) graphene in the next section.

A. Crystal structure of MoS_2

The crystal structure of single-layer MoS_2 is shown in Fig. 1. It is characterized by the point group D_{3h} and space group $P\bar{6}m2$ (# 187). Three Wyckoff positions have multiplicity $m = 1$, the positions of the Mo atom, the midpoint between a pair of top and bottom S atoms, and the center of the hexagon. Hence, as discussed in Sec. II G, three choices $\alpha = a, b, c$ emerge for the origin of the coordinate system: (a) origin at the center of the hexagon [Fig. 1(a)], (b) origin at a Mo atom [Fig. 1(b)], and (c) origin at the midpoint between a top and bottom S atom [Fig. 1(c)]. In either case, the Mo atoms have site symmetry D_{3h} and Wyckoff multiplicity $m = 1$. Yet the Wyckoff letters for these positions listed in Table I depend on the coordinate system [52]. For coordinate system (a), the Mo and S atoms have Wyckoff letters e and h respectively, whereas these letters become a and i in coordinate system (b), and c and g in coordinate system (c). The S atoms have site symmetry C_{3v} and multiplicity $m = 2$. The positions of Mo and S atoms in unit cell j are denoted by $\mathbf{R}_j^{\mathrm{Mo}(\alpha)}$ and $\mathbf{R}_j^{\mathrm{S}\mu(\alpha)}$ respectively. For the S atom, the top (bottom) atoms are labeled $\mu = 1$ ($\mu = 2$). There are yet other coordinate systems that can be used for MoS_2. For example, Ref. [31] used a coordinate system that differs from coordinate system (a) by a reflection about the xz plane. Here, we do not consider these additional coordinate systems [23].

The Brillouin zone for single-layer MoS_2 is shown in Fig. 1(e). In the following, we will focus on the $\mathbf{\Gamma}$ point $\mathbf{k} = 0$, the $\mathbf{K}$, and the $\mathbf{M}$ points. The star of the $\mathbf{K}$ point includes two inequivalent wave vectors denoted $\mathbf{K}$ and $\mathbf{K}'$. The star of the $\mathbf{M}$ point includes three inequivalent wave vectors denoted $\mathbf{M}_1$, $\mathbf{M}_2$, and $\mathbf{M}_3$.

TABLE I. Site symmetries in monolayer MoS_2 and single-layer (SLG), bilayer (BLG) and tri-layer (TLG) graphene. We include here the Wyckoff positions occupied by atoms as well as the unoccupied center of the hexagon denoted by $\mathbf{R}_j^{\rm center}$. The coordinate systems $\alpha = a, b, c$ for MoS_2 and TLG are depicted in Figs. 1 and 7, respectively.

	(α)			
MoS_2		($P\bar{6}m2$, # 187, D_{3h})		
positions $\mathbf{R}_j^{W\mu(\alpha)}$		$\mathbf{R}_j^{\rm Mo(\alpha)}$	$\{\mathbf{R}_j^{\rm S1(\alpha)}, \mathbf{R}_j^{\rm S2(\alpha)}\}$	$\mathbf{R}_j^{\rm center(\alpha)}$
site symmetry		$\bar{6}m2$ (D_{3h})	$3m$ (C_{3v})	$\bar{6}m2$ (D_{3h})
multiplicity		1	2	1
Wyckoff letter	(a)	e	h	a
	(b)	a	i	c
	(c)	c	g	e
SLG		($P6/mmm$, # 191, D_{6h})		
positions $\mathbf{R}_j^{W\mu}$		$\{\mathbf{R}_j^{c1}, \mathbf{R}_j^{c2}\}$	$\mathbf{R}_j^{\rm center}$	
site symmetry		$\bar{6}m2$ (D_{3h})	$6/mmm$ (D_{6h})	
multiplicity		2	1	
Wyckoff letter		c	a	
BLG		($P\bar{3}m1$, # 164, D_{3d})		
positions $\mathbf{R}_j^{W\mu}$		$\{\mathbf{R}_j^{c1}, \mathbf{R}_j^{c2}\}$	$\{\mathbf{R}_j^{d1}, \mathbf{R}_j^{d2}\}$	
site symmetry		$3m$ (C_{3v})	$3m$ (C_{3v})	
multiplicity		2	2	
Wyckoff letter		c	d	
	(α)			
TLG		($P\bar{6}m2$, # 187, D_{3h})		
positions $\mathbf{R}_j^{W\mu(\alpha)}$		$\mathbf{R}_j^{A}$	$\mathbf{R}_j^{B}$	$\{\mathbf{R}_j^{A'1}, \mathbf{R}_j^{A'2}\}$	$\{\mathbf{R}_j^{B'1}, \mathbf{R}_j^{B'2}\}$
site symmetry		$\bar{6}m2$ (D_{3h})	$\bar{6}m2$ (D_{3h})	$3m$ (C_{3v})	$3m$ (C_{3v})
multiplicity		1	1	2	2
Wyckoff letter	(a)	c	e	g	h
	(b)	e	a	h	i
	(c)	a	c	i	g

The point group of single-layer MoS_2 is D_{3h}. This is also the point group of the wave vector at the $\mathbf{\Gamma}$ point. It contains a 120° counter-clockwise rotation C_3 about the z axis. The reflection plane of σ_h is the xy-plane and $S_3 = \sigma_h C_3$. The rotation axes of the three two-fold rotations $C_2^{\prime(i)}$ are the axes $i = 1, 2, 3$ shown in Fig. 1. These axes are also shown as dashed lines in Fig. 2(a). The reflection plane of $\sigma_v^{(i)}$ is the plane passing through the axis i and the z axis. The characters of D_{3h} are listed in Table XXV (Appendix C). We label the IRs of the crystallographic point groups following Koster *et al.* [56].

At the $\mathbf{K}$ point [Fig. 2(b)], the point group of the wave vector becomes $\mathcal{G}_{\mathbf{K}} = C_{3h}$ whose characters are listed in Table XXVII (Appendix C). Finally, at the inequivalent points $\mathbf{M}_i$ ($i = 1, 2, 3$), the group of the wave vector is $\mathcal{G}_{\mathbf{M}} = C_{2v}$, the character table of which is reproduced in Table XXVIII (Appendix C). This group contains the two-fold rotation C_2, the axis of which is indicated as dashed line in Figs. 2(c)-(e), the reflection σ_v about the xy plane, and the reflection σ_v' for which the reflection plane includes the dashed line and the z axis.

The primitive lattice vectors $\mathbf{a}_1$ and $\mathbf{a}_2$ are

$$\mathbf{a}_1 = \frac{a}{2}\begin{pmatrix} 1 \\ \sqrt{3} \end{pmatrix}, \quad \mathbf{a}_2 = \frac{a}{2}\begin{pmatrix} 1 \\ -\sqrt{3} \end{pmatrix}, \tag{81}$$

where a is the lattice constant. Ignoring for brevity the z component, the positions $\mathbf{t}_{\rm Mo}^{\alpha}$ of Mo and $\mathbf{t}_{\rm S}^{\alpha}$ of S in the unit cell are

$$\mathbf{t}_{\rm Mo}^{a} = \frac{a}{2}\begin{pmatrix} 1 \\ \frac{1}{\sqrt{3}} \end{pmatrix}, \qquad \mathbf{t}_{\rm S}^{a} = \frac{a}{2}\begin{pmatrix} 1 \\ -\frac{1}{\sqrt{3}} \end{pmatrix}, \tag{82a}$$

$$\mathbf{t}_{\rm Mo}^{b} = \frac{a}{2}\begin{pmatrix} 0 \\ 0 \end{pmatrix}, \qquad \mathbf{t}_{\rm S}^{b} = \frac{a}{2}\begin{pmatrix} 0 \\ -\frac{2}{\sqrt{3}} \end{pmatrix}, \tag{82b}$$

$$\mathbf{t}_{\rm Mo}^{c} = \frac{a}{2}\begin{pmatrix} 0 \\ \frac{2}{\sqrt{3}} \end{pmatrix}, \qquad \mathbf{t}_{\rm S}^{c} = \frac{a}{2}\begin{pmatrix} 0 \\ 0 \end{pmatrix}, \tag{82c}$$

where the superscript $\alpha = a, b, c$ denotes the coordinate system. The primitive vectors $\mathbf{b}_1$ and $\mathbf{b}_2$ of the reciprocal lattice are

$$\mathbf{b}_1 = \frac{2\pi}{a}\begin{pmatrix} 1 \\ 1/\sqrt{3} \end{pmatrix}, \quad \mathbf{b}_2 = \frac{2\pi}{a}\begin{pmatrix} 1 \\ -1/\sqrt{3} \end{pmatrix}. \tag{83}$$

The two inequivalent corner points of the Brillouin zone

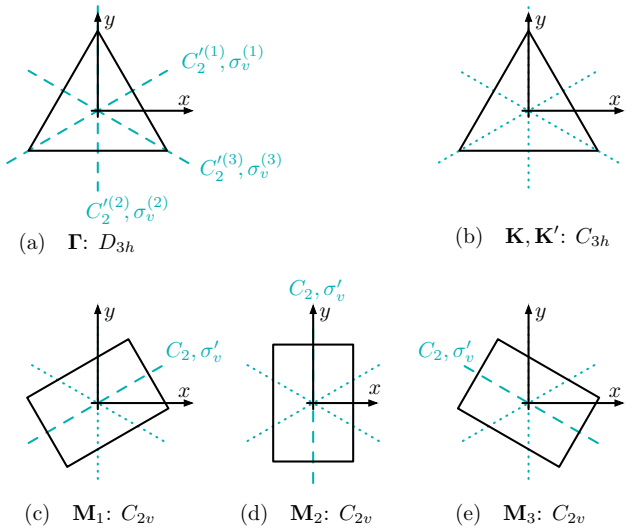

(a) $\mathbf{\Gamma}$: D_{3h} (b) $\mathbf{K}, \mathbf{K}'$: C_{3h}

(c) $\mathbf{M}_1$: C_{2v} (d) $\mathbf{M}_2$: C_{2v} (e) $\mathbf{M}_3$: C_{2v}

FIG. 2. Groups of the wave vector in monolayer MoS_2 and TLG. (a) The point $\mathbf{\Gamma}$ has the point group D_{3h} with the z axis (out of plane) as the three-fold rotation axis. The dashed lines (i) are the axes for two-fold rotations $C_2'^{(i)}$ with $i = 1, 2, 3$. The reflection $\sigma_v^{(i)}$ is about a plane that includes the dashed axis i and the z axis. (b) The points $\mathbf{K}$ and $\mathbf{K}'$ have the point group C_{3h} with three-fold rotations about the z axis. The reflection plane of σ_h is the xy-plane. The dotted lines indicate the two-fold rotation axes that appear in the point group D_{3h} but are not symmetry elements of C_{3h}. (c)-(e) The points $\mathbf{M}_1$, $\mathbf{M}_2$, and $\mathbf{M}_1$ have the point group C_{2v}. The dashed line is the axis of the two-fold rotation C_2. The reflection plane of σ_v is the xy-plane. The reflection plane of σ_v' contains the dashed line and the z axis.

are

$$\mathbf{K} = \frac{2\pi}{a}\begin{pmatrix} 2/3 \\ 0 \end{pmatrix}, \quad \mathbf{K}' = \frac{2\pi}{a}\begin{pmatrix} -2/3 \\ 0 \end{pmatrix}, \tag{84}$$

and the $\mathbf{M}$ points are

$$\mathbf{M}_1 = \frac{\pi}{a}\begin{pmatrix} 1 \\ 1/\sqrt{3} \end{pmatrix}, \quad \mathbf{M}_2 = \frac{2\pi}{a}\begin{pmatrix} 0 \\ 1/\sqrt{3} \end{pmatrix}, \quad \mathbf{M}_3 = \frac{\pi}{a}\begin{pmatrix} -1 \\ 1/\sqrt{3} \end{pmatrix}, \tag{85}$$

see Fig. 1(e).

B. Rearrangement of IRs of Bloch states in MoS_2

The crystal structure of monolayer MoS_2 can be described by three different coordinate systems $\alpha = a, b, c$ shown in Fig. 1. This provides an example for the rearrangement of the IRs of Bloch states discussed in general terms in Sec. II G. The coordinate systems α and β are related via a translation $\boldsymbol{\tau}_{\alpha\beta}$. For the shifts $a \to b$, $b \to c$, and $c \to a$, the translation vectors (apart from a lattice vector) are given by

$$\boldsymbol{\tau}_{ab} = \boldsymbol{\tau}_{bc} = \boldsymbol{\tau}_{ca} = \frac{a}{2}\begin{pmatrix} 1 \\ 1/\sqrt{3} \end{pmatrix} \tag{86}$$

and $\boldsymbol{\tau}_{\beta\alpha} = -\boldsymbol{\tau}_{\alpha\beta}$.

TABLE II. Rearrangement of the IRs of C_{3h} at the $\mathbf{K}$ point of monolayer MoS_2 when we go from one of the three coordinate systems $\alpha = a, b, c$ to a different coordinate system β (see Fig. 1).

a	Γ_1	Γ_2	Γ_3	Γ_4	Γ_5	Γ_6
b	Γ_3	Γ_1	Γ_2	Γ_6	Γ_4	Γ_5
c	Γ_2	Γ_3	Γ_1	Γ_5	Γ_6	Γ_4

For wave vectors $\mathbf{k}$ inside the BZ such as the $\mathbf{\Gamma}$ point as well as for the $\mathbf{M}$ points, the RARs $\Gamma^{\mathbf{\Gamma}}_{\alpha\beta}$ and $\Gamma^{\mathbf{M}}_{\alpha\beta}$ are given by Eq. (67) with $\mathbf{b}_g = 0$ for all $g \in \mathcal{G}_{\mathbf{k}}$. These RARs are, therefore, given by the identity representation Γ_1, i.e., at both the $\mathbf{\Gamma}$ and $\mathbf{M}$ points the labeling of Bloch states is independent of the coordinate system. However, a shift of the coordinate system rearranges the IRs at the $\mathbf{K}$ point. Using Eq. (67b) at the $\mathbf{K}$ point, where the group of the wave vector is C_{3h}, we get

$$\mathbf{b}_E = \mathbf{b}_{\sigma_h} = 0, \tag{87a}$$

$$\mathbf{b}_{C_3} = \mathbf{b}_{S_3} = -\mathbf{b}_1 = -\frac{2\pi}{a}\begin{pmatrix} 1 \\ 1/\sqrt{3} \end{pmatrix}, \tag{87b}$$

$$\mathbf{b}_{C_3^{-1}} = \mathbf{b}_{S_3^{-1}} = -\mathbf{b}_2 = -\frac{2\pi}{a}\begin{pmatrix} 1 \\ -1/\sqrt{3} \end{pmatrix}. \tag{87c}$$

For the shifts $a \to b$, $b \to c$, and $c \to a$, we thus have using Eq. (67)

$$\mathscr{D}^{\mathbf{K}}_{\alpha\beta}(E) = \mathscr{D}^{\mathbf{K}}_{\alpha\beta}(\sigma_h) = \exp(-i\mathbf{b}_E \cdot \boldsymbol{\tau}_{\alpha\beta}) = 1, \tag{88a}$$

$$\mathscr{D}^{\mathbf{K}}_{\alpha\beta}(C_3) = \mathscr{D}^{\mathbf{K}}_{\alpha\beta}(S_3) = \exp(-i\mathbf{b}_{C_3} \cdot \boldsymbol{\tau}_{\alpha\beta}) = \omega^{-4}, \tag{88b}$$

$$\mathscr{D}^{\mathbf{K}}_{\alpha\beta}(C_3^{-1}) = \mathscr{D}^{\mathbf{K}}_{\alpha\beta}(S_3^{-1}) = \exp(-i\mathbf{b}_{C_3^{-1}} \cdot \boldsymbol{\tau}_{\alpha\beta}) = \omega^{4} \tag{88c}$$

with $\omega \equiv \exp(i\pi/6)$. This implies $\Gamma^{\mathbf{K}}_{ab} = \Gamma^{\mathbf{K}}_{bc} = \Gamma^{\mathbf{K}}_{ca} = \Gamma_3$. Since $\boldsymbol{\tau}_{\beta\alpha} = -\boldsymbol{\tau}_{\alpha\beta}$, we have $\Gamma^{\mathbf{K}}_{ba} = \Gamma^{\mathbf{K}}_{cb} = \Gamma^{\mathbf{K}}_{ac} = \Gamma_3^* = \Gamma_2$. Hence, at the $\mathbf{K}$ point, for a Bloch state transforming in one coordinate system according to a certain IR, we can multiply this IR with either Γ_2 or Γ_3 to obtain the IR of the same Bloch state in a different coordinate system. The multiplication table for the IRs of C_{3h} is reproduced in Table XXX (Appendix C). Table II shows how the IRs of C_{3h} are rearranged when we go from one of the three coordinate systems $\alpha = a, b, c$ to a different coordinate system β. At the $\mathbf{K}'$ point, Eq. (66) gives

$$\Gamma^{\mathbf{K}'}_{\alpha\beta} = \Gamma^{-\mathbf{K}}_{\alpha\beta} = \Gamma^{\mathbf{K}*}_{\alpha\beta}. \tag{89}$$

TABLE III. Mapping of polar vectors $\mathbf{P}$ and axial vectors $\mathbf{A}$ under $g = C_3$, C_3^{-1}, $\sigma_v^{(i)}$, and σ_h, where the images are expressed in terms of the original components of these vectors. C_3 is a 120° counter-clockwise rotation about the z axis while $\sigma_v^{(i)}$ is a reflection about the plane containing the z axis and the axis i defined in Fig. 2. We have $\omega \equiv \exp(i\pi/6)$. Note $S_3^{\pm 1} = \sigma_h \times C_3^{\pm 1}$ and $C_2'^{(i)} = \sigma_h \times \sigma_v^{(i)}$.

	$C_3^{\pm 1}$	$\sigma_v^{(1)}/\sigma_v^{(3)}$	$\sigma_v^{(2)}$	σ_h
P_x	$-\frac{1}{2}P_x \mp \frac{\sqrt{3}}{2}P_y$	$\frac{1}{2}P_x \pm \frac{\sqrt{3}}{2}P_y$	$-P_x$	P_x
P_y	$\pm\frac{\sqrt{3}}{2}P_x - \frac{1}{2}P_y$	$\pm\frac{\sqrt{3}}{2}P_x - \frac{1}{2}P_y$	P_y	P_y
P_z	P_z	P_z	P_z	$-P_z$
P_+	$\omega^{\pm 4}P_+$	$-\omega^{\mp 4}P_-$	$-P_-$	P_+
P_-	$\omega^{\mp 4}P_-$	$-\omega^{\pm 4}P_+$	$-P_+$	P_-
A_x	$-\frac{1}{2}A_x \mp \frac{\sqrt{3}}{2}A_y$	$-\frac{1}{2}A_x \mp \frac{\sqrt{3}}{2}A_y$	A_x	$-A_x$
A_y	$\pm\frac{\sqrt{3}}{2}A_x - \frac{1}{2}A_y$	$\mp\frac{\sqrt{3}}{2}A_x + \frac{1}{2}A_y$	$-A_y$	$-A_y$
A_z	A_z	$-A_z$	$-A_z$	A_z
A_+	$\omega^{\pm 4}A_+$	$\omega^{\mp 4}A_-$	A_-	$-A_+$
A_-	$\omega^{\mp 4}A_-$	$\omega^{\pm 4}A_+$	A_+	$-A_-$

C. Atomic orbitals $\phi_\nu^W(\delta\mathbf{r})$ at $\mathbf{k} = \mathbf{\Gamma}$, K, and M

The conduction and valence bands in MoS_2 are dominated by Mo d and S p orbitals [24]. At the points $\mathbf{\Gamma}$, $\mathbf{K}$, and $\mathbf{M}$, the groups of the wave vectors $\mathcal{G}_\mathbf{k}$ are D_{3h}, C_{3h}, and C_{2v}, respectively, with character tables reproduced in Tables XXV, XXVII, and XXVIII. We use Eq. (A1) to project these functions onto functions transforming according to the IRs of the various groups $\mathcal{G}_\mathbf{k}$. The relevant symmetry operations are defined in Fig. 2 and Table III considering both polar vectors $\mathbf{P}$ such as position $\mathbf{r}$ and axial vectors $\mathbf{A}$. The two inequivalent points $\mathbf{K}$ and $\mathbf{K}'$ are related by a vertical reflection that transforms the component x into $-x$ while keeping the y and z components fixed. Table IV summarizes the IRs of the p and d orbitals. We note that these results are fully consistent with the full rotation group compatibility tables in Ref. [56].

D. Transformation of plane waves $q_\mathbf{k}(\mathbf{R}_j^{\mathrm{Mo}(\alpha)})$

We now determine the IRs of the plane waves $q_\mathbf{k}(\mathbf{R}_j^{\mathrm{Mo}(\alpha)})$ for the coordinate systems $\alpha = a, b, c$ at the $\mathbf{\Gamma}$, $\mathbf{K}$, and $\mathbf{M}$ points of the Brillouin zone. Since the Wyckoff letter corresponding to the positions of the Mo atoms has multiplicity $m = 1$, we can use either Eq. (42) or Eq. (44) to determine the phase $\mathcal{D}_\mathbf{k}^{\mathrm{Mo}(\alpha)}(g)$ acquired by the plane waves $q_\mathbf{k}(\mathbf{R}_j^{\mathrm{Mo}(\alpha)})$ under a transformation g. We can then derive the IRs of the plane waves using the projection operators (A1). The results are summarized in Table VII.

E. Transformation of plane waves $q_\mathbf{k}(\mathbf{R}_j^{\mathrm{S}\mu(\alpha)})$

The S atoms are located at Wyckoff positions with multiplicity $m = 2$, so that we represent the plane wave at the positions $\mathbf{R}_j^{\mathrm{S}\mu(\alpha)}$ as a two-component spinor

$$Q_\mathbf{k}(\mathfrak{R}_j^{S(\alpha)}) = q_\mathbf{k}(\mathbf{R}_j^{S1(\alpha)}) + q_\mathbf{k}(\mathbf{R}_j^{S2(\alpha)}) \equiv \begin{pmatrix} 1 \\ 1 \end{pmatrix}. \quad (90)$$

We can then use Eq. (33) to determine the phases acquired under symmetry transformations. To obtain the plane wave IRs, it is again advantageous to consider the simplest coordinate system. For the S atoms, this is coordinate system (c) where the origin of the coordinate system is at the midpoint between the S atoms in the top and bottom layer of a unit cell. In this case, the transformation g maps $\mathbf{R}_1^{\mathrm{S}\mu(c)}$ either onto itself or onto $\mathbf{R}_1^{\mathrm{S}\mu'(c)}$ with $\mu \neq \mu'$, so that Eq. (33) becomes

$$\mathcal{D}_\mathbf{k}^{\mathrm{S}(c)}(g)_{\mu'\mu} = \exp[i\mathbf{k}\cdot(\mathbf{R}_1^{\mathrm{S}\mu'(c)} - \mathbf{R}_1^{\mathrm{S}\mu'(c)})] = 1 \quad (91)$$

for all $g \in \mathcal{G}_\mathbf{k}$. We can then determine the IRs of the plane waves for the coordinate systems (a) and (b) by using the respective RAR derived in Sec. III B. The results are summarized in Table VII.

F. IRs of Bloch states in MoS_2

The full symmetry-adapted Bloch functions are written as products of symmetrized plane waves and symmetrized atomic orbitals. The five symmetry-adapted d orbitals of the Mo atom times the plane wave $q_\mathbf{k}(\mathbf{R}_j^{\mathrm{Mo}(\alpha)})$ and the three symmetry-adapted p orbitals of the S atoms times the plane waves $q_\mathbf{k}(\mathbf{R}_j^{\mathrm{S}1(\alpha)}) \pm q_\mathbf{k}(\mathbf{R}_j^{\mathrm{S}2(\alpha)})$ therefore comprises eleven symmetry-adapted basis functions for MoS_2 [30]. The corresponding IRs are listed in Table VIII for the $\mathbf{\Gamma}$, $\mathbf{K}$, and $\mathbf{M}$ points. We list in Tables IX, X, and XI the sets of Bloch states transforming according to an IR of $\mathcal{G}_\mathbf{k}$ for the wave vectors $\mathbf{k} = \mathbf{\Gamma}, \mathbf{K}, \mathbf{M}$. Using these symmetrized Bloch functions, the TB Hamiltonian for a wave vector $\mathbf{k}$ can be written in a block-diagonal form, where each block refers to the basis functions transforming according to an IR Γ_I of $\mathcal{G}_\mathbf{k}$ [57]. To classify the additional degeneracy of the Bloch states due to time-reversal symmetry, we evaluate Eq. (79). All IRs of the space group for the stars $\{\mathbf{\Gamma}\}$, $\{\mathbf{K}\}$, and $\{\mathbf{M}\}$ belong to case (a).

TABLE IV. Symmetry-adapted p and d atomic orbitals for the point groups D_{3h}, C_{3h} and C_{2v} with coordinate systems defined in Fig. 2 (MoS_2 and TLG). For C_{2v}, the symmetrized atomic orbital $\phi_\nu^{[i]}$ corresponds to the coordinate systems used for the point $\mathbf{M}_i$ in Figs. 2(c)-(e). The orbital $[i(j)]$ takes the upper (lower) sign. The IRs of the atomic orbitals listed here are consistent with the compatibility relations in Table VI.

D_{3h}		C_{3h}		C_{2v}		
ϕ_ν	IR	ϕ_ν	IR	$\phi_\nu^{[1(3)]}$	$\phi_\nu^{[2]}$	IR
p_z	Γ_4	p_z	Γ_4	p_z	p_z	Γ_4
$\{p_x, p_y\}$	Γ_6	$p_x + ip_y$	Γ_2	$p_x \mp \sqrt{3}p_y$	p_x	Γ_2
		$p_x - ip_y$	Γ_3	$\sqrt{3}p_x \pm p_y$	p_y	Γ_1
d_{z^2}	Γ_1	d_{z^2}	Γ_1	d_{z^2}	d_{z^2}	Γ_1
$\{d_{xz}, d_{yz}\}$	Γ_5	$d_{xz} + id_{yz}$	Γ_5	$d_{xz} \mp \sqrt{3}d_{yz}$	d_{xz}	Γ_3
		$d_{xz} - id_{yz}$	Γ_6	$\sqrt{3}d_{xz} \pm d_{yz}$	d_{yz}	Γ_4
$\{d_{x^2-y^2}, d_{xy}\}$	Γ_6	$d_{x^2-y^2} + id_{xy}$	Γ_3	$d_{x^2-y^2} \pm \sqrt{3}d_{xy}$	$d_{x^2-y^2}$	Γ_1
		$d_{x^2-y^2} - id_{xy}$	Γ_2	$\sqrt{3}d_{x^2-y^2} \mp d_{xy}$	d_{xy}	Γ_2

TABLE V. Symmetry-adapted p orbitals for the point groups D_{6h}, D_{3h}, and D_{2h} for the coordinate systems shown in Fig. 4 (SLG) and D_{3d}, D_3, and C_{2h} for the coordinate system shown in Fig. 6 (BLG). For D_{2h} and C_{2h}, the symmetrized atomic orbital $\phi_\nu^{[i]}$ corresponds to the coordinate systems used for the point $\mathbf{M}_i$ in Figs. 4(c)-(e) and 6(c)-(e) respectively. The orbital $[i(j)]$ takes the upper (lower) sign.

D_{6h}		D_{3h}		D_{2h}			D_{3d}		D_3		C_{2h}		
ϕ_ν	IR	ϕ_ν	IR	$\phi_\nu^{[1(3)]}$	$\phi_\nu^{[2]}$	IR	ϕ_ν	IR	ϕ_ν	IR	$\phi_\nu^{[1(3)]}$	$\phi_\nu^{[2]}$	IR
p_z	Γ_2^-	p_z	Γ_4	p_z	p_z	Γ_3^-	p_z	Γ_2^-	p_z	Γ_2	p_z	p_z	Γ_2^-
$\{p_x, p_y\}$	Γ_5^-	$\{p_x, p_y\}$	Γ_6	$p_x \mp \sqrt{3}p_y$	p_x	Γ_4^-	$\{p_x, p_y\}$	Γ_3^-	$\{p_x, p_y\}$	Γ_3	$p_x \mp \sqrt{3}p_y$	p_x	Γ_1^-
				$\sqrt{3}p_x \pm p_y$	p_y	Γ_2^-					$\sqrt{3}p_x \pm p_y$	p_y	Γ_2^-

TABLE VI. Compatibility relations for the IRs of D_{3h} and the IRs of its subgroups C_{3h} and C_{2v} using the coordinate system in Fig. 2. The three different orientations of coordinate systems for C_{2v} in Figs. 2(c)-(e) follow the same compatibility relations.

D_{3h}	Γ_1	Γ_2	Γ_3	Γ_4	Γ_5	Γ_6
C_{3h}	Γ_1	Γ_1	Γ_4	Γ_4	$\Gamma_5 + \Gamma_6$	$\Gamma_2 + \Gamma_3$
C_{2v}	Γ_1	Γ_2	Γ_3	Γ_4	$\Gamma_3 + \Gamma_4$	$\Gamma_1 + \Gamma_2$

TABLE VII. Symmetrized plane waves $\mathbb{Q}_{\mathbf{k}}^{I\beta}(\boldsymbol{\mathfrak{R}}_j^W)$ for monolayer MoS_2 and single-layer (SLG), bilayer (BLG) and tri-layer (TLG) graphene at the $\mathbf{\Gamma}$, $\mathbf{K}$, and $\mathbf{M}$ points for the positions occupied by atoms. The symmetrized plane waves $\mathbb{Q}_{\mathbf{K}'}^{I\beta}(\boldsymbol{\mathfrak{R}}_j^W)$ at $\mathbf{K}' = -\mathbf{K}$ are obtained from the expressions given for $\mathbf{K}$ by replacing $\mathbf{K}$ by $\mathbf{K}'$. The corresponding IRs are the complex conjugates of the IRs at $\mathbf{K}$. The group $\mathcal{G}_{\mathbf{k}}$ of the wave vector and the plane wave IRs are shown. At the $\mathbf{K}$ point, we distinguish between the three coordinate systems $\alpha = a, b, c$ for MoS_2 and TLG with atomic positions $\mathbf{R}_j^{W(\alpha)\mu}$ depicted in Figs. 1 and 7, respectively. The IRs for the coordinate systems α are then denoted by $\Gamma_{i/j/k}$. The definition of the symmetrized plane waves at the points $\mathbf{M}_i$ of SLG and BLG contains prefactors γ_i, where $\gamma_1 = \gamma_3 = -1$, and $\gamma_2 = +1$.

	$\mathbf{k} = \mathbf{\Gamma}$		$\mathbf{k} = \mathbf{K}$		$\mathbf{k} = \mathbf{M}_1, \mathbf{M}_2, \mathbf{M}_3$	
MoS_2:	D_{3h}		C_{3h}		C_{2v}	
Mo	Γ_1	$q_{\mathbf{\Gamma}}(\mathbf{R}_j^{\mathrm{Mo}})$	$\Gamma_{2/1/3}$	$q_{\mathbf{K}}(\mathbf{R}_j^{\mathrm{Mo}})$	Γ_1	$q_{\mathbf{M}_i}(\mathbf{R}_j^{\mathrm{Mo}})$
S	Γ_1, Γ_4	$q_{\mathbf{\Gamma}}(\mathbf{R}_j^{\mathrm{S}1}) \pm q_{\mathbf{\Gamma}}(\mathbf{R}_j^{\mathrm{S}2})$	$\Gamma_{3/2/1}, \Gamma_{6/5/4}$	$q_{\mathbf{K}}(\mathbf{R}_j^{\mathrm{S}1}) \pm q_{\mathbf{K}}(\mathbf{R}_j^{\mathrm{S}2})$	Γ_1, Γ_4	$q_{\mathbf{M}_i}(\mathbf{R}_j^{\mathrm{S}1}) \pm q_{\mathbf{M}_i}(\mathbf{R}_j^{\mathrm{S}2})$
SLG:	D_{6h}		D_{3h}		D_{2h}	
c	Γ_1^+, Γ_3^-	$q_{\mathbf{\Gamma}}(\mathbf{R}_j^{c1}) \pm q_{\mathbf{\Gamma}}(\mathbf{R}_j^{c2})$	Γ_6	$\{q_{\mathbf{K}}(\mathbf{R}_j^{c1}), q_{\mathbf{K}}(\mathbf{R}_j^{c2})\}$	Γ_1^+, Γ_2^-	$q_{\mathbf{M}_i}(\mathbf{R}_j^{c1}) \pm \gamma_i\, q_{\mathbf{M}_i}(\mathbf{R}_j^{c2})$
BLG:	D_{3d}		D_3		C_{2h}	
c	Γ_1^+, Γ_2^-	$q_{\mathbf{\Gamma}}(\mathbf{R}_j^{c1}) \pm q_{\mathbf{\Gamma}}(\mathbf{R}_j^{c2})$	Γ_1, Γ_2	$q_{\mathbf{K}}(\mathbf{R}_j^{c1}) \pm q_{\mathbf{K}}(\mathbf{R}_j^{c2})$	Γ_1^+, Γ_2^-	$q_{\mathbf{M}_i}(\mathbf{R}_j^{c1}) \pm q_{\mathbf{M}_i}(\mathbf{R}_j^{c2})$
d	Γ_1^+, Γ_2^-	$q_{\mathbf{\Gamma}}(\mathbf{R}_j^{d1}) \pm q_{\mathbf{\Gamma}}(\mathbf{R}_j^{d2})$	Γ_3	$\{q_{\mathbf{K}}(\mathbf{R}_j^{d1}), q_{\mathbf{K}}(\mathbf{R}_j^{d2})\}$	Γ_1^+, Γ_2^-	$q_{\mathbf{M}_i}(\mathbf{R}_j^{d1}) \pm \gamma_i\, q_{\mathbf{M}_i}(\mathbf{R}_j^{d2})$
TLG:	D_{3h}		C_{3h}		C_{2v}	
A	Γ_1	$q_{\mathbf{\Gamma}}(\mathbf{R}_j^{\mathrm{A}})$	$\Gamma_{3/2/1}$	$q_{\mathbf{K}}(\mathbf{R}_j^{\mathrm{A}})$	Γ_1	$q_{\mathbf{M}_i}(\mathbf{R}_j^{\mathrm{A}})$
B	Γ_1	$q_{\mathbf{\Gamma}}(\mathbf{R}_j^{\mathrm{B}})$	$\Gamma_{2/1/3}$	$q_{\mathbf{K}}(\mathbf{R}_j^{\mathrm{B}})$	Γ_1	$q_{\mathbf{M}_i}(\mathbf{R}_j^{\mathrm{B}})$
A'	Γ_1, Γ_4	$q_{\mathbf{\Gamma}}(\mathbf{R}_j^{\mathrm{A}'1}) \pm q_{\mathbf{\Gamma}}(\mathbf{R}_j^{\mathrm{A}'2})$	$\Gamma_{1/3/2}, \Gamma_{4/6/5}$	$q_{\mathbf{K}}(\mathbf{R}_j^{\mathrm{A}'1}) \pm q_{\mathbf{K}}(\mathbf{R}_j^{\mathrm{A}'2})$	Γ_1, Γ_4	$q_{\mathbf{M}_i}(\mathbf{R}_j^{\mathrm{A}'1}) \pm q_{\mathbf{M}_i}(\mathbf{R}_j^{\mathrm{A}'2})$
B'	Γ_1, Γ_4	$q_{\mathbf{\Gamma}}(\mathbf{R}_j^{\mathrm{B}'1}) \pm q_{\mathbf{\Gamma}}(\mathbf{R}_j^{\mathrm{B}'2})$	$\Gamma_{3/2/1}, \Gamma_{6/5/4}$	$q_{\mathbf{K}}(\mathbf{R}_j^{\mathrm{B}'1}) \pm q_{\mathbf{K}}(\mathbf{R}_j^{\mathrm{B}'2})$	Γ_1, Γ_4	$q_{\mathbf{M}_i}(\mathbf{R}_j^{\mathrm{B}'1}) \pm q_{\mathbf{M}_i}(\mathbf{R}_j^{\mathrm{B}'2})$

TABLE VIII. IRs of the plane waves ($\Gamma_{\mathbf{k}}^q$), the atomic orbitals ϕ_ν ($\Gamma_{\mathbf{k}}^\phi$), and the full Bloch functions ($\Gamma_{\mathbf{k}}^\Phi = \Gamma_{\mathbf{k}}^q \times \Gamma_{\mathbf{k}}^\phi$) for the Mo and S atoms at the points $\mathbf{k} = \mathbf{\Gamma}$, $\mathbf{K}$, and $\mathbf{M}_i$. At $\mathbf{K}$, we distinguish between the three coordinate systems $\alpha = a, b, c$. For the plane waves at $\mathbf{K}'$, the IR $\Gamma_{\mathbf{K}'(i/j/k)}^q$ is the complex conjugate of the IR $\Gamma_{\mathbf{K}(i/j/k)}^q$. At the points $\mathbf{M}_i$ ($i = 1, 2, 3$), the atomic orbitals are denoted by $\phi_\nu^{[i]}$.

	$\mathbf{k} = \mathbf{\Gamma}$ (D_{3h})				$\mathbf{k} = \mathbf{K}, \mathbf{K}'$ (C_{3h})					$\mathbf{k} = \mathbf{M}_1, \mathbf{M}_2, \mathbf{M}_3$ (C_{2v})				
	$\Gamma_{\mathbf{\Gamma}}^q$	ϕ_ν	$\Gamma_{\mathbf{\Gamma}}^\phi$	$\Gamma_{\mathbf{\Gamma}}^\Phi$	$\Gamma_{\mathbf{K}(a/b/c)}^q$	ϕ_ν	$\Gamma_{\mathbf{K}}^\phi$	$\Gamma_{\mathbf{K}(a/b/c)}^\Phi$	$\Gamma_{\mathbf{K}'(a/b/c)}^\Phi$	$\Gamma_{\mathbf{M}}^q$	$\phi_\nu^{[1(3)]}$	$\phi_\nu^{[2]}$	$\Gamma_{\mathbf{M}}^\phi$	$\Gamma_{\mathbf{M}}^\Phi$
Mo	Γ_1	d_{z^2}	Γ_1	Γ_1	$\Gamma_{2/1/3}$	d_{z^2}	Γ_1	$\Gamma_{2/1/3}$	$\Gamma_{3/1/2}$	Γ_1	d_{z^2}	d_{z^2}	Γ_1	Γ_1
		$\{d_{x^2-y^2}, d_{xy}\}$	Γ_6	Γ_6		$d_{x^2-y^2} + id_{xy}$	Γ_3	$\Gamma_{1/3/2}$	$\Gamma_{2/3/1}$		$d_{x^2-y^2} \pm \sqrt{3}d_{xy}$	$d_{x^2-y^2}$	Γ_1	Γ_1
						$d_{x^2-y^2} - id_{xy}$	Γ_2	$\Gamma_{3/2/1}$	$\Gamma_{1/2/3}$		$\sqrt{3}d_{x^2-y^2} \mp d_{xy}$	d_{xy}	Γ_2	Γ_2
		$\{d_{xz}, d_{yz}\}$	Γ_5	Γ_5		$d_{xz} + id_{yz}$	Γ_5	$\Gamma_{6/5/4}$	$\Gamma_{4/5/6}$		$d_{xz} \mp \sqrt{3}d_{yz}$	d_{xz}	Γ_3	Γ_3
						$d_{xz} - id_{yz}$	Γ_6	$\Gamma_{4/6/5}$	$\Gamma_{5/6/4}$		$\sqrt{3}d_{xz} \pm d_{yz}$	d_{yz}	Γ_4	Γ_4
S	Γ_1, Γ_4	p_z	Γ_4	Γ_4	$\Gamma_{3/2/1}, \Gamma_{6/5/4}$	p_z	Γ_4	$\Gamma_{6/5/4}$	$\Gamma_{5/6/4}$	Γ_1, Γ_4	p_z	p_z	Γ_4	Γ_4
				Γ_1				$\Gamma_{3/2/1}$	$\Gamma_{2/3/1}$					Γ_1
		$\{p_x, p_y\}$	Γ_6	Γ_6		$p_x + ip_y$	Γ_2	$\Gamma_{1/3/2}$	$\Gamma_{3/1/2}$		$p_x \mp \sqrt{3}p_y$	p_x	Γ_2	Γ_2
								$\Gamma_{4/6/5}$	$\Gamma_{6/4/5}$					Γ_3
				Γ_5		$p_x - ip_y$	Γ_3	$\Gamma_{2/1/3}$	$\Gamma_{1/2/3}$		$\sqrt{3}p_x \pm p_y$	p_y	Γ_1	Γ_1
								$\Gamma_{5/4/6}$	$\Gamma_{4/5/6}$					Γ_4

TABLE IX. Symmetry-adapted TB Bloch functions in MoS_2 at $\mathbf{k} = \mathbf{\Gamma}$ with group of the wave vector $\mathcal{G}_{\mathbf{\Gamma}} = D_{3h}$. The Bloch functions are written as a product of the plane wave $q_{\mathbf{\Gamma}}(\mathbf{R}_j^{\mathrm{Mo}})$ and d orbitals for Mo atoms and the plane waves $q^{\pm}_{\mathbf{\Gamma}}(\mathbf{R}_j^{\mathrm{S}}) = q_{\mathbf{\Gamma}}(\mathbf{R}_j^{\mathrm{S1}}) \pm q_{\mathbf{\Gamma}}(\mathbf{R}_j^{\mathrm{S2}})$ and p orbitals for S atoms. Also, $q_{\mathbf{\Gamma}}(\mathbf{R}_j^{W})\,\{d_\mu, d_\nu\}$ is a short-hand notation for the pair of Bloch functions $\{q_{\mathbf{\Gamma}}(\mathbf{R}_j^{W})\,d_\mu, q_{\mathbf{\Gamma}}(\mathbf{R}_j^{W})\,d_\nu\}$. The last column indicates the degeneracy of Bloch states due to time-reversal symmetry discussed in Sec. II H.

IRs	Mo	S	TR
Γ_1	$q_{\mathbf{\Gamma}}(\mathbf{R}_j^{\mathrm{Mo}})\,d_{z^2}$	$q^{-}_{\mathbf{\Gamma}}(\mathbf{R}_j^{\mathrm{S}})\,p_z$	a
Γ_4		$q^{+}_{\mathbf{\Gamma}}(\mathbf{R}_j^{\mathrm{S}})\,p_z$	a
Γ_5	$q_{\mathbf{\Gamma}}(\mathbf{R}_j^{\mathrm{Mo}})\,\{d_{xz}, d_{yz}\}$	$q^{-}_{\mathbf{\Gamma}}(\mathbf{R}_j^{\mathrm{S}})\,\{p_x, p_y\}$	a
Γ_6	$q_{\mathbf{\Gamma}}(\mathbf{R}_j^{\mathrm{Mo}})\,\{d_{x^2-y^2}, d_{xy}\}$	$q^{+}_{\mathbf{\Gamma}}(\mathbf{R}_j^{\mathrm{S}})\,\{p_x, p_y\}$	a

TABLE X. Symmetry-adapted TB Bloch functions in MoS_2 at $\mathbf{k} = \mathbf{K}, \mathbf{K}'$ with group of the wave vector $\mathcal{G}_{\mathbf{K}} = \mathcal{G}_{\mathbf{K}'} = C_{3h}$. The Bloch functions are written as a product of the plane wave $q_{\mathbf{k}}(\mathbf{R}_j^{\mathrm{Mo}})$ and d orbitals for Mo atoms and the plane waves $q^{\pm}_{\mathbf{k}}(\mathbf{R}_j^{\mathrm{S}}) = q_{\mathbf{k}}(\mathbf{R}_j^{\mathrm{S1}}) \pm q_{\mathbf{k}}(\mathbf{R}_j^{\mathrm{S2}})$ and p orbitals for S atoms. The IRs $\Gamma_{i/j/k}$ correspond to the coordinate system $\alpha = a/b/c$ in Fig. 1.

$\mathbf{K}$	$\mathbf{K}' = -\mathbf{K}$	Mo	S	TR
$\Gamma_{1/3/2}$	$\Gamma^*_{1/3/2} = \Gamma_{1/2/3}$	$q_{\mathbf{k}}(\mathbf{R}_j^{\mathrm{Mo}})\,(d_{x^2-y^2} \pm i d_{xy})$	$q^{+}_{\mathbf{k}}(\mathbf{R}_j^{\mathrm{S}})\,(p_x \pm i p_y)$	a
$\Gamma_{2/1/3}$	$\Gamma^*_{2/1/3} = \Gamma_{3/1/2}$	$q_{\mathbf{k}}(\mathbf{R}_j^{\mathrm{Mo}})\,d_{z^2}$	$q^{+}_{\mathbf{k}}(\mathbf{R}_j^{\mathrm{S}})\,(p_x \mp i p_y)$	a
$\Gamma_{3/2/1}$	$\Gamma^*_{3/2/1} = \Gamma_{2/3/1}$	$q_{\mathbf{k}}(\mathbf{R}_j^{\mathrm{Mo}})\,(d_{x^2-y^2} \mp i d_{xy})$	$q^{-}_{\mathbf{k}}(\mathbf{R}_j^{\mathrm{S}})\,p_z$	a
$\Gamma_{4/6/5}$	$\Gamma^*_{4/6/5} = \Gamma_{4/5/6}$	$q_{\mathbf{k}}(\mathbf{R}_j^{\mathrm{Mo}})\,(d_{xz} \mp i d_{yz})$	$q^{-}_{\mathbf{k}}(\mathbf{R}_j^{\mathrm{S}})\,(p_x \pm i p_y)$	a
$\Gamma_{5/4/6}$	$\Gamma^*_{5/4/6} = \Gamma_{6/4/5}$		$q^{-}_{\mathbf{k}}(\mathbf{R}_j^{\mathrm{S}})\,(p_x \mp i p_y)$	a
$\Gamma_{6/5/4}$	$\Gamma^*_{6/5/4} = \Gamma_{5/6/4}$	$q_{\mathbf{k}}(\mathbf{R}_j^{\mathrm{Mo}})\,(d_{xz} \pm i d_{yz})$	$q^{+}_{\mathbf{k}}(\mathbf{R}_j^{\mathrm{S}})\,p_z$	a

TABLE XI. Symmetry-adapted TB Bloch functions in MoS_2 at $\mathbf{k} = \mathbf{M}$ with group of the wave vector $\mathcal{G}_{\mathbf{M}} = C_{2v}$. The Bloch functions are written as a product of the plane wave $q_{\mathbf{M}}(\mathbf{R}_j^{\mathrm{Mo}})$ and d orbitals for Mo atoms and the plane waves $q^{\pm}_{\mathbf{M}}(\mathbf{R}_j^{\mathrm{S}}) = q_{\mathbf{M}}(\mathbf{R}_j^{\mathrm{S1}}) \pm q_{\mathbf{M}}(\mathbf{R}_j^{\mathrm{S2}})$ and p orbitals for S atoms.

	$\mathbf{M}_1(\mathbf{M}_3)$		$\mathbf{M}_2$		
IRs	Mo	S	Mo	S	TR
Γ_1	$q_{\mathbf{M}}(\mathbf{R}_j^{\mathrm{Mo}})\,d_{z^2}$;	$q^{-}_{\mathbf{M}}(\mathbf{R}_j^{\mathrm{S}})\,p_z$;	$q_{\mathbf{M}}(\mathbf{R}_j^{\mathrm{Mo}})\,d_{z^2}$;	$q^{-}_{\mathbf{M}}(\mathbf{R}_j^{\mathrm{S}})\,p_z$;	a
	$q_{\mathbf{M}}(\mathbf{R}_j^{\mathrm{Mo}})\,(d_{x^2-y^2} \pm \sqrt{3} d_{xy})$	$q^{+}_{\mathbf{M}}(\mathbf{R}_j^{\mathrm{S}})\,(\sqrt{3} p_x \pm p_y)$	$q_{\mathbf{M}}(\mathbf{R}_j^{\mathrm{Mo}})\,d_{x^2-y^2}$	$q^{+}_{\mathbf{M}}(\mathbf{R}_j^{\mathrm{S}})\,p_y$	
Γ_2	$q_{\mathbf{M}}(\mathbf{R}_j^{\mathrm{Mo}})\,(\sqrt{3} d_{x^2-y^2} \mp d_{xy})$	$q^{+}_{\mathbf{M}}(\mathbf{R}_j^{\mathrm{S}})\,(p_x \mp \sqrt{3} p_y)$	$q_{\mathbf{M}}(\mathbf{R}_j^{\mathrm{Mo}})\,d_{xy}$	$q^{+}_{\mathbf{M}}(\mathbf{R}_j^{\mathrm{S}})\,p_x$	a
Γ_3	$q_{\mathbf{M}}(\mathbf{R}_j^{\mathrm{Mo}})\,(d_{xz} \mp \sqrt{3} d_{yz})$	$q^{-}_{\mathbf{M}}(\mathbf{R}_j^{\mathrm{S}})\,(p_x \mp \sqrt{3} p_y)$	$q_{\mathbf{M}}(\mathbf{R}_j^{\mathrm{Mo}})\,d_{xz}$	$q^{-}_{\mathbf{M}}(\mathbf{R}_j^{\mathrm{S}})\,p_x$	a
Γ_4	$q_{\mathbf{M}}(\mathbf{R}_j^{\mathrm{Mo}})\,(\sqrt{3} d_{xz} \pm d_{yz})$	$q^{+}_{\mathbf{M}}(\mathbf{R}_j^{\mathrm{S}})\,p_z$;	$q_{\mathbf{M}}(\mathbf{R}_j^{\mathrm{Mo}})\,d_{yz}$	$q^{+}_{\mathbf{M}}(\mathbf{R}_j^{\mathrm{S}})\,p_z$;	a
		$q^{-}_{\mathbf{M}}(\mathbf{R}_j^{\mathrm{S}})\,(\sqrt{3} p_x \pm p_y)$		$q^{-}_{\mathbf{M}}(\mathbf{R}_j^{\mathrm{S}})\,p_y$	

IV. BAND SYMMETRIES IN FEW-LAYER GRAPHENE

We can also apply the general formalism in Sec. II to identify the band symmetries in other quasi-2D materials such as single-layer (SLG), bilayer (BLG), and trilayer (TLG) graphene.

A. Crystal structure of few-layer graphene

Like the crystal structure of monolayer MoS_2, the crystal structures of SLG, BLG, and TLG belong to the hexagonal crystal system. Therefore, we use the same expressions for the primitive lattice vectors [Eq. (81)] and reciprocal lattice vectors [Eq. (83)]; and we have the same high-symmetry points in the BZ denoted $\mathbf{\Gamma}$, $\mathbf{K}$ [Eq. (84)], and $\mathbf{M}$ [Eq. (85)]. The space groups for few-layer graphene are listed in Table I. This table also contains the site symmetries of the high-symmetry points for these crystal structures.

1. *Single-layer graphene*

Figure 3 shows the crystal structure of SLG. It is characterized by the point group D_{6h} (space group $P6/mmm$, # 191). The carbon atoms form two distinct Bravais lattices denoted as sublattices A and B. The atomic positions denoted by $\{\mathbf{R}_j^{c1}, \mathbf{R}_j^{c2}\}$ have site symmetries characterized by the point group D_{3h} and Wyckoff letter c. The center of the hexagon, characterized by site symmetry D_{6h} is the only Wyckoff position with multiplicity $m = 1$. This point is the origin of the coordinate system for this crystal structure. The positions of the C atoms in the unit cell are given by

$$\mathbf{t}_{c_1} = \frac{a}{2}\begin{pmatrix} 1 \\ -\frac{1}{\sqrt{3}} \end{pmatrix}, \quad \mathbf{t}_{c_2} = \frac{a}{2}\begin{pmatrix} 1 \\ \frac{1}{\sqrt{3}} \end{pmatrix}. \tag{92}$$

The point group D_{6h} of the crystal, which also characterizes the $\mathbf{\Gamma}$ point of the BZ, contains two-fold, three-fold and six-fold rotations C_2, C_3 and C_6 where the z axis is the rotation axis. The rotation axes of the three two-fold rotation $C_2^{\prime(i)}$ and $C_2^{\prime\prime(jk)}$ are the corresponding dashed lines shown in Fig. 4(a). The reflection planes for $\sigma_v^{(i)}$ and $\sigma_d^{(ij)}$ are perpendicular to the xy-plane passing through the corresponding dashed lines. The reflection σ_h is along the xy-plane and $S_n = C_n\sigma_h$. At the $\mathbf{K}$ point, the group of the wave vector is $\mathcal{G}_{\mathbf{K}} = D_{3h}$ containing three two-fold rotations $C_2^{\prime(ij)}$ about the corresponding dashed axes in Fig. 4(b). The reflection plane of $\sigma_v^{(ij)}$ is perpendicular to the xy plane along the rotation axis of $C_2^{\prime(ij)}$. The three-fold rotation axis is the z axis, and σ_h is a reflection about the xy-plane. The group of the wave vector at the $\mathbf{M}_i$ points is $\mathcal{G}_{\mathbf{M}} = D_{2h}$ containing the symmetry operations C_2, C_2', C_2'', σ_v, σ_v', and σ_v'' with rotation axes and reflection planes shown in Figs. 4(c)-(e). The character table for D_{2h} is reproduced in Table XXVI (Appendix C).

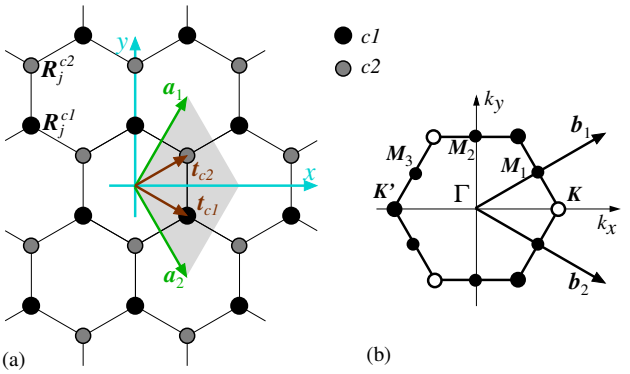

FIG. 3. (a) Crystal structure of single-layer graphene characterized by the point group D_{6h}. The shaded region shows a unit cell ($j = 1$). The C atoms are located at Wyckoff position c with multiplicity $m = 2$, hence the label $c1$ and $c2$ on one unit cell. The primitive lattice vectors are denoted $\mathbf{a}_1$ and $\mathbf{a}_2$. The positions of C atoms in unit cell j are denoted by $\mathbf{R}_j^{c1}$ and $\mathbf{R}_j^{c2}$. The vectors $\mathbf{t}_{c1}$ and $\mathbf{t}_{c2}$ are the positions of the atomic positions of C in the unit cell. (b) The first Brillouin zone with basic reciprocal lattice vectors $\mathbf{b}_1$ and $\mathbf{b}_2$.

2. *Bilayer graphene*

The point group D_{3d} (space group $P\bar{3}m1$, # 164) characterizes BLG as shown in Fig. 5. The only Wyckoff position with multiplicity $m = 1$ is the midpoint of two C atoms on top of each other. We use this point as the origin of the coordinate system. The atomic positions in BLG are the Wyckoff positions c and d, each with multiplicity $m = 2$ and site symmetry C_{3v}. The two atoms in one Wyckoff letter are labeled $\mu = 1$ ($\mu = 2$) for the atom in the top (bottom) layer. The layers are arranged in an AB stacking, so that the atomic position $\mathbf{R}_j^{c1}$ is located on top of $\mathbf{R}_j^{c2}$. Ignoring the z component, the positions of the C atoms in the unit cell are

$$\mathbf{t}_{c\mu} = \frac{a}{2}\begin{pmatrix} 0 \\ 0 \end{pmatrix}, \quad \mathbf{t}_{d1} = \frac{a}{2}\begin{pmatrix} 0 \\ \frac{2}{\sqrt{3}} \end{pmatrix}, \quad \mathbf{t}_{d2} = \frac{a}{2}\begin{pmatrix} 1 \\ \frac{1}{\sqrt{3}} \end{pmatrix}. \tag{93}$$

The three-fold proper and six-fold improper rotation axis is the z axis. The axis of the two-fold rotation $C_2^{\prime(ij)}$ is the corresponding dashed line in Fig. 6(a). The three reflection planes corresponding to $\sigma_d^{(i)}$ are perpendicular to the xy-plane passing through the corresponding dashed line. The group of the wave vector is $\mathcal{G}_{\mathbf{K}} = D_3$ at the $\mathbf{K}$ point with three-fold rotations about the z axis and three two-fold rotations $C_2^{\prime(jk)}$ about the corresponding dashed line in Fig. 6(b). At the $\mathbf{M}_i$ points, the group of the wave vector is $\mathcal{G}_{\mathbf{M}} = C_{2h}$, where σ_h is perpendicular to the xy-plane passing through the corresponding dashed line in Figs. 6(c)-(e), and the two-fold rotation C_2 is about the

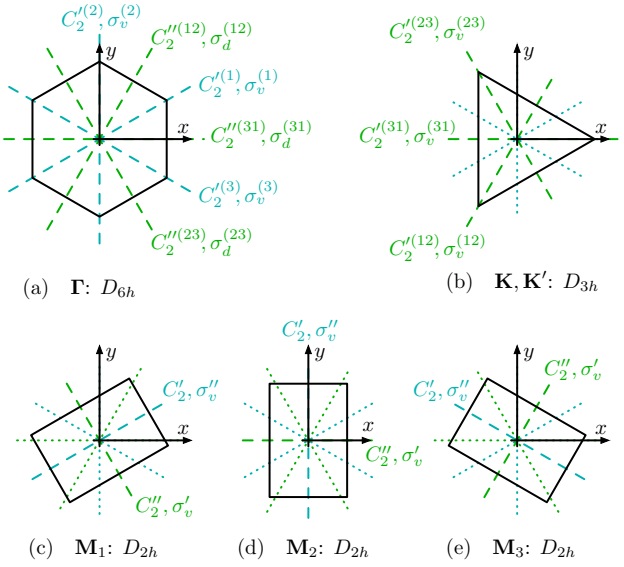

FIG. 4. Groups of the wave vector in SLG. (a) The point $\mathbf{\Gamma}$ has the point group D_{6h} with the z axis (out of plane) as the axis for the n-fold rotations C_n ($n = 2, 3, 6$) and the xy-plane as the reflection plane for σ_h. The dashed lines (i and ij) are the axes for two-fold rotations $C_2^{\prime(i)}$ and $C_2^{\prime\prime(ij)}$ with $i, j = 1, 2, 3$. The reflection $\sigma_v^{(i)}$ [$\sigma_d^{(ij)}$] is about a plane that includes the corresponding dashed axis and the z axis. (b) The points $\mathbf{K}$ and $\mathbf{K}'$ have the point group D_{3h} with three-fold rotations about the z axis. The dashed lines are the axes for the two-fold rotations $C_2^{\prime(ij)}$. The reflection plane of $\sigma_v^{(ij)}$ contains the corresponding dashed lines and the z axis. The reflection plane of σ_h is the xy-plane. The dotted lines indicate the two-fold rotation axes that appear in the point group D_{6h} but are not symmetry elements of D_{3h}. (c)-(e) The points $\mathbf{M}_1$, $\mathbf{M}_2$, and $\mathbf{M}_1$ have the point group D_{2h}. The rotation axis of C_2 is the z axis and the reflection plane of σ_v is the xy-plane. The dashed lines are the axes of the two-fold rotations C_2' and C_2''. The reflection planes of σ_v' and σ_v'' contain the corresponding dashed line and the z axis.

corresponding dashed line. The character table for C_{2h} is reproduced in Table XXIX (Appendix C).

3. *Trilayer graphene*

Lastly, Fig. 7 shows the crystal structure of TLG. This system has the same space group $P\bar{6}m2$, # 187 as monolayer MoS_2 (point group D_{3h}). We designate the Wyckoff positions of the carbon atoms in the middle layer as A and B with site symmetry group D_{3h}, and the remaining positions as $A'\mu$ and $B'\mu$ with $\mu = 1$ ($\mu = 2$) for the top (bottom) layer with site symmetry group C_{3v}. The points A and B as well as the center of the hexagon in the middle layer are Wyckoff positions with multiplicity $m = 1$, which we use as the origin of the three coordinate systems defined in Fig. 7. We therefore associate with each Wyckoff letter W an index (α) corresponding to the coordinate systems $\alpha = a, b, c$. Ignoring the z com-

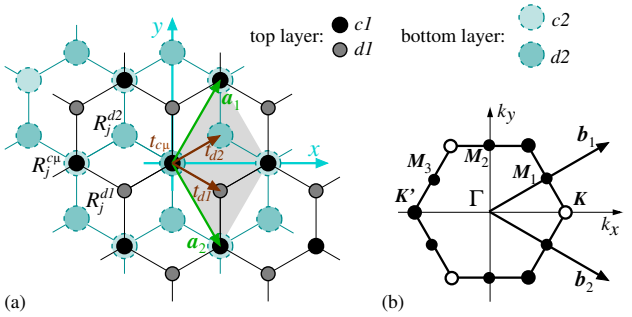

FIG. 5. (a) Crystal structure of bilayer graphene characterized by the point group D_{3d}. The shaded region shows a unit cell ($j = 1$). The C atoms are located on Wyckoff positions c and d each with multiplicity $m = 2$. The atomic position in unit cell j are denoted by $\mathbf{R}_j^{c\mu}$ and $\mathbf{R}_j^{d\mu}$ with $\mu = 1$ ($\mu = 2$) corresponding to the atom at the top (bottom) layer. The vectors $\mathbf{t}_{c\mu}$ and $\mathbf{t}_{d\mu}$ give the positions of the C atoms within a unit cell. The primitive lattice vectors are denoted by $\mathbf{a}_1$ and $\mathbf{a}_2$. (b) The first Brillouin zone with basic reciprocal lattice vectors $\mathbf{b}_1$ and $\mathbf{b}_2$.

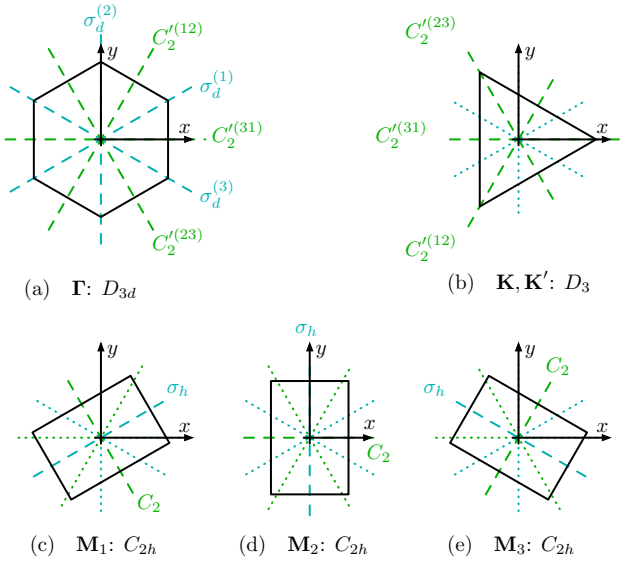

FIG. 6. Groups of the wave vector in BLG. (a) The point $\mathbf{\Gamma}$ has the point group D_{3d} with the z axis (out of plane) as the axis for the three-fold proper rotation C_3 and the six-fold improper rotation S_6. The green dashed lines ij are the axes for two-fold rotations $C_2^{\prime\prime(ij)}$ with $i, j = 1, 2, 3$. The reflection $\sigma_d^{(i)}$ is about a plane that includes the corresponding blue dashed axis and the z axis. (b) The points $\mathbf{K}$ and $\mathbf{K}'$ have the point group D_3 with three-fold rotations about the z axis. The dashed lines are the axes for the two-fold rotations $C_2^{\prime(ij)}$. The dotted lines indicate the reflection planes that appear in the point group D_{3d} but are not symmetry elements of D_3. (c)-(e) The points $\mathbf{M}_1$, $\mathbf{M}_2$, and $\mathbf{M}_1$ have the point group C_{2h}. The green dashed line is the axis of the two-fold rotation C_2. The reflection plane of σ_h contains the blue dashed line and the z axis.

ponent, the positions of the C atoms in the unit cell for the three coordinate systems are

$$\mathbf{t}^a_A = \frac{a}{2}\begin{pmatrix} 1 \\ -\frac{1}{\sqrt{3}} \end{pmatrix}, \qquad \mathbf{t}^a_{A'\mu} = \frac{a}{2}\begin{pmatrix} 0 \\ 0 \end{pmatrix}, \tag{94a}$$

$$\mathbf{t}^a_B = \frac{a}{2}\begin{pmatrix} 1 \\ \frac{1}{\sqrt{3}} \end{pmatrix}, \qquad \mathbf{t}^a_{B'\mu} = \frac{a}{2}\begin{pmatrix} 1 \\ -\frac{1}{\sqrt{3}} \end{pmatrix}, \tag{94b}$$

$$\mathbf{t}^b_A = \frac{a}{2}\begin{pmatrix} 0 \\ -\frac{2}{\sqrt{3}} \end{pmatrix}, \qquad \mathbf{t}^b_{A'\mu} = \frac{a}{2}\begin{pmatrix} -1 \\ -\frac{1}{\sqrt{3}} \end{pmatrix}, \tag{94c}$$

$$\mathbf{t}^b_B = \frac{a}{2}\begin{pmatrix} 0 \\ 0 \end{pmatrix}, \qquad \mathbf{t}^b_{B'\mu} = \frac{a}{2}\begin{pmatrix} 0 \\ -\frac{2}{\sqrt{3}} \end{pmatrix}, \tag{94d}$$

$$\mathbf{t}^c_A = \frac{a}{2}\begin{pmatrix} 0 \\ 0 \end{pmatrix}, \qquad \mathbf{t}^c_{A'\mu} = \frac{a}{2}\begin{pmatrix} -1 \\ \frac{1}{\sqrt{3}} \end{pmatrix}, \tag{94e}$$

$$\mathbf{t}^c_B = \frac{a}{2}\begin{pmatrix} 0 \\ \frac{2}{\sqrt{3}} \end{pmatrix}, \qquad \mathbf{t}^c_{B'\mu} = \frac{a}{2}\begin{pmatrix} 0 \\ 0 \end{pmatrix}, \tag{94f}$$

where the superscripts $\alpha = a, b, c$ denote the coordinate system. The positions of the six atoms in unit cell j are denoted by $\mathbf{R}^A_j$, $\mathbf{R}^B_j$, $\mathbf{R}^{A'\mu}_j$ and $\mathbf{R}^{B'\mu}_j$. In standard notation [58], the positions A, B , $A'\mu$ and $B'\mu$ are characterized by the Wyckoff letters c, e, g, and h respectively in coordinate system (a), by e, a, h, and i in coordinate system (b), and by a, c, i, and g in coordinate system (c), see Table I.

The point group D_{3h} of the crystal structure of TLG is the same as for MoS_2 with coordinate system shown in Fig. 2(a). The group of the wave vector at $\mathbf{K}$ is $\mathcal{G}_{\mathbf{K}} = C_{3h}$ with coordinate system shown in Fig. 2(b). At the three points $\mathbf{M}_i$ the group of the wave vector is $\mathcal{G}_{\mathbf{M}} = C_{2v}$ with coordinate system shown in Figs. 2(c)-(e), which contains the two-fold rotation C_2 about the dashed line, reflection σ'_v about the dashed line and the z axis, and reflection σ_v about the xy plane.

B. IRs of Bloch states in graphene

In graphene, the bands near the Fermi level are dominated by the p orbitals of the C atoms. For SLG, using the coordinate systems in Fig. 4, the IRs of the symmetry-adapted p orbitals are listed in Table V for the points $\mathbf{\Gamma}$, $\mathbf{K}$, and $\mathbf{M}$ with groups of the wave vector D_{6h}, D_{3h}, and D_{2h} respectively. For BLG, Fig. 6 shows the coordinate systems used for the points $\mathbf{\Gamma}$, $\mathbf{K}$, and $\mathbf{M}$ with group of the wave vector D_{3d}, D_3 and C_{2h}, respectively. The IRs of the p orbitals at these points are listed in Table V. The coordinate systems used for TLG are the same as the ones for MoS_2 [Fig. 2], so that the IRs of the p orbitals can be taken from Table IV. The symmetry-adapted plane waves with the corresponding IRs are summarized in Table VII.

The IRs of the full Bloch functions for SLG, BLG, and TLG are listed in Table XII. The sets of Bloch states transforming as an IR in $\mathcal{G}_{\mathbf{k}}$ for the wave vectors $\mathbf{k} = \mathbf{\Gamma}, \mathbf{K}, \mathbf{M}$ are listed in Tables XIII, XIV, and XV for SLG, Tables XVI, XVII, and XVIII for BLG, and Tables XIX, XX, and XXI for TLG.

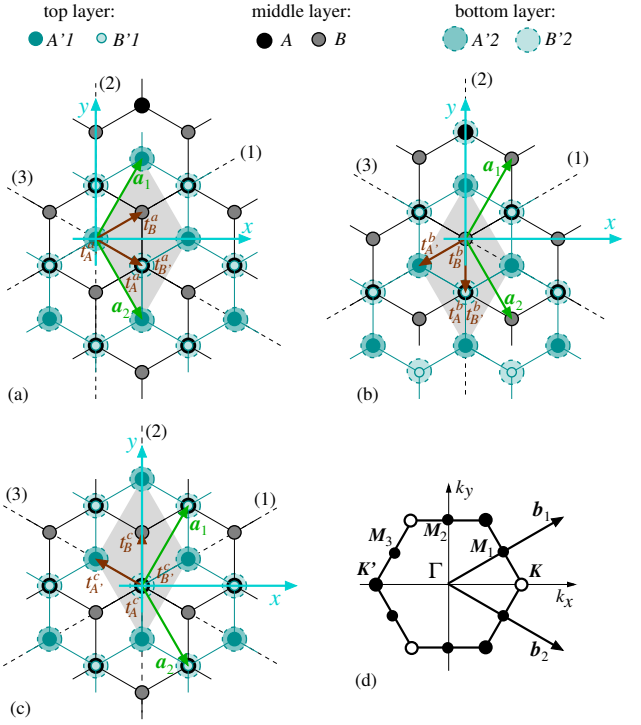

FIG. 7. Crystal structure of trilayer graphene. Three coordinate systems $\alpha = a, b, c$ are considered with (a) the origin located at the atom A, (b) origin at atom B, and (c) origin at the midpoint between $B'1$ and $B'2$. The dashed axes (1), (2) and (3) are the two-fold rotation axes of the point group D_{3h}. The shaded region shows a unit cell ($j = 1$). The vectors $\mathbf{t}^\alpha_A$, $\mathbf{t}^\alpha_B$, $\mathbf{t}^\alpha_{A'}$ and $\mathbf{t}^\alpha_{B'}$ give the positions of the C atoms labeled A, B, $A'\mu$ and $B'\mu$ within a unit cell respectively. For the A' and B' atom, the top (bottom) atoms are labeled $\mu = 1$ ($\mu = 2$). The positions of these atoms in unit cell j are denoted by $\mathbf{R}^{A(\alpha)}_j$, $\mathbf{R}^{B(\alpha)}_j$, $\mathbf{R}^{A'\mu(\alpha)}_j$, and $\mathbf{R}^{B'\mu(\alpha)}_j$ respectively. (d) The first Brillouin zone.

TABLE XII. IRs of the plane waves ($\Gamma^q_{\mathbf{k}}$), the atomic orbitals ϕ_ν ($\Gamma^\phi_{\mathbf{k}}$), and the full Bloch functions ($\Gamma^\Phi_{\mathbf{k}} = \Gamma^q_{\mathbf{k}} \times \Gamma^\phi_{\mathbf{k}}$) for single-layer (SLG), bilayer (BLG), and tri-layer graphene (TLG) at the points $\mathbf{k} = \mathbf{\Gamma}$, $\mathbf{K}$, and $\mathbf{M}_i$. The positions of C atoms in SLG are characterized by the Wyckoff letter c with multiplicity $m = 2$. For BLG, the atomic positions have Wyckoff letters c and d each with multiplicity $m = 2$. For TLG, the Wyckoff letters of the atomic positions are denoted A and B with multiplicity $m = 1$, and A' and B' with multiplicity $m = 2$. For TLG at $\mathbf{K}$, we need to distinguish between the three coordinate systems $\alpha = a, b, c$. The IRs of $\mathcal{G}_{\mathbf{K}}$ and $\mathcal{G}_{\mathbf{K}'}$ in SLG and BLG are real, so that $\Gamma^q_{\mathbf{K}} = \Gamma^q_{\mathbf{K}'}$ and $\Gamma^\phi_{\mathbf{K}} = \Gamma^\phi_{\mathbf{K}'}$, whereas in TLG the IR $\Gamma^q_{\mathbf{K}'(i/j/k)}$ is the complex conjugate of $\Gamma^q_{\mathbf{K}(i/j/k)}$. At the points $\mathbf{M}_i$ ($i = 1, 2, 3$), the atomic orbitals are denoted by $\phi^{[i]}_\nu$.

	$\mathbf{k} = \mathbf{\Gamma}$				$\mathbf{k} = \mathbf{K}$				$\mathbf{k} = \mathbf{M}_1, \mathbf{M}_2, \mathbf{M}_3$				
	$\Gamma^q_{\mathbf{\Gamma}}$	ϕ_ν	$\Gamma^\phi_{\mathbf{\Gamma}}$	$\Gamma^\Phi_{\mathbf{\Gamma}}$	$\Gamma^q_{\mathbf{K}}$	ϕ_ν	$\Gamma^\phi_{\mathbf{K}}$	$\Gamma^\Phi_{\mathbf{K}}$	$\Gamma^q_{\mathbf{M}}$	$\phi^{[1(3)]}_\nu$	$\phi^{[2]}_\nu$	$\Gamma^\phi_{\mathbf{M}}$	$\Gamma^\Phi_{\mathbf{M}}$
SLG	D_{6h}				D_{3h}				D_{2h}				
c	Γ_1^+, Γ_3^-	p_z	Γ_2^-	Γ_2^- / Γ_3^+	Γ_6	p_z	Γ_4	Γ_5	Γ_1^+, Γ_2^-	p_z	p_z	Γ_3^-	Γ_3^- / Γ_4^+
		$\{p_x, p_y\}$	Γ_5^-	Γ_5^-		$\{p_x, p_y\}$	Γ_6	Γ_1 / Γ_2		$p_x \mp \sqrt{3}p_y$	p_x	Γ_4^-	Γ_4^- / Γ_3^+
				Γ_6^+				Γ_6		$\sqrt{3}p_x \pm p_y$	p_y	Γ_2^-	Γ_2^- / Γ_1^+
BLG	D_{3d}				D_3				C_{2h}				
c	Γ_1^+, Γ_2^-	p_z	Γ_2^-	Γ_2^- / Γ_1^+	Γ_1, Γ_2	p_z	Γ_2	Γ_2 / Γ_1	Γ_1^+, Γ_2^-	p_z	p_z	Γ_2^-	Γ_2^- / Γ_1^+
		$\{p_x, p_y\}$	Γ_3^-	Γ_3^-		$\{p_x, p_y\}$	Γ_3	Γ_3		$p_x \mp \sqrt{3}p_y$	p_x	Γ_1^-	Γ_1^- / Γ_2^+
				Γ_3^+				Γ_3		$\sqrt{3}p_x \pm p_y$	p_y	Γ_2^-	Γ_2^- / Γ_1^+
d	Γ_1^+, Γ_2^-	p_z	Γ_2^-	Γ_2^- / Γ_1^+	Γ_3	p_z	Γ_2	Γ_3	Γ_1^+, Γ_2^-	p_z	p_z	Γ_2^-	Γ_2^- / Γ_1^+
		$\{p_x, p_y\}$	Γ_3^-	Γ_3^-		$\{p_x, p_y\}$	Γ_3	Γ_1 / Γ_2		$p_x \mp \sqrt{3}p_y$	p_x	Γ_1^-	Γ_1^- / Γ_2^+
				Γ_3^+				Γ_3		$\sqrt{3}p_x \pm p_y$	p_y	Γ_2^-	Γ_2^- / Γ_1^+
TLG	D_{3h}				C_{3h}				C_{2v}				
	$\Gamma^q_{\mathbf{\Gamma}}$	ϕ_ν	$\Gamma^\phi_{\mathbf{\Gamma}}$	$\Gamma^\Phi_{\mathbf{\Gamma}}$	$\Gamma^q_{\mathbf{K}(a/b/c)}$	ϕ_ν	$\Gamma^\phi_{\mathbf{K}}$	$\Gamma^\Phi_{\mathbf{K}(a/b/c)}$ / $\Gamma^\Phi_{\mathbf{K}'(a/b/c)}$	$\Gamma^q_{\mathbf{M}}$	$\phi^{[1(3)]}_\nu$	$\phi^{[2]}_\nu$	$\Gamma^\phi_{\mathbf{M}}$	$\Gamma^\Phi_{\mathbf{M}}$
A	Γ_1	p_z	Γ_4	Γ_4	$\Gamma_{3/2/1}$	p_z	Γ_4	$\Gamma_{6/5/4}$ / $\Gamma_{5/6/4}$	Γ_1	p_z	p_z	Γ_4	Γ_4
		$\{p_x, p_y\}$	Γ_6	Γ_6		$p_x + ip_y$	Γ_2	$\Gamma_{1/3/2}$ / $\Gamma_{3/1/2}$		$p_x \mp \sqrt{3}p_y$	p_x	Γ_2	Γ_2
						$p_x - ip_y$	Γ_3	$\Gamma_{2/1/3}$ / $\Gamma_{1/2/3}$		$\sqrt{3}p_x \pm p_y$	p_y	Γ_1	Γ_1
B	Γ_1	p_z	Γ_4	Γ_4	$\Gamma_{2/1/3}$	p_z	Γ_4	$\Gamma_{5/4/6}$ / $\Gamma_{6/4/5}$	Γ_1	p_z	p_z	Γ_4	Γ_4
		$\{p_x, p_y\}$	Γ_6	Γ_6		$p_x + ip_y$	Γ_2	$\Gamma_{3/2/1}$ / $\Gamma_{1/2/3}$		$p_x \mp \sqrt{3}p_y$	p_x	Γ_2	Γ_2
						$p_x - ip_y$	Γ_3	$\Gamma_{1/3/2}$ / $\Gamma_{2/3/1}$		$\sqrt{3}p_x \pm p_y$	p_y	Γ_1	Γ_1
A'	Γ_1, Γ_4	p_z	Γ_4	Γ_4 / Γ_1	$\Gamma_{1/3/2}, \Gamma_{4/6/5}$	p_z	Γ_4	$\Gamma_{4/6/5}$ / $\Gamma_{4/5/6}$ / $\Gamma_{1/3/2}$ / $\Gamma_{1/2/3}$	Γ_1, Γ_4	p_z	p_z	Γ_4	Γ_4 / Γ_1
		$\{p_x, p_y\}$	Γ_6	Γ_6		$p_x + ip_y$	Γ_2	$\Gamma_{2/1/3}$ / $\Gamma_{2/3/1}$ / $\Gamma_{5/4/6}$ / $\Gamma_{5/6/4}$		$p_x \mp \sqrt{3}p_y$	p_x	Γ_2	Γ_2 / Γ_3
				Γ_5		$p_x - ip_y$	Γ_3	$\Gamma_{3/2/1}$ / $\Gamma_{3/1/2}$ / $\Gamma_{6/5/4}$ / $\Gamma_{6/4/5}$		$\sqrt{3}p_x \pm p_y$	p_y	Γ_1	Γ_1 / Γ_4
B'	Γ_1, Γ_4	p_z	Γ_4	Γ_4 / Γ_1	$\Gamma_{3/2/1}, \Gamma_{6/5/4}$	p_z	Γ_4	$\Gamma_{6/5/4}$ / $\Gamma_{5/6/4}$ / $\Gamma_{3/2/1}$ / $\Gamma_{2/3/1}$	Γ_1, Γ_4	p_z	p_z	Γ_4	Γ_4 / Γ_1
		$\{p_x, p_y\}$	Γ_6	Γ_6		$p_x + ip_y$	Γ_2	$\Gamma_{1/3/2}$ / $\Gamma_{3/1/2}$ / $\Gamma_{4/6/5}$ / $\Gamma_{6/4/5}$		$p_x \mp \sqrt{3}p_y$	p_x	Γ_2	Γ_2 / Γ_3
				Γ_5		$p_x - ip_y$	Γ_3	$\Gamma_{2/1/3}$ / $\Gamma_{1/2/3}$ / $\Gamma_{5/4/6}$ / $\Gamma_{4/5/6}$		$\sqrt{3}p_x \pm p_y$	p_y	Γ_1	Γ_1 / Γ_4

TABLE XIII. Symmetry-adapted TB Bloch functions in SLG at $\mathbf{k} = \mathbf{\Gamma}$ with group of the wave vector $\mathcal{G}_{\mathbf{\Gamma}} = D_{6h}$. The C atoms are located at Wyckoff position c of multiplicity 2. The Bloch functions are written as a product of the plane waves $q^{\pm}_{\mathbf{\Gamma}}(\mathbf{R}^c_j) = q_{\mathbf{\Gamma}}(\mathbf{R}^{c1}_j) \pm q_{\mathbf{\Gamma}}(\mathbf{R}^{c2}_j)$ and the p orbitals of the C atoms. Also, $q_{\mathbf{\Gamma}}(\mathbf{R}^W_j)\,\{p_x, p_y\}$ is a short-hand notation for the pair of Bloch functions $\{q_{\mathbf{\Gamma}}(\mathbf{R}^W_j)\,p_x, q_{\mathbf{\Gamma}}(\mathbf{R}^W_j)\,p_y\}$. The last column indicates the degeneracy of Bloch states due to time-reversal symmetry discussed in Sec. II H.

IRs	Bloch function	TR
Γ^-_2	$q^-_{\mathbf{\Gamma}}(\mathbf{R}^c_j)\,p_z$	a
Γ^+_3	$q^+_{\mathbf{\Gamma}}(\mathbf{R}^c_j)\,p_z$	a
Γ^-_5	$q^+_{\mathbf{\Gamma}}(\mathbf{R}^c_j)\,\{p_x, p_y\}$	a
Γ^+_6	$q^-_{\mathbf{\Gamma}}(\mathbf{R}^c_j)\,\{p_x, p_y\}$	a

TABLE XIV. Symmetry-adapted TB Bloch functions in SLG at $\mathbf{k} = \mathbf{K}$ with group of the wave vector $\mathcal{G}_{\mathbf{K}} = D_{3h}$. The same form of the symmetry-adapted TB Bloch functions and corresponding IRs work for $\mathbf{k} = \mathbf{K}'$, that is we replace $\mathbf{K}$ with $\mathbf{K}'$.

IRs	Bloch function	TR
Γ_1	$q_{\mathbf{K}}(\mathbf{R}^{c1}_j)\,p_y + q_{\mathbf{K}}(\mathbf{R}^{c2}_j)\,p_x$	a
Γ_2	$q_{\mathbf{K}}(\mathbf{R}^{c1}_j)\,p_y - q_{\mathbf{K}}(\mathbf{R}^{c2}_j)\,p_x$	a
Γ_5	$\{q_{\mathbf{K}}(\mathbf{R}^{c1}_j)\,p_z, q_{\mathbf{K}}(\mathbf{R}^{c2}_j)\,p_z\}$	a
Γ_6	$\{q_{\mathbf{K}}(\mathbf{R}^{c1}_j)\,p_x, q_{\mathbf{K}}(\mathbf{R}^{c2}_j)\,p_y\}$	a

TABLE XV. Symmetry-adapted TB Bloch functions in SLG at $\mathbf{k} = \mathbf{M}$ with group of the wave vector $\mathcal{G}_{\mathbf{M}} = D_{2h}$.

IRs	$\mathbf{M}_1$ ($\mathbf{M}_3$)	$\mathbf{M}_2$	TR
Γ^+_1	$q^+_{\mathbf{M}}(\mathbf{R}^c_j)(\sqrt{3}p_x \pm p_y)$	$q^-_{\mathbf{M}}(\mathbf{R}^c_j)\,p_y$	a
Γ^-_2	$q^-_{\mathbf{M}}(\mathbf{R}^c_j)(\sqrt{3}p_x \pm p_y)$	$q^+_{\mathbf{M}}(\mathbf{R}^c_j)\,p_y$	a
Γ^+_3	$q^+_{\mathbf{M}}(\mathbf{R}^c_j)(p_x \mp \sqrt{3}p_y)$	$q^-_{\mathbf{M}}(\mathbf{R}^c_j)\,p_x$	a
Γ^-_3	$q^-_{\mathbf{M}}(\mathbf{R}^c_j)\,p_z$	$q^+_{\mathbf{M}}(\mathbf{R}^c_j)\,p_z$	a
Γ^+_4	$q^+_{\mathbf{M}}(\mathbf{R}^c_j)\,p_z$	$q^-_{\mathbf{M}}(\mathbf{R}^c_j)\,p_z$	a
Γ^-_4	$q^-_{\mathbf{M}}(\mathbf{R}^c_j)(p_x \mp \sqrt{3}p_y)$	$q^+_{\mathbf{M}}(\mathbf{R}^c_j)\,p_x$	a

TABLE XVI. Symmetry-adapted TB Bloch functions in BLG at $\mathbf{k} = \mathbf{\Gamma}$ with group of the wave vector $\mathcal{G}_{\mathbf{\Gamma}} = D_{3d}$. The C atoms are located at Wyckoff positions $W = c, d$ each of multiplicity 2. $q^{\pm}_{\mathbf{\Gamma}}(\mathbf{R}^W_j)\,\{p_x, p_y\}$ is a short-hand notation for the pair of Bloch functions $\{q^{\pm}_{\mathbf{\Gamma}}(\mathbf{R}^W_j)\,p_x, q^{\pm}_{\mathbf{\Gamma}}(\mathbf{R}^W_j)\,p_y\}$.

IRs	$W = c, d$	TR
Γ^+_1	$q^-_{\mathbf{\Gamma}}(\mathbf{R}^W_j)\,p_z$	a
Γ^-_2	$q^+_{\mathbf{\Gamma}}(\mathbf{R}^W_j)\,p_z$	a
Γ^+_3	$q^-_{\mathbf{\Gamma}}(\mathbf{R}^W_j)\,\{p_x, p_y\}$	a
Γ^-_3	$q^+_{\mathbf{\Gamma}}(\mathbf{R}^W_j)\,\{p_x, p_y\}$	a

TABLE XVII. Symmetry-adapted TB Bloch functions in BLG at $\mathbf{k} = \mathbf{K}$ with group of the wave vector $\mathcal{G}_{\mathbf{K}} = D_3$. $q^{\pm}_{\mathbf{K}}(\mathbf{R}^W_j)\,\{p_x, p_y\}$ is a short-hand notation for the pair of Bloch functions $\{q^{\pm}_{\mathbf{K}}(\mathbf{R}^W_j)\,p_x, q^{\pm}_{\mathbf{K}}(\mathbf{R}^W_j)\,p_y\}$. The same form of the symmetry-adapted TB Bloch functions and corresponding IRs work for $\mathbf{k} = \mathbf{K}'$, that is we replace $\mathbf{K}$ with $\mathbf{K}'$.

IRs	c	d	TR
Γ_1	$q^-_{\mathbf{K}}(\mathbf{R}^c_j)\,p_z$	$q_{\mathbf{K}}(\mathbf{R}^{d1}_j)\,p_y + q_{\mathbf{K}}(\mathbf{R}^{d2}_j)\,p_x$	a
Γ_2	$q^+_{\mathbf{K}}(\mathbf{R}^c_j)\,p_z$	$q_{\mathbf{K}}(\mathbf{R}^{d1}_j)\,p_y - q_{\mathbf{K}}(\mathbf{R}^{d2}_j)\,p_x$	a
Γ_3	$q^-_{\mathbf{K}}(\mathbf{R}^c_j)\,\{p_x, p_y\}$; $q^+_{\mathbf{K}}(\mathbf{R}^c_j)\,\{p_x, p_y\}$	$\{q_{\mathbf{K}}(\mathbf{R}^{d1}_j)\,p_z, q_{\mathbf{K}}(\mathbf{R}^{d2}_j)\,p_z\}$; $\{q_{\mathbf{K}}(\mathbf{R}^{d1}_j)\,p_x, q_{\mathbf{K}}(\mathbf{R}^{d2}_j)\,p_y\}$	a

TABLE XVIII. Symmetry-adapted TB Bloch functions in BLG at $\mathbf{k}=\mathbf{M}$ with group of the wave vector $\mathcal{G}_{\mathbf{M}}=C_{2h}$.

	$\mathbf{k}=\mathbf{M}_1\,(\mathbf{M}_3)$		$\mathbf{k}=\mathbf{M}_2$		
IRs	c	d	c	d	TR
Γ_1^+	$q^-_{\mathbf{M}}(\mathbf{R}_j^c)\,p_z$;	$q^+_{\mathbf{M}}(\mathbf{R}_j^d)\,p_z$;	$q^-_{\mathbf{M}}(\mathbf{R}_j^c)\,p_z$;	$q^-_{\mathbf{M}}(\mathbf{R}_j^d)\,p_z$;	a
	$q^-_{\mathbf{M}}(\mathbf{R}_j^c)\,(\sqrt{3}p_x\pm p_y)$	$q^+_{\mathbf{M}}(\mathbf{R}_j^d)\,(\sqrt{3}p_x\pm p_y)$	$q^-_{\mathbf{M}}(\mathbf{R}_j^c)\,p_y$	$q^-_{\mathbf{M}}(\mathbf{R}_j^d)\,p_y$	
Γ_1^-	$q^+_{\mathbf{M}}(\mathbf{R}_j^c)\,(p_x\mp\sqrt{3}p_y)$	$q^-_{\mathbf{M}}(\mathbf{R}_j^d)\,(p_x\mp\sqrt{3}p_y)$	$q^+_{\mathbf{M}}(\mathbf{R}_j^c)\,p_x$	$q^+_{\mathbf{M}}(\mathbf{R}_j^d)\,p_x$	a
Γ_2^+	$q^-_{\mathbf{M}}(\mathbf{R}_j^c)\,(p_x\mp\sqrt{3}p_y)$	$q^+_{\mathbf{M}}(\mathbf{R}_j^d)\,(p_x\mp\sqrt{3}p_y)$	$q^-_{\mathbf{M}}(\mathbf{R}_j^c)\,p_x$	$q^-_{\mathbf{M}}(\mathbf{R}_j^d)\,p_x$	a
Γ_2^-	$q^+_{\mathbf{M}}(\mathbf{R}_j^c)\,p_z$;	$q^-_{\mathbf{M}}(\mathbf{R}_j^d)\,p_z$;	$q^+_{\mathbf{M}}(\mathbf{R}_j^c)\,p_z$;	$q^+_{\mathbf{M}}(\mathbf{R}_j^d)\,p_z$;	a
	$q^+_{\mathbf{M}}(\mathbf{R}_j^c)\,(\sqrt{3}p_x\pm p_y)$	$q^-_{\mathbf{M}}(\mathbf{R}_j^d)\,(\sqrt{3}p_x\pm p_y)$	$q^+_{\mathbf{M}}(\mathbf{R}_j^c)\,p_y$	$q^+_{\mathbf{M}}(\mathbf{R}_j^d)\,p_y$	

TABLE XIX. Symmetry-adapted TB Bloch functions in TLG at $\mathbf{k}=\mathbf{\Gamma}$ with group of the wave vector $\mathcal{G}_{\mathbf{\Gamma}}=D_{3h}$. The C atoms are located at Wyckoff positions $W=A,B$ ($W=A',B'$) of multiplicity 1 (2). $q_{\mathbf{\Gamma}}(\mathbf{R}_j^W)\,\{p_x,p_y\}$ is a short-hand notation for the pair of Bloch functions $\{q_{\mathbf{\Gamma}}(\mathbf{R}_j^W)\,p_x, q_{\mathbf{\Gamma}}(\mathbf{R}_j^W)\,p_y\}$.

IRs	$W=A,B$	$W=A',B'$	TR
Γ_1		$q^-_{\mathbf{\Gamma}}(\mathbf{R}_j^W)\,p_z$	a
Γ_4	$q_{\mathbf{\Gamma}}(\mathbf{R}_j^W)\,p_z$	$q^+_{\mathbf{\Gamma}}(\mathbf{R}_j^W)\,p_z$	a
Γ_5		$q^-_{\mathbf{\Gamma}}(\mathbf{R}_j^W)\,\{p_x,p_y\}$	a
Γ_6	$q_{\mathbf{\Gamma}}(\mathbf{R}_j^W)\,\{p_x,p_y\}$	$q^+_{\mathbf{\Gamma}}(\mathbf{R}_j^W)\,\{p_x,p_y\}$	a

TABLE XX. Symmetry-adapted TB Bloch functions in TLG at $\mathbf{k}=\mathbf{K},\mathbf{K}'$ with group of the wave vector $\mathcal{G}_{\mathbf{K}}=\mathcal{G}_{\mathbf{K}'}=C_{3h}$. The IRs $\Gamma_{i/j/k}$ correspond to the coordinate system $\alpha=a/b/c$ in Fig. 7. The IRs at $\mathbf{K}'$ are the complex conjugates of the IRs at $\mathbf{K}$.

$\mathbf{K}$	$\mathbf{K}'=-\mathbf{K}$	A	B	A'	B'	TR
$\Gamma_{1/3/2}$	$\Gamma^*_{1/3/2}=\Gamma_{1/2/3}$	$q_{\mathbf{K}}(\mathbf{R}_j^A)\,(p_x\pm ip_y)$	$q_{\mathbf{K}}(\mathbf{R}_j^B)\,(p_x\mp ip_y)$	$q^-_{\mathbf{K}}(\mathbf{R}_j^{A'})\,p_z$	$q^+_{\mathbf{K}}(\mathbf{R}_j^{B'})\,(p_x\pm ip_y)$	a
$\Gamma_{2/1/3}$	$\Gamma^*_{2/1/3}=\Gamma_{3/1/2}$	$q_{\mathbf{K}}(\mathbf{R}_j^A)\,(p_x\mp ip_y)$		$q^+_{\mathbf{K}}(\mathbf{R}_j^{A'})\,(p_x\pm ip_y)$	$q^+_{\mathbf{K}}(\mathbf{R}_j^{B'})\,(p_x\mp ip_y)$	a
$\Gamma_{3/2/1}$	$\Gamma^*_{3/2/1}=\Gamma_{2/3/1}$		$q_{\mathbf{K}}(\mathbf{R}_j^B)\,(p_x\pm ip_y)$	$q^+_{\mathbf{K}}(\mathbf{R}_j^{A'})\,(p_x\mp ip_y)$	$q^-_{\mathbf{K}}(\mathbf{R}_j^{A'})\,p_z$	a
$\Gamma_{4/6/5}$	$\Gamma^*_{4/6/5}=\Gamma_{4/5/6}$			$q^+_{\mathbf{K}}(\mathbf{R}_j^{A'})\,p_z$	$q^-_{\mathbf{K}}(\mathbf{R}_j^{B'})\,(p_x\pm ip_y)$	a
$\Gamma_{5/4/6}$	$\Gamma^*_{5/4/6}=\Gamma_{6/4/5}$		$q_{\mathbf{K}}(\mathbf{R}_j^B)\,p_z$	$q^-_{\mathbf{K}}(\mathbf{R}_j^{A'})\,(p_x\pm ip_y)$	$q^-_{\mathbf{K}}(\mathbf{R}_j^{B'})\,(p_x\mp ip_y)$	a
$\Gamma_{6/5/4}$	$\Gamma^*_{6/5/4}=\Gamma_{5/6/4}$	$q_{\mathbf{K}}(\mathbf{R}_j^A)\,p_z$		$q^-_{\mathbf{K}}(\mathbf{R}_j^{A'})\,(p_x\mp ip_y)$	$q^+_{\mathbf{K}}(\mathbf{R}_j^{B'})\,p_z$	a

TABLE XXI. Symmetry-adapted TB Bloch functions in TLG at $\mathbf{k}=\mathbf{M}$ with group of the wave vector $\mathcal{G}_{\mathbf{M}}=C_{2v}$.

	$\mathbf{k}=\mathbf{M}_1\,(\mathbf{M}_3)$		$\mathbf{k}=\mathbf{M}_2$		
IRs	$W=A,B$	$W=A',B'$	$W=A,B$	$W=A',B'$	TR
Γ_1	$q_{\mathbf{M}}(\mathbf{R}_j^W)\,(\sqrt{3}p_x\pm p_y)$	$q^+_{\mathbf{M}}(\mathbf{R}_j^W)\,p_z$;	$q_{\mathbf{M}}(\mathbf{R}_j^W)\,p_y$	$q^-_{\mathbf{M}}(\mathbf{R}_j^W)\,p_z$;	a
		$q^+_{\mathbf{M}}(\mathbf{R}_j^W)\,(\sqrt{3}p_x\pm p_y)$		$q^+_{\mathbf{M}}(\mathbf{R}_j^W)\,p_y$	
Γ_2	$q_{\mathbf{M}}(\mathbf{R}_j^W)\,(p_x\mp\sqrt{3}p_y)$	$q^+_{\mathbf{M}}(\mathbf{R}_j^W)\,(p_x\mp\sqrt{3}p_y)$	$q_{\mathbf{M}}(\mathbf{R}_j^W)\,p_x$	$q^+_{\mathbf{M}}(\mathbf{R}_j^W)\,p_x$	a
Γ_3		$q^-_{\mathbf{M}}(\mathbf{R}_j^W)\,(p_x\mp\sqrt{3}p_y)$		$q^-_{\mathbf{M}}(\mathbf{R}_j^W)\,p_x$	a
Γ_4	$q_{\mathbf{M}}(\mathbf{R}_j^W)\,p_z$	$q^-_{\mathbf{M}}(\mathbf{R}_j^W)\,p_z$;	$q_{\mathbf{M}}(\mathbf{R}_j^W)\,p_z$	$q^+_{\mathbf{M}}(\mathbf{R}_j^W)\,p_z$;	a
		$q^-_{\mathbf{M}}(\mathbf{R}_j^W)\,(\sqrt{3}p_x\pm p_y)$		$q^-_{\mathbf{M}}(\mathbf{R}_j^W)\,p_y$	

V. SELECTION RULES: EFFECT OF BAND IR REARRANGEMENT

We show in the following that the selection rules for the observable matrix elements of a Hermitian operator $\mathbb{O}$ taken between Bloch states are not affected by the rearrangement of band IRs discussed in Sec. II G provided the perturbation of a crystal represented by the operator $\mathbb{O}$ preserves translational invariance. This condition for the operator $\mathbb{O}$ is certainly obeyed by the dipole operator $\mathbb{O} = \mathbf{r}$ representing optical transitions, but it does not apply to localized perturbations such as point defects for which anyway the specific location of the defect plays a crucial role [3]. We consider a translation $\boldsymbol{\tau}$ of the coordinate system as introduced in Sec. II G, so that $T = \{\mathbb{1}|\boldsymbol{\tau}\}$ is a unitary operator with $T^\dagger = T^{-1}$. This transforms both the states and operators. A state $|\psi_{J\beta}\rangle$ in the old coordinate system transforming according to the IR Γ_J becomes $|\psi_{J'\beta'}\rangle = T|\psi_{J\beta}\rangle$ transforming according to $\Gamma_{J'} = \Gamma_{\boldsymbol{\tau}} \times \Gamma_J$, with $\Gamma_{\boldsymbol{\tau}} = \{\mathscr{D}^{\mathbf{k}}_{\boldsymbol{\tau}}(g) = \exp(-i\mathbf{b}_g \cdot \boldsymbol{\tau}) : g \in \mathscr{G}_{\mathbf{k}}\}$ [Eq. (67)]. Similarly, $\langle\psi_{I\alpha}|$ transforming according to the IR Γ^*_I becomes $\langle\psi_{I'\alpha'}| = \langle\psi_{I\alpha}|T^\dagger$ transforming according to $\Gamma^*_{I'} = \Gamma^*_{\boldsymbol{\tau}} \times \Gamma^*_I$. Invariance of the operator $\mathbb{O}$ under translations T implies $[\mathbb{O}, T] = 0$, or

$$\mathbb{O}' \equiv T\,\mathbb{O}\,T^{-1} = \mathbb{O}, \tag{95}$$

so that both $\mathbb{O}$ and $\mathbb{O}'$ transform according to the same representation (which need not be irreducible)

$$\Gamma_{\mathbb{O}} = \Gamma_{\mathbb{O}'}. \tag{96}$$

Hence, we get (note $\Gamma^*_{\boldsymbol{\tau}} \times \Gamma_{\boldsymbol{\tau}} = \Gamma_1$)

$$\Gamma^*_{I'} \times \Gamma_{\mathbb{O}'} \times \Gamma_{J'} = \Gamma^*_I \times \Gamma_{\mathbb{O}} \times \Gamma_J, \tag{97}$$

i.e., in the unprimed and primed coordinate system we get the same selection rules. In the primed coordinate system, the matrix elements become

$$\begin{aligned}
\mathbb{O}'_{\alpha'\beta'} &= \langle\psi_{I'\alpha'}|\mathbb{O}'|\psi_{J'\beta'}\rangle && \text{(98a)}\\
&= \langle\psi_{I\alpha}|T^{-1}T\,\mathbb{O}\,T^{-1}T\,|\psi_{J\beta}\rangle && \text{(98b)}\\
&= \langle\psi_{I\alpha}|\mathbb{O}|\psi_{J\beta}\rangle && \text{(98c)}\\
&= \mathbb{O}_{\alpha\beta}. && \text{(98d)}
\end{aligned}$$

Note that for multi-dimensional IRs Γ_J and $\Gamma_{J'} = \Gamma_{\boldsymbol{\tau}} \times \Gamma_J$, we can always choose the representation matrices such that $T|\psi_{J\beta}\rangle = |\psi_{J'\beta}\rangle$, and similarly $\langle\psi_{I\alpha}|T^\dagger = \langle\psi_{I'\alpha}|$, so that Eq. (98) becomes $\mathbb{O}'_{\alpha\beta} = \mathbb{O}_{\alpha\beta}$.

VI. THEORY OF INVARIANTS

A. General theory

The Bloch eigenstates $\Psi^{I\beta}_{n\mathbf{k}}(\mathbf{r})$ at a wave vector $\mathbf{k}$ transform according to an IR Γ_I of the group of the wave vector $\mathscr{G}_{\mathbf{k}}$. The knowledge of these IRs suffices to construct the general form of the effective Hamiltonian characterizing the Bloch eigenstates near the expansion point $\mathbf{k}$ consistent with the symmetry operations in $\mathscr{G}_{\mathbf{k}}$. This method is known as the theory of invariants [3]. The Hamiltonian can be expressed in terms of a general tensor operator denoted as $\boldsymbol{\mathscr{K}}$ that may depend on, e.g., the kinetic wave vector $\boldsymbol{\kappa}$ measured from $\mathbf{k}$, external electric and magnetic fields $\boldsymbol{\mathscr{E}}$ and $\boldsymbol{\mathscr{B}}$, strain $\boldsymbol{\epsilon}$ and spin $\mathbf{S}$. For all group elements $g \in \mathscr{G}_{\mathbf{k}}$, the Hamiltonian $\mathscr{H}(\boldsymbol{\mathscr{K}})$ obeys the invariance condition [3]

$$\mathscr{D}(g)\mathscr{H}(g^{-1}\boldsymbol{\mathscr{K}})\mathscr{D}^{-1}(g) = \mathscr{H}(\boldsymbol{\mathscr{K}}). \tag{99}$$

According to the theory of invariants, each block $\mathscr{H}_{II'}$ of the matrix $\mathscr{H}$ corresponding to a pair of bands transforming according to the IRs Γ_I and $\Gamma_{I'}$ has the form

$$\mathscr{H}_{II'}(\boldsymbol{\mathscr{K}}) = \sum_{i,J} a^{II'}_{iJ} \sum_{l=1}^{L_J} X^J_l \mathscr{K}^{i,J*}_l, \tag{100}$$

where J labels the L_J-dimensional IRs Γ_J contained in the product representation $\Gamma^*_I \times \Gamma_{I'}$, the basis matrices X^J_l and the irreducible tensor operators $\mathscr{K}^i_J$ constructed from the perturbations $\boldsymbol{\mathscr{K}}$ transform according to the IR Γ_J, and $a^{II'}_{iJ}$ are constant prefactors. The index i labels the irreducible tensor operators transforming as Γ_J. In general, we have multiple blocks $\mathscr{H}_{II'}(\boldsymbol{\mathscr{K}})$ corresponding to different bands n and n' transforming according to Γ_I and $\Gamma_{I'}$. To simplify the notation, we drop these additional indices.

B. Effect of band IR rearrangements

A translation of the coordinate system by $\boldsymbol{\tau}$ changes the IR of an eigenfunction $\Psi^I_{n\mathbf{k}}(\mathbf{r})$ from Γ_I to $\Gamma_J = \Gamma_{\boldsymbol{\tau}} \times \Gamma_I$, see Eq. (68). We have

$$\begin{aligned}
\Gamma^*_J \times \Gamma_{J'} &= (\Gamma_{\boldsymbol{\tau}} \times \Gamma_I)^* \times (\Gamma_{\boldsymbol{\tau}} \times \Gamma_{I'}) && \text{(101a)}\\
&= \Gamma^*_I \times \Gamma_{I'}, && \text{(101b)}
\end{aligned}$$

where we used $\Gamma^*_{\boldsymbol{\tau}} \times \Gamma_{\boldsymbol{\tau}} = \Gamma_1$ for one-dimensional IRs $\Gamma_{\boldsymbol{\tau}}$. Therefore, the IRs contained in $\Gamma^*_J \times \Gamma_{J'}$ are equal to the IRs contained in $\Gamma^*_I \times \Gamma_{I'}$. This implies that translations $\boldsymbol{\tau}$ of the coordinate system resulting in a rearrangement of the IRs assigned to the eigenfunctions do not affect the invariant expansion of the Hamiltonian $\mathscr{H}(\boldsymbol{\mathscr{K}})$.

C. Invariant Hamiltonian for MoS_2

As an application of the theory of invariants, we consider monolayer MoS_2. In this material, the lowest conduction and highest valence band are at the points $\mathbf{K}$ and $\mathbf{K}'$ [29], hence we focus on these points (where $\mathscr{G}_{\mathbf{K}} = C_{3h}$). Table III lists the mapping of axial ($\mathbf{A}$) and polar vectors ($\mathbf{P}$) under the relevant symmetry operations. This allows one to confirm the examples for

basis functions listed for C_{3h} in Table XXVII. Crystal momentum $\boldsymbol{\kappa}$ and an electric field $\boldsymbol{\mathscr{E}}$ transform like polar vectors, whereas spin $\mathbf{S}$ and a magnetic field $\boldsymbol{\mathscr{B}}$ transform like axial vectors. Hence we immediately obtain from Table XXVII the lowest-order tensor operators listed in the second column of Table XXII. In general, we obtain higher-order tensor operators using the Clebsch-Gordan coefficients that are tabulated in, e.g., Ref. [56]. However, this procedure is greatly simplified if all IRs of the relevant group are one-dimensional, which holds for C_{3h}. In such a case, the higher-order tensor operators can be constructed using the multiplication table for the IRs that is reproduced for C_{3h} in Table XXX. Irreducible tensor operators are generally not unique. Given two irreducible tensor operators $\mathscr{K}$ and $\mathscr{K}'$ transforming according to the same IR Γ_I, any linear combinations of these tensors transforms likewise irreducibly according to Γ_I [5]. We exploit this freedom to choose linear combinations of irreducible tensors such as κ_-^3 and κ_+^3 that have also a well-defined behavior under time reversal symmetry (see Sec. VI D).

We can also consider the effects of strain. When stress deforms a crystalline solid, the symmetry of the system is altered which changes the energy spectrum of the material. Suppose under a deformation a point $\mathbf{r}$ in a solid undergoes a displacement $\mathbf{u}(\mathbf{r})$. For small homogeneous strain, the symmetric strain tensor is defined as $(i,j=x,y,z)$ [59]

$$\epsilon_{ij} = \frac{1}{2}\left(\frac{\partial u_i}{\partial r_j} + \frac{\partial u_j}{\partial r_i} + \frac{\partial u_k}{\partial r_i}\frac{\partial u_k}{\partial r_j}\right). \tag{102}$$

However, considering MoS_2 as a quasi-2D material, strain due to a perpendicular stress component is not relevant. The components ϵ_{ij} transform like the symmetrized products $\{\kappa_i,\kappa_j\}$ [3] so that we get the lowest-order operators listed in the second column of Table XXII while mixed higher-order tensor operators are listed in the third column of Table XXII.

Since the IRs of C_{3h} are all one-dimensional, the Hamiltonian blocks (100) at the points $\mathbf{K}$ and $\mathbf{K}'$ of MoS_2 are one-dimensional. The 1×1 basis matrices X_1^J can be absorbed into the prefactors $a_{iJ}^{II'}$. Hence, Eq. (100) can be simplified to

$$\mathscr{H}_{II'}(\boldsymbol{\mathscr{K}}) = \sum_i a_i^{II'}\mathscr{K}_l^{i,J*}. \tag{103}$$

The IRs corresponding to the eleven bands at $\mathbf{K}$ and $\mathbf{K}'$ that are dominated by the Mo d and S p orbitals are listed in Table XXIII. Here we focus on constructing a generic 6×6 Hamiltonian consisting of a sequence of bands transforming as $\Gamma_{1/3/2},\Gamma_{2/1/3},\Gamma_{3/2/1},\Gamma_{4/6/5},\Gamma_{5/4/6}$, and $\Gamma_{6/5/4}$ respectively, (realized, e.g., by the bands v_1,c_1,c_3,c_2,v_3, and v_2; additional bands will replicate the behavior obtained for these bands). For these bands, the Hamiltonian matrix elements $\mathscr{H}^{\mathbf{K}}(\boldsymbol{\mathscr{K}})_{II'}$ contain tensors $\mathscr{K}$ transforming as

$$(\Gamma_I^*\times\Gamma_{I'}) = \begin{pmatrix} \Gamma_1 & \Gamma_2 & \Gamma_3 & \Gamma_4 & \Gamma_5 & \Gamma_6\\ \Gamma_3 & \Gamma_1 & \Gamma_2 & \Gamma_6 & \Gamma_4 & \Gamma_5\\ \Gamma_2 & \Gamma_3 & \Gamma_1 & \Gamma_5 & \Gamma_6 & \Gamma_4\\ \Gamma_4 & \Gamma_5 & \Gamma_6 & \Gamma_1 & \Gamma_2 & \Gamma_3\\ \Gamma_6 & \Gamma_4 & \Gamma_5 & \Gamma_3 & \Gamma_1 & \Gamma_2\\ \Gamma_5 & \Gamma_6 & \Gamma_4 & \Gamma_2 & \Gamma_3 & \Gamma_1 \end{pmatrix}, \tag{104}$$

see Table XXX (Appendix C).

D. Time reversal

At the points $\mathbf{K}$ and $\mathbf{K}'=-\mathbf{K}$ with $\mathscr{G}_{\mathbf{K}}=C_{3h}$, the Bloch functions $\Psi_{\mathbf{K}}^I$ and the corresponding time reversed functions $\Theta\,\Psi_{\mathbf{K}}^I$ are linearly dependent on each other [case (a) according to Eq. (79), see also Table X]. Also, the eigenfunctions at $\mathbf{K}$ can be mapped onto the eigenfunctions at $-\mathbf{K}$ by a vertical reflection $R=\sigma_v^{(2)}$ or a 180° rotation $C_2'^{(2)}$, which is case (2) as defined in Eq. (80). [These two operations R are elements of the group D_{3h}, the point group of MoS_2, see Fig. 2(a).] Hence, for a Bloch state $\Psi_{\mathbf{K}}^I$ of band I, the time reversed state $\Theta\,\Psi_{\mathbf{K}}^I$ and the spatially transformed state $R\,\Psi_{\mathbf{K}}^I$, with $R=\sigma_v^{(2)},C_2'^{(2)}$, obey the linear relation

$$\Theta\,\Psi_{\mathbf{K}}^I = (\Psi_{\mathbf{K}}^I)^* = t_R^I R\,\Psi_{\mathbf{K}}^I, \tag{105}$$

where t_R^I is a phase factor (a unitary matrix if the dimensions of the IRs Γ_I and Γ_I^* was larger than one) that depends on the choice for the operation R. For the phase conventions used in Table XXIV, we have

$$t_{\sigma_v^{(2)}}^I = \begin{cases} 1, & I=1,2,3\\ -1, & I=4,5,6, \end{cases} \tag{106a}$$

$$t_{C_2'^{(2)}}^I = 1, \quad I=1,\ldots,6. \tag{106b}$$

The matrix $\mathscr{H}(\boldsymbol{\mathscr{K}})$ must then satisfy the additional condition

$$(t_R)^{-1}\,\mathscr{H}(R^{-1}\,\boldsymbol{\mathscr{K}})\,t_R = \mathscr{H}^*(\zeta\,\boldsymbol{\mathscr{K}}) = \mathscr{H}^t(\zeta\,\boldsymbol{\mathscr{K}}). \tag{107}$$

where t_R is a diagonal matrix with elements $(t_R)_{II}=t_R^I$, $\zeta=+1$ (-1) for quantities that are even (odd) under time reversal such as $\boldsymbol{\mathscr{E}}$ and $\boldsymbol{\epsilon}$ ($\boldsymbol{\kappa}$, $\boldsymbol{\mathscr{B}}$, and $\mathbf{S}$), $*$ denotes complex conjugation and t transposition. The components of polar vectors $\mathbf{P}$ and axial vectors $\mathbf{A}$ transform under $\sigma_v^{(2)}$ and $C_2'^{(2)}$ as follows (see Table III)

$$\sigma_v^{(2)}\,P_\pm = -P_\mp, \qquad C_2'^{(2)}\,P_\pm = -P_\mp, \tag{108a}$$

$$\sigma_v^{(2)}\,P_z = P_z, \qquad C_2'^{(2)}\,P_z = -P_z, \tag{108b}$$

$$\sigma_v^{(2)}\,A_\pm = A_\mp, \qquad C_2'^{(2)}\,A_\pm = -A_\mp, \tag{108c}$$

$$\sigma_v^{(2)}\,A_z = -A_z, \qquad C_2'^{(2)}\,A_z = -A_z. \tag{108d}$$

It follows from Eq. (107) whether off-diagonal terms in $\mathscr{H}(\boldsymbol{\mathscr{K}})$ have real or imaginary prefactors. Tensor operators that give rise to invariants with real prefactors

TABLE XXII. Irreducible tensor operators for the point group C_{3h}. For off-diagonal terms in the Hamiltonian $\mathscr{H}(\boldsymbol{\mathscr{K}})$, using the phase conventions in Table XXIV, the bold-face tensor operators give rise to invariants with purely real prefactors, while the remaining tensor operators give rise to invariants with purely imaginary prefactors. At the same time, these phase conventions and time-reversal symmetry imply that invariants appearing on the diagonal of $\mathscr{H}(\boldsymbol{\mathscr{K}})$ (which transform as Γ_1) can only be formed from tensor operators listed in bold, the remaining tensor operators correspond to invariants that are forbidden by time reversal symmetry. Tensors transforming according to Γ_3 and Γ_6 are the Hermitean adjoint of the tensors transforming according to Γ_2 and Γ_5, respectively. Notation: $V_\pm = V_x \pm iV_y$ with $\mathbf{V} = \boldsymbol{\kappa}, \boldsymbol{\mathscr{B}}, \boldsymbol{\mathscr{C}}$, and $\epsilon_\pm = \epsilon_{xx} - \epsilon_{yy} \pm 2i\epsilon_{xy}$, $\epsilon_\parallel = \epsilon_{xx} + \epsilon_{yy}$.

	lowest order	higher order
Γ_1	$\mathbb{1}; \boldsymbol{\mathscr{B}_z}; \boldsymbol{S_z}; \boldsymbol{\epsilon_\parallel}$	$\boldsymbol{\kappa^2}; \boldsymbol{\kappa_-^3 + \kappa_+^3}; i\kappa_-^3 - i\kappa_+^3; \boldsymbol{\kappa^4}; \kappa_-\mathscr{C}_+ + \kappa_+\mathscr{C}_-; \boldsymbol{i\kappa_-\mathscr{C}_+ - i\kappa_+\mathscr{C}_-}; \boldsymbol{\kappa^2\mathscr{B}_z}; \boldsymbol{\kappa^2 S_z}$; $\boldsymbol{\kappa_-\epsilon_- + \kappa_+\epsilon_+}; i\kappa_-\epsilon_- - i\kappa_+\epsilon_+; \boldsymbol{\kappa^2\epsilon_\parallel}; \boldsymbol{\mathscr{B}_z S_z}; \boldsymbol{\mathscr{B}_- S_+ + \mathscr{B}_+ S_-}; i\mathscr{B}_- S_+ - i\mathscr{B}_+ S_-; \boldsymbol{\mathscr{B}_z\epsilon_\parallel}$; $\mathscr{C}_-\epsilon_- + \mathscr{C}_+\epsilon_+; \boldsymbol{i\mathscr{C}_-\epsilon_- - i\mathscr{C}_+\epsilon_+}; \boldsymbol{S_z\epsilon_\parallel}; \boldsymbol{\kappa_-\mathscr{B}_- S_- + \kappa_+\mathscr{B}_+ S_+}; i\kappa_-\mathscr{B}_- S_- - i\kappa_+\mathscr{B}_+ S_+$; $\mathscr{C}_z(\kappa_+ S_- + \kappa_- S_+); \boldsymbol{i\mathscr{C}_z(\kappa_+ S_- - \kappa_- S_+)}; \boldsymbol{\mathscr{B}_z(\kappa_-\epsilon_- + \kappa_+\epsilon_+)}; i\mathscr{B}_z(\kappa_-\epsilon_- - \kappa_+\epsilon_+)$; $\kappa_+\mathscr{C}_+\epsilon_- + \kappa_-\mathscr{C}_-\epsilon_+; \boldsymbol{i\kappa_+\mathscr{C}_+\epsilon_- - i\kappa_-\mathscr{C}_-\epsilon_+}$
Γ_2	$\boldsymbol{\kappa_+}; \mathscr{C}_+; \boldsymbol{\epsilon_-}$	$\boldsymbol{\kappa_-^2}; \boldsymbol{\kappa^2\kappa_+}; \boldsymbol{\kappa^2\kappa_-^2}; \boldsymbol{\kappa_+^4}; \kappa_-\mathscr{C}_-; \kappa^2\mathscr{C}_+; \boldsymbol{\kappa_+^2\mathscr{C}_-}; \boldsymbol{\kappa_+\mathscr{B}_z}; \boldsymbol{\kappa_-^2\mathscr{B}_z}; \boldsymbol{\kappa_+ S_z}; \boldsymbol{\kappa_-^2 S_z}; \boldsymbol{\kappa_-\epsilon_+}; \boldsymbol{\kappa^2\epsilon_-}$; $\mathscr{C}_+ S_z; \mathscr{C}_z S_+; \boldsymbol{\mathscr{C}_-\epsilon_+}; \mathscr{B}_z\mathscr{C}_+; \mathscr{B}_+\mathscr{C}_z; \boldsymbol{\mathscr{B}_- S_-}; \boldsymbol{\kappa_+\mathscr{B}_+ S_-}; \kappa_+\mathscr{C}_+\epsilon_+$
Γ_4	$\mathscr{C}_z$	$\boldsymbol{\kappa_+\mathscr{B}_- + \kappa_-\mathscr{B}_+}; i\kappa_+\mathscr{B}_- - i\kappa_-\mathscr{B}_+; \boldsymbol{\kappa_+ S_- + \kappa_- S_+}; i\kappa_+ S_- - i\kappa_- S_+$; $\mathscr{B}_-\mathscr{C}_+ + \mathscr{B}_+\mathscr{C}_-; \boldsymbol{i\mathscr{B}_-\mathscr{C}_+ - i\mathscr{B}_+\mathscr{C}_-}; \mathscr{C}_+ S_- + \mathscr{C}_- S_+; \boldsymbol{i\mathscr{C}_+ S_- - i\mathscr{C}_- S_+}$; $\mathscr{B}_-\epsilon_- + \mathscr{B}_+\epsilon_+; \boldsymbol{i\mathscr{B}_-\epsilon_- - i\mathscr{B}_+\epsilon_+}; S_-\epsilon_- + S_+\epsilon_+; \boldsymbol{iS_-\epsilon_- - iS_+\epsilon_+}$
Γ_5	$\boldsymbol{\mathscr{B}_+}; \boldsymbol{S_+}$	$\kappa_+\mathscr{C}_z; \kappa_-^2\mathscr{C}_z; \boldsymbol{\kappa_-\mathscr{B}_-}; \boldsymbol{\kappa_- S_-}; \boldsymbol{\kappa^2\mathscr{B}_+}; \boldsymbol{\kappa^2 S_+}; \boldsymbol{\kappa_+^2\mathscr{B}_-}; \boldsymbol{\kappa_+^2 S_-}; \boldsymbol{\mathscr{C}_z\mathscr{C}_+}; \mathscr{C}_-\mathscr{B}_-; \mathscr{C}_- S_-$; $\boldsymbol{\mathscr{B}_+\mathscr{B}_z}; \boldsymbol{\mathscr{B}_+ S_z}; \boldsymbol{\mathscr{B}_z S_+}; \boldsymbol{S_z S_+}; \mathscr{C}_z\epsilon_-; \boldsymbol{\mathscr{B}_-\epsilon_+}; \boldsymbol{S_-\epsilon_+}; \kappa_+\mathscr{C}_- S_+; \boldsymbol{\kappa_-\mathscr{C}_z\epsilon_+}; \boldsymbol{\kappa_+\mathscr{B}_+\epsilon_+}; \boldsymbol{\kappa_+ S_+\epsilon_+}$

TABLE XXIII. IRs $\Gamma_{i/j/k}$ for the eleven TB bands [30] in MoS_2 obtained from Mo d and S p orbitals at the $\mathbf{K}$ point for coordinate systems $\alpha = a/b/c$ in Fig. 1. We denote the bands by $c_4, \ldots, c_1, v_1, \ldots, v_7$ arranged in order of decreasing energy. The seven bands $c_3, \ldots, v_4$ are used in Ref. [31], while the three bands c_3, c_1, and v_1 are used in Ref. [60]. The main (second) atomic orbital for each band is given in the third (fourth) column (compare Table X).

band	IR	main orbital	second orbital
c_4	$\Gamma_{6/5/4}$	$d_{xz} + id_{yz}$	p_z
c_3	$\Gamma_{3/2/1}$	$d_{x^2-y^2} - id_{xy}$	p_z
c_2	$\Gamma_{4/6/5}$	$d_{xz} - id_{yz}$	$p_x + ip_y$
c_1	$\Gamma_{2/1/3}$	d_{z^2}	$p_x - ip_y$
v_1	$\Gamma_{1/3/2}$	$d_{x^2-y^2} + id_{xy}$	$p_x + ip_y$
v_2	$\Gamma_{6/5/4}$	p_z	$d_{xz} + id_{yz}$
v_3	$\Gamma_{5/4/6}$	$p_x - ip_y$	
v_4	$\Gamma_{3/2/1}$	p_z	$d_{x^2-y^2} - id_{xy}$
v_5	$\Gamma_{1/3/2}$	$p_x + ip_y$	$d_{x^2-y^2} + id_{xy}$
v_6	$\Gamma_{2/1/3}$	$p_x - ip_y$	d_{z^2}
v_7	$\Gamma_{4/6/5}$	$p_x + ip_y$	$d_{xz} - id_{yz}$

are marked in bold in Table XXII. Furthermore, condition (107) provides a general criterion which terms are allowed by time-reversal symmetry on the diagonal of the Hamiltonian [when the tensor operators must transform according to the identity IR Γ_1, see Eq. (104)]. Here, our phase conventions imply that invariants (with real prefactors) can only be formed from tensor operators marked in bold in Table XXII. Thus, for example, on the diagonal of the Hamiltonian the third-order trigonal term $\kappa_+^3 + \kappa_-^3 = 2\kappa_x(\kappa_x^2 - 3\kappa_y^2)$, as well as the field-dependent terms $i\kappa_-\mathscr{C}_+ - i\kappa_+\mathscr{C}_- = 2(\kappa_y\mathscr{C}_x - \kappa_x\mathscr{C}_y)$ and $\mathscr{B}_+ S_- + \mathscr{B}_- S_+ = 2(\mathscr{B}_x S_x + \mathscr{B}_y S_y)$ are allowed by symmetry and thus present in the Hamiltonian. However, the terms $i\kappa_-^3 - i\kappa_+^3 = 2\kappa_y(3\kappa_x^2 - \kappa_y^2)$, $\kappa_+\mathscr{C}_- + \kappa_-\mathscr{C}_+ = 2(\kappa_x\mathscr{C}_x + \kappa_y\mathscr{C}_y)$ and $i\mathscr{B}_- S_+ - i\mathscr{B}_+ S_- = 2(\mathscr{B}_y S_x - \mathscr{B}_x S_y)$ are allowed by spatial symmetry; but these terms are forbidden by time-reversal symmetry and hence do not appear in the Hamiltonian. (They are allowed, though, as off-diagonal terms coupling different bands transforming according to the same IR, when these terms will have imaginary prefactors.)

Using the transformation R, one can derive the effective Hamiltonian for the valley $\mathbf{K}'$ using the transformation

$$\mathscr{H}^{\mathbf{K}'}(\boldsymbol{\mathscr{K}}) = \mathscr{H}^{\mathbf{K}}(R^{-1}\,\boldsymbol{\mathscr{K}}). \tag{109}$$

Alternatively, time reversal can be used, see Eq. (107). Note that the definition of $\mathscr{H}^{\mathbf{K}'}(\boldsymbol{\mathscr{K}})$ relative to $\mathscr{H}^{\mathbf{K}}(\boldsymbol{\mathscr{K}})$ depends on the phase conventions used for the basis functions $\Psi^I_{\mathbf{K}'}$ relative to the phase conventions used for $\Psi^I_{\mathbf{K}}$.

E. Analysis of the invariant expansion

The invariant Hamiltonian at the point $\mathbf{K}$ of the BZ becomes in lowest order of the wave vector $\boldsymbol{\kappa}$ and spin-orbit coupling (spin $\mathbf{S}$)

$$\mathscr{H}(\boldsymbol{\kappa}, \mathbf{S}) = \mathscr{H}_0 + \mathscr{H}_\kappa + \mathscr{H}_{\rm so} \tag{110}$$

with

$$\mathscr{H}_0 = \begin{pmatrix} E_1 & 0 & 0 & 0 & 0 & 0 \\ 0 & E_2 & 0 & 0 & 0 & 0 \\ 0 & 0 & E_3 & 0 & 0 & 0 \\ 0 & 0 & 0 & E_4 & 0 & 0 \\ 0 & 0 & 0 & 0 & E_5 & 0 \\ 0 & 0 & 0 & 0 & 0 & E_6 \end{pmatrix}, \tag{111a}$$

TABLE XXIV. Linear relation between the Bloch functions at $\mathbf{K}' = -\mathbf{K}$ obtained via time reversal Θ and via a spatial transformation R applied to a Bloch function $\Psi^I_{\mathbf{K}}$ at wave vector $\mathbf{k} = \mathbf{K}$. The $\mathbf{K}$ point in the Brillouin zone is mapped onto $-\mathbf{K}$ by a vertical reflection $R = \sigma_v^{(2)}$ and by a rotation $R = C_2'^{(2)}$, see Fig. 2(a).

IR	$\Psi^I_{\mathbf{K}}$	$\Theta\,\Psi^I_{\mathbf{K}}$	$\sigma_v^{(2)}\,\Psi^I_{\mathbf{K}}$	$C_2'^{(2)}\,\Psi^I_{\mathbf{K}}$
Γ_1	$q_{\mathbf{K}}(\mathbf{R}_j^{\mathrm{Mo}})\,(d_{x^2-y^2}+id_{xy})$;	$q_{\mathbf{K}'}(\mathbf{R}_j^{\mathrm{Mo}})\,(d_{x^2-y^2}-id_{xy})$;	$\Theta\,\Psi^1_{\mathbf{K}}$	$\Theta\,\Psi^1_{\mathbf{K}}$
	$iq^+_{\mathbf{K}}(\mathbf{R}_j^{\mathrm{S}})\,(p_x+ip_y)$	$-iq^+_{\mathbf{K}'}(\mathbf{R}_j^{\mathrm{S}})\,(p_x-ip_y)$		
Γ_2	$q_{\mathbf{K}}(\mathbf{R}_j^{\mathrm{Mo}})\,d_{z^2}$;	$q_{\mathbf{K}'}(\mathbf{R}_j^{\mathrm{Mo}})\,d_{z^2}$;	$\Theta\,\Psi^2_{\mathbf{K}}$	$\Theta\,\Psi^2_{\mathbf{K}}$
	$iq^+_{\mathbf{K}}(\mathbf{R}_j^{\mathrm{S}})\,(p_x-ip_y)$	$-iq^+_{\mathbf{K}'}(\mathbf{R}_j^{\mathrm{S}})\,(p_x+ip_y)$		
Γ_3	$q_{\mathbf{K}}(\mathbf{R}_j^{\mathrm{Mo}})\,(d_{x^2-y^2}-id_{xy})$;	$q_{\mathbf{K}'}(\mathbf{R}_j^{\mathrm{Mo}})\,(d_{x^2-y^2}+id_{xy})$;	$\Theta\,\Psi^3_{\mathbf{K}}$	$\Theta\,\Psi^3_{\mathbf{K}}$
	$q^-_{\mathbf{K}}(\mathbf{R}_j^{\mathrm{S}})\,p_z$	$q^-_{\mathbf{K}'}(\mathbf{R}_j^{\mathrm{S}})\,p_z$		
Γ_4	$q_{\mathbf{K}}(\mathbf{R}_j^{\mathrm{Mo}})\,(d_{xz}-id_{yz})$;	$q_{\mathbf{K}'}(\mathbf{R}_j^{\mathrm{Mo}})\,(d_{xz}+id_{yz})$;	$-\Theta\,\Psi^4_{\mathbf{K}}$	$\Theta\,\Psi^4_{\mathbf{K}}$
	$q^-_{\mathbf{K}}(\mathbf{R}_j^{\mathrm{S}})\,(p_x+ip_y)$	$q^-_{\mathbf{K}'}(\mathbf{R}_j^{\mathrm{S}})\,(p_x-ip_y)$		
Γ_5	$q^-_{\mathbf{K}}(\mathbf{R}_j^{\mathrm{S}})\,(p_x-ip_y)$	$q^-_{\mathbf{K}'}(\mathbf{R}_j^{\mathrm{S}})\,(p_x+ip_y)$	$-\Theta\,\Psi^5_{\mathbf{K}}$	$\Theta\,\Psi^5_{\mathbf{K}}$
Γ_6	$q_{\mathbf{K}}(\mathbf{R}_j^{\mathrm{Mo}})\,(d_{xz}+id_{yz})$;	$q_{\mathbf{K}'}(\mathbf{R}_j^{\mathrm{Mo}})\,(d_{xz}-id_{yz})$;	$-\Theta\,\Psi^6_{\mathbf{K}}$	$\Theta\,\Psi^6_{\mathbf{K}}$
	$iq^+_{\mathbf{K}}(\mathbf{R}_j^{\mathrm{S}})\,p_z$	$-iq^+_{\mathbf{K}'}(\mathbf{R}_j^{\mathrm{S}})\,p_z$		

$$\mathscr{H}_{\boldsymbol{\kappa}} = \begin{pmatrix} 0 & \gamma_{12}\kappa_+ & \gamma_{13}\kappa_- & 0 & 0 & 0 \\ \gamma_{12}\kappa_- & 0 & \gamma_{23}\kappa_+ & 0 & 0 & 0 \\ \gamma_{13}\kappa_+ & \gamma_{23}\kappa_- & 0 & 0 & 0 & 0 \\ 0 & 0 & 0 & 0 & \gamma_{45}\kappa_+ & \gamma_{46}\kappa_- \\ 0 & 0 & 0 & \gamma_{45}\kappa_- & 0 & \gamma_{56}\kappa_+ \\ 0 & 0 & 0 & \gamma_{46}\kappa_+ & \gamma_{56}\kappa_- & 0 \end{pmatrix}, \tag{111b}$$

$$\mathscr{H}_{\mathrm{so}} = \begin{pmatrix} \lambda_{11}S_z & 0 & 0 & 0 & \lambda_{15}S_+ & \lambda_{16}S_- \\ 0 & \lambda_{22}S_z & 0 & \lambda_{24}S_- & 0 & \lambda_{26}S_+ \\ 0 & 0 & \lambda_{33}S_z & \lambda_{34}S_+ & \lambda_{35}S_- & 0 \\ 0 & \lambda_{24}S_+ & \lambda_{34}S_- & \lambda_{44}S_z & 0 & 0 \\ \lambda_{15}S_- & 0 & \lambda_{35}S_+ & 0 & \lambda_{55}S_z & 0 \\ \lambda_{16}S_+ & \lambda_{26}S_- & 0 & 0 & 0 & \lambda_{66}S_z \end{pmatrix}, \tag{111c}$$

where E_I, γ_{ij}, and λ_{ij} are material-dependent real parameters.

The lowest-order strain-dependent terms become

$$\mathscr{H}_{\boldsymbol{\epsilon}} = \begin{pmatrix} \xi_{11}\epsilon_\parallel & \xi_{12}\epsilon_- & \xi_{13}\epsilon_+ & 0 & 0 & 0 \\ \xi_{12}\epsilon_+ & \xi_{22}\epsilon_\parallel & \xi_{23}\epsilon_- & 0 & 0 & 0 \\ \xi_{13}\epsilon_- & \xi_{23}\epsilon_+ & \xi_{33}\epsilon_\parallel & 0 & 0 & 0 \\ 0 & 0 & 0 & \xi_{44}\epsilon_\parallel & \xi_{45}\epsilon_- & \xi_{46}\epsilon_+ \\ 0 & 0 & 0 & \xi_{45}\epsilon_+ & \xi_{55}\epsilon_\parallel & \xi_{56}\epsilon_- \\ 0 & 0 & 0 & \xi_{46}\epsilon_- & \xi_{56}\epsilon_+ & \xi_{66}\epsilon_\parallel \end{pmatrix} \tag{112}$$

with real parameters ξ_{ij}. The effect of electric and magnetic fields $\boldsymbol{\mathscr{E}}$ and $\boldsymbol{\mathscr{B}}$ can also be included in the Hamiltonian (110). For the electric field, we add on the diagonal a scalar potential $e\boldsymbol{\mathscr{E}}\cdot\mathbf{r}$ and we replace crystal momentum by kinetic momentum $\hbar\boldsymbol{\kappa} = -i\hbar\boldsymbol{\nabla} + e\mathbf{A}$, where $\mathbf{A}$ is the vector potential due to the magnetic field. In addition, we may have terms that depend explicitly on the fields $\boldsymbol{\mathscr{E}}$ and $\boldsymbol{\mathscr{B}}$. The in-plane components $\mathscr{E}_x$ and $\mathscr{E}_y$ transform spatially like the wave vector components κ_x and κ_y. However, $\boldsymbol{\mathscr{E}}$ is even under time reversal symmetry, whereas $\boldsymbol{\kappa}$ is odd. In lowest order, the $\boldsymbol{\mathscr{E}}$ dependent terms become

$$\mathscr{H}_{\boldsymbol{\mathscr{E}}} = \begin{pmatrix} 0 & \eta_{12}\mathscr{E}_+ & \eta_{13}\mathscr{E}_- & \eta_{14}\mathscr{E}_z & 0 & 0 \\ \eta_{12}^*\mathscr{E}_- & 0 & \eta_{23}\mathscr{E}_+ & 0 & \eta_{25}\mathscr{E}_z & 0 \\ \eta_{13}^*\mathscr{E}_+ & \eta_{23}^*\mathscr{E}_- & 0 & 0 & 0 & \eta_{36}\mathscr{E}_z \\ \eta_{14}^*\mathscr{E}_z & 0 & 0 & 0 & \eta_{45}\mathscr{E}_+ & \eta_{46}\mathscr{E}_- \\ 0 & \eta_{25}^*\mathscr{E}_z & 0 & \eta_{45}^*\mathscr{E}_- & 0 & \eta_{56}\mathscr{E}_+ \\ 0 & 0 & \eta_{36}^*\mathscr{E}_z & \eta_{46}^*\mathscr{E}_+ & \eta_{56}^*\mathscr{E}_- & 0 \end{pmatrix} \tag{113}$$

with imaginary prefactors η_{ij}. Since $\boldsymbol{\mathscr{B}}$ transforms in the same way as the spin $\mathbf{S}$ both under spatial transformations and time reversal, the $\boldsymbol{\mathscr{B}}$-dependent terms are similar to Eq. (111c)

$$\mathscr{H}_{\boldsymbol{\mathscr{B}}} = \begin{pmatrix} \beta_{11}\mathscr{B}_z & 0 & 0 & 0 & \beta_{15}\mathscr{B}_+ & \beta_{16}\mathscr{B}_- \\ 0 & \beta_{22}\mathscr{B}_z & 0 & \beta_{24}\mathscr{B}_- & 0 & \beta_{26}\mathscr{B}_+ \\ 0 & 0 & \beta_{33}\mathscr{B}_z & \beta_{34}\mathscr{B}_+ & \beta_{35}\mathscr{B}_- & 0 \\ 0 & \beta_{24}\mathscr{B}_+ & \beta_{34}\mathscr{B}_- & \beta_{44}\mathscr{B}_z & 0 & 0 \\ \beta_{15}\mathscr{B}_- & 0 & \beta_{35}\mathscr{B}_+ & 0 & \beta_{55}\mathscr{B}_z & 0 \\ \beta_{16}\mathscr{B}_+ & \beta_{26}\mathscr{B}_- & 0 & 0 & 0 & \beta_{66}\mathscr{B}_z \end{pmatrix} \tag{114}$$

with real parameters β_{ij}.

We can project the multi-band Hamiltonian (110) on a subspace containing the bands of interest using quasi-degenerate perturbation theory or Löwdin partitioning [5]. This gives rise to higher-order terms in the effective Hamiltonian that may include also mixed terms proportional to products of $\boldsymbol{\kappa}$, $\mathbf{S}$, $\boldsymbol{\epsilon}$, $\boldsymbol{\mathscr{E}}$, and $\boldsymbol{\mathscr{B}}$. In particular, in the presence of a magnetic field $\boldsymbol{\mathscr{B}}$, the components of crystal momentum $\hbar\boldsymbol{\kappa} = -i\hbar\boldsymbol{\nabla} + e\mathbf{A}$ do not commute, $[\kappa_x, \kappa_y] = (e/i\hbar)\mathscr{B}_z$, so that antisymmetrized products of κ_x and κ_y appearing in higher-order perturbation theory give rise to terms proportional to $\mathscr{B}_z$. Similarly, terms

proportional to in-plane electric fields $\mathscr{E}_x, \mathscr{E}_y$ appear because of the presence of the scalar potential $e\boldsymbol{\mathscr{E}} \cdot \mathbf{r}$ and the relation $[r_i, \kappa_j] = i\delta_{ij}$.

VII. CONCLUSIONS

Starting from a TB approach, we have developed a comprehensive theory to derive the IRs characterizing the Bloch eigenstates in a crystal by decomposing the TB basis functions into localized symmetry-adapted atomic orbitals and crystal-periodic symmetry-adapted plane waves. Both the symmetry-adapted atomic orbitals and the symmetry-adapted plane waves can easily be tabulated, thus accelerating the design and exploration of new materials. The symmetry-adapted basis functions block-diagonalize the TB Hamiltonian, which naturally facilitates further analysis of the band structure. While our analysis focused for clarity on symmorphic space groups, our theory can readily be generalized to non-symmorphic groups.

The present work was motivated by the goal to develop a systematic theory of effective multi-band Hamiltonians for the dynamics of Bloch electrons in external fields that break the symmetry of the crystal structure. Yet our general symmetry analysis of Bloch states will likely be useful for other applications, too.

ACKNOWLEDGMENTS

We appreciate stimulating discussions with G. Burkard, A. Kormányos, and U. Zülicke This work was supported by the NSF under Grant No. DMR-1310199. Work at Argonne was supported by DOE BES under Contract No. DE-AC02-06CH11357.

Appendix A: Projection operators

A general method to identify the IRs of the eigenstates of a Hamiltonian uses projection operators [3, 19, 38, 39]. Given a symmetry group G with IRs Γ_I, we can project a general function $f(\mathbf{r})$ onto its components $f_{I\beta}(\mathbf{r})$ transforming according to the βth component of the IR Γ_I of G. Here the projection operators $\Pi_{I\beta}$ are

$$\Pi_{I\beta} \equiv \frac{n_I}{h} \sum_g \mathscr{D}_I(g)^*_{\beta\beta}\, P(g), \tag{A1}$$

where h is the order of the group G, n_I is the dimensionality of the IR Γ_I, $\mathscr{D}_I(g)$ are the representation matrices for Γ_I, and $P(g)$ are the symmetry operators corresponding to $g \in G$. Often, we denote $P(g)$ simply as g. If we are not interested in a particular component β of Γ_I, we can use the "coarse-grained" projection operators

$$\Pi_I \equiv \sum_\beta \Pi_{I\beta} = \frac{n_I}{h} \sum_g \chi_I(g)^*\, P(g), \tag{A2}$$

where $\chi_I(g) \equiv \operatorname{tr} \mathscr{D}_I(g)$ are the characters for Γ_I. For one-dimensional IRs, the operators Π_I become equivalent to $\Pi_{I\beta}$. The projection operators obey the completeness relation

$$\sum_{I,\beta} \Pi_{I\beta} = \sum_I \Pi_I = \mathbb{1}. \tag{A3}$$

Appendix B: Rearrangement lemma for IRs

Generally, if Γ_0 is a one-dimensional IR of a group G, then for any IR Γ_I of G, the product representation $\Gamma_{I'} = \Gamma_0 \times \Gamma_I$ is irreducible. If two IRs Γ_I and Γ_J of G are (in)equivalent, then the IRs $\Gamma_{I'} = \Gamma_0 \times \Gamma_I$ and $\Gamma_{J'} = \Gamma_0 \times \Gamma_J$ are also (in)equivalent. Hence, a multiplication of the IRs of G by Γ_0 simply rearranges the sequence of IRs of G. These statements can be proven as follows: For the element $g \in G$, we denote the characters for the IRs Γ_0 and Γ_I by $\chi_0(g)$ and $\chi_I(g)$ respectively. Hence the character of the representation $\Gamma_{I'}$ becomes $\chi_{I'}(g) = \chi_0(g)\,\chi_I(g)$. Since Γ_0 is one-dimensional, its characters are also its unitary representation matrices obeying $|\chi_0(g)|^2 = 1$. Using the orthogonality relations for characters we get

$$\sum_g |\chi_{I'}(g)|^2 = \sum_g |\chi_0(g)\,\chi_I(g)|^2 \tag{B1a}$$

$$= \sum_g |\chi_0(g)|^2\, |\chi_I(g)|^2 \tag{B1b}$$

$$= \sum_g |\chi_I(g)|^2 = h, \tag{B1c}$$

where h is the order of the group. Hence $\Gamma_{I'} = \Gamma_0 \times \Gamma_I$ is irreducible if Γ_I is irreducible. Now consider two IRs $\Gamma_{I'} = \Gamma_0 \times \Gamma_I$ and $\Gamma_{J'} = \Gamma_0 \times \Gamma_J$. Using again the orthogonality relations for characters we get

$$\sum_g \chi^*_{I'}(g)\chi_{J'}(g) = \sum_g \chi^*_I(g)\,\chi^*_0(g)\,\chi_0(g)\,\chi_J(g) \tag{B2a}$$

$$= \sum_g \chi^*_I(g)\,\chi_J(g) = h\,\delta_{IJ}, \tag{B2b}$$

so that $\Gamma_{I'}$ and $\Gamma_{J'}$ are indeed (in)equivalent if Γ_I and Γ_J are (in)equivalent.

Appendix C: Group tables

Character tables and basis functions for the groups D_{3h}, D_{2h}, C_{3h}, C_{2v}, and C_{2h} are reproduced in Tables XXV – XXIX following the designations by Koster *et al.* [39]. The second column in each table gives the designations for the IRs used by Dresselhaus *et al.* [39]. Examples of basis functions that transform irreducibly according to the different IRs are listed in the last column. These functions are expressed in terms of the cartesian components of polar ($\mathbf{P}$) and axial ($\mathbf{A}$) vectors using

the coordinate systems defined for the respective groups in Figs. 2, 4, and 6. Finally, we reproduce in Table XXX the multiplication table for the IRs of the group C_{3h} [56].

TABLE XXV. Character table and basis functions for the group D_{3h} [56]. The coordinate system for the basis functions is defined in Fig. 2(a).

		E	$2C_3$	$3C_2'^{(i)}$	σ_h	$2S_3$	$3\sigma_v^{(jk)}$	bases
Γ_1	A_1'	1	1	1	1	1	1	$\mathbb{1}$
Γ_2	A_2'	1	1	-1	1	1	-1	A_z
Γ_3	A_1''	1	1	1	-1	-1	-1	P_zA_z
Γ_4	A_2''	1	1	-1	-1	-1	1	P_z
Γ_5	E''	2	-1	0	-2	1	0	A_x, A_y
Γ_6	E'	2	-1	0	2	-1	0	P_x, P_y

TABLE XXVI. Character table and basis functions for the group D_{2h} [56]. The coordinate system for the basis functions is defined in Fig. 4(c-e).

		E	C_2	C_2'	C_2''	I	σ_v	σ_v'	σ_v''	bases $[c(e)]$	$[d]$
Γ_1^+	A_{1g}	1	1	1	1	1	1	1	1	$\mathbb{1}$	$\mathbb{1}$
Γ_2^+	B_{2g}	1	-1	1	-1	1	-1	1	-1	$\sqrt{3}A_x \pm A_y$	A_y
Γ_3^+	B_{1g}	1	1	-1	-1	1	1	-1	-1	A_z	A_z
Γ_4^+	B_{3g}	1	-1	-1	1	1	-1	-1	1	$A_x \mp \sqrt{3}A_y$	A_x
Γ_1^-	A_{1u}	1	1	1	1	-1	-1	-1	-1		$P_xP_yP_z$
Γ_2^-	B_{2u}	1	-1	1	-1	-1	1	-1	1	$\sqrt{3}P_x \pm P_y$	P_y
Γ_3^-	B_{1u}	1	1	-1	-1	-1	-1	1	1	P_z	P_z
Γ_4^-	B_{3u}	1	-1	-1	1	-1	1	1	-1	$P_x \mp \sqrt{3}P_y$	P_x

TABLE XXVII. Character table and basis functions for the group C_{3h} with $\omega \equiv \exp(i\pi/6)$ [56]. The coordinate system for the basis functions is defined in Fig. 2(b).

		E	C_3	C_3^{-1}	σ_h	S_3	S_3^{-1}	bases
Γ_1	A'	1	1	1	1	1	1	$\mathbb{1}; A_z$
Γ_2	E_1'	1	ω^4	ω^{-4}	1	ω^4	ω^{-4}	P_+
Γ_3	E_2'	1	ω^{-4}	ω^4	1	ω^{-4}	ω^4	P_-
Γ_4	A''	1	1	1	-1	-1	-1	P_z
Γ_5	E_1''	1	ω^4	ω^{-4}	-1	$-\omega^4$	$-\omega^{-4}$	A_+
Γ_6	E_2''	1	ω^{-4}	ω^4	-1	$-\omega^{-4}$	$-\omega^4$	A_-

TABLE XXVIII. Character table and basis functions for the group C_{2v} [56]. The coordinate system for the basis functions is defined in Fig. 2(c-e).

		E	C_2	σ_v	σ_v'	bases $[c(e)]$	$[d]$
Γ_1	A_1	1	1	1	1	$\mathbb{1}; \sqrt{3}P_x \pm P_y$	$\mathbb{1}; P_y$
Γ_2	B_1	1	-1	1	-1	$P_x \mp \sqrt{3}P_y; A_z$	$P_x; A_z$
Γ_3	A_2	1	1	-1	-1	$\sqrt{3}A_x \pm A_y$	A_y
Γ_4	B_2	1	-1	-1	1	$P_z; A_x \mp \sqrt{3}A_y$	$P_z; A_x$

TABLE XXIX. Character table and basis functions for the group C_{2h} [56]. The coordinate system for the basis functions is defined in Fig. 6(c-e).

		E	C_2	I	σ_h	bases $[c(e)]$	$[d]$
Γ_1^+	A_g	1	1	1	1	$\mathbb{1}; A_x \mp \sqrt{3}A_y$	$\mathbb{1}; A_x$
Γ_2^+	B_g	1	-1	1	-1	$\sqrt{3}A_x \pm A_y; A_z$	$A_y; A_z$
Γ_1^-	A_u	1	1	-1	-1	$P_x \mp \sqrt{3}P_y$	P_x
Γ_2^-	B_u	1	-1	-1	1	$\sqrt{3}P_x \pm P_y; P_z$	$P_y; P_z$

TABLE XXX. Multiplication table for the IRs of the group C_{3h} [56].

Γ_1	Γ_2	Γ_3	Γ_4	Γ_5	Γ_6	$\Gamma_i \times \Gamma_j$
Γ_1	Γ_2	Γ_3	Γ_4	Γ_5	Γ_6	Γ_1
	Γ_3	Γ_1	Γ_5	Γ_6	Γ_4	Γ_2
		Γ_2	Γ_6	Γ_4	Γ_5	Γ_3
			Γ_1	Γ_2	Γ_3	Γ_4
				Γ_3	Γ_1	Γ_5
					Γ_2	Γ_6

[1] J. M. Luttinger and W. Kohn, Motion of electrons and holes in perturbed periodic fields, Phys. Rev. **97**, 869 (1955).

[2] C. Kittel, *Quantum Theory of Solids* (Wiley, New York, 1963).

[3] G. L. Bir and G. E. Pikus, *Symmetry and Strain-Induced Effects in Semiconductors* (Wiley, New York, 1974).

[4] G. Bastard, *Wave Mechanics Applied to Semiconductor Heterostructures* (Les Editions de Physique, Les Ulis, 1988).

[5] R. Winkler, *Spin-Orbit Coupling Effects in Two-Dimensional Electron and Hole Systems* (Springer, Berlin, 2003).

[6] G. Dresselhaus, A. F. Kip, and C. Kittel, Cyclotron resonance of electrons and holes in silicon and germanium crystals, Phys. Rev. **98**, 368 (1955).

[7] N. O. Lipari and A. Baldereschi, Angular momentum theory and localized states in solids: Investigation of shallow acceptor states in semiconductors, Phys. Rev. Lett. **25**, 1660 (1970).

[8] K. Suzuki and J. C. Hensel, Quantum resonances in the valence bands of germanium. I. Theoretical considerations, Phys. Rev. B **9**, 4184 (1974).

[9] J. C. Hensel and K. Suzuki, Quantum resonances in the valence bands of germanium. II. Cyclotron resonances in uniaxially stressed crystals, Phys. Rev. B **9**, 4219 (1974).

[10] H.-R. Trebin, U. Rössler, and R. Ranvaud, Quantum resonances in the valence bands of zinc-blende semiconductors. I. Theoretical aspects, Phys. Rev. B **20**, 686 (1979).

[11] R. Ranvaud, H.-R. Trebin, U. Rössler, and F. H. Pollak, Quantum resonances in the valence bands of zinc-blende semiconductors. II. Results for p-InSb under uniaxial stress, Phys. Rev. B **20**, 701 (1979).

[12] E. L. Ivchenko and G. E. Pikus, *Superlattices and Other Heterostructures*, 2nd ed. (Springer, Berlin, 1997).

[13] H. Haug and S. W. Koch, *Quantum Theory of the Optical and Electronic Properties of Semiconductors*, 4th ed. (World Scientific, Singapore, 2004).

[14] A. H. Castro Neto, F. Guinea, N. M. R. Peres, K. S. Novoselov, and A. K. Geim, The electronic properties of graphene, Rev. Mod. Phys. **81**, 109 (2009).

[15] T. Ihn, *Semiconductor Nanostructures* (Oxford University Press, Oxford, 2010).

[16] A. Kormányos, G. Burkard, M. Gmitra, J. Fabian, V. Zólyomi, N. D. Drummond, and V. Fal'ko, $\boldsymbol{k}\cdot\boldsymbol{p}$ theory for two-dimensional transition metal dichalcogenide semiconductors, 2D Mater. **2**, 022001 (2015).

[17] J. M. Luttinger, Quantum theory of cyclotron resonances in semiconductors: General theory, Phys. Rev. **102**, 1030 (1956).

[18] E. O. Kane, The $\mathbf{k}\cdot\mathbf{p}$ method, in *Semiconductors and Semimetals*, Vol. 1, edited by R. K. Willardson and A. C. Beer (Academic, New York, 1966) Chap. 3, pp. 75–100.

[19] E. Wigner, *Group Theory and its Application to the Quantum Mechanics of Atomic Spectra* (Academic, New York, 1959).

[20] J. L. Birman, M. Lax, and R. Loudon, Intervalley-scattering selection rules in III-V semiconductors, Phys. Rev. **145**, 620 (1966).

[21] T. N. Morgan, Symmetry of electron states in GaP, Phys. Rev. Lett. **21**, 819 (1968).

[22] J. F. Cornwell, Origin dependence of the symmetry labelling of electron and phonon states in crystals, Phys. Stat. Sol. B **43**, 763 (1971).

[23] J. F. Cornwell, Dependence of the symmetry labelling of electron and phonon states in crystals on orientation, Phys. Stat. Sol. B **52**, 275 (1972).

[24] L. F. Mattheiss, Band structures of transition-metal-dichalcogenide layer compounds, Phys. Rev. B **8**, 3719 (1973).

[25] K. F. Mak, C. Lee, J. Hone, J. Shan, and T. F. Heinz, Atomically thin MoS_2: A new direct-gap semiconductor, Phys. Rev. Lett. **105**, 136805 (2010).

[26] J. K. Ellis, M. J. Lucero, and G. E. Scuseria, The indirect to direct band gap transition in multilayered MoS_2 as predicted by screened hybrid density functional theory, Appl. Phys. Lett. **99**, 261908 (2011).

[27] E. S. Kadantsev and P. Hawrylak, Electronic structure of a single MoS_2 monolayer, Solid State Commun. **152**, 909 (2012).

[28] W. S. Yun, S. W. Han, S. C. Hong, I. G. Kim, and J. D. Lee, Thickness and strain effects on electronic structures of transition metal dichalcogenides: 2H-MX_2 semiconductors (M = Mo, W; X = S, Se, Te), Phys. Rev. B **85**, 033305 (2012).

[29] D. Xiao, G.-B. Liu, W. Feng, X. Xu, and W. Yao, Coupled spin and valley physics in monolayers of MoS_2 and other group-VI dichalcogenides, Phys. Rev. Lett. **108**, 196802 (2012).

[30] E. Cappelluti, R. Roldán, J. A. Silva-Guillén, P. Ordejón, and F. Guinea, Tight-binding model and direct-gap/indirect-gap transition in single-layer and multilayer MoS_2, Phys. Rev. B **88**, 075409 (2013).

[31] A. Kormányos, V. Zólyomi, N. D. Drummond, P. Rakyta, G. Burkard, and V. I. Fal'ko, Monolayer MoS_2: Trigonal warping, the Γ valley, and spin-orbit coupling effects, Phys. Rev. B **88**, 045416 (2013).

[32] D. Jariwala, V. K. Sangwan, L. J. Lauhon, T. J. Marks, and M. C. Hersam, Emerging device applications for semiconducting two-dimensional transition metal dichalcogenides, ACS Nano **8**, 1102 (2014).

[33] P. Ajayan, P. Kim, and K. Banerjee, Two-dimensional van der Waals materials, Phys. Today **69**, 38 (2016).

[34] S. Manzeli, D. Ovchinnikov, D. Pasquier, O. V. Yazyev, and A. Kis, 2D transition metal dichalcogenides, Nature Reviews Materials **2**, 17033 (2017).

[35] G. Wang, A. Chernikov, M. M. Glazov, T. F. Heinz, X. Marie, T. Amand, and B. Urbaszek, Colloquium: Excitons in atomically thin transition metal dichalcogenides, Rev. Mod. Phys. **90**, 021001 (2018).

[36] R. Winkler and U. Zülicke, Invariant expansion for the trigonal band structure of graphene, Phys. Rev. B **82**, 245313 (2010).

[37] R. Winkler and U. Zülicke, Electromagnetic coupling of spins and pseudospins in bilayer graphene, Phys. Rev. B **91**, 205312 (2015).

[38] H.-W. Streitwolf, *Group Theory in Solid-State Physics* (Macdonald, London, 1971).

[39] M. S. Dresselhaus, G. Dresselhaus, and A. Jorio, *Group Theory* (Springer, Berlin, 2008).

[40] B. Bradlyn, L. Elcoro, J. Cano, M. G. Vergniory, Z. Wang, C. Felser, M. I. Aroyo, and B. A. Bernevig, Topological quantum chemistry (2017).

[41] B. Bradlyn, L. Elcoro, M. G. Vergniory, J. Cano, Z. Wang, C. Felser, M. I. Aroyo, and B. A. Bernevig, Band connectivity for topological quantum chemistry: Band structures as a graph theory problem, Phys. Rev. B **97**, 035138 (2018).

[42] J. Cano, B. Bradlyn, Z. Wang, L. Elcoro, M. G. Vergniory, C. Felser, M. I. Aroyo, and B. A. Bernevig, Building blocks of topological quantum chemistry: Elementary band representations, Phys. Rev. B **97**, 035139 (2018).

[43] G. Burns and A. M. Glazer, *Space Groups for Solid State Scientists*, 3rd ed. (Academic, Amsterdam, 2013).

[44] J. C. Slater and G. F. Koster, Simplified LCAO method for the periodic potential problem, Phys. Rev. **94**, 1498 (1954).

[45] C. Eckart, The application of group theory to the quantum dynamics of monatomic systems, Rev. Mod. Phys. **2**, 305 (1930).

[46] This assumption facilitates a discussion of the symmetry of the basis functions (5). Functions (5) with a finite overlap between nearest neighbors that are needed in a TB calculation must have the same symmetry as the simplified functions discussed here. The symmetry of these functions cannot change discontinuously when the overlap between the atomic orbitals is switched off.

[47] The $2l+1$ atomic orbitals for a given magnitude l of orbital angular momentum transform according to an IR of the full rotation group. The compatibility tables for decomposing the IRs of the full rotation group into IRs of the crystallographic point groups are listed in Ref. [56]. Here we require a more complete solution of this problem where we also construct the linear combinations of angular-momentum eigenstates that transform irreducibly according to the different IRs of $\mathcal{G}_{\mathbf{k}}$. This problem does not depend on, e.g., the principal quantum numbers of these orbitals. We note that for sufficiently large l (for any $\mathcal{G}_{\mathbf{k}}$ if $l \geq 6$) these $2l+1$ atomic orbitals contribute to all (even or odd if $\mathcal{G}_{\mathbf{k}}$ includes inversion) IRs of $\mathcal{G}_{\mathbf{k}}$, which limits possibilities to decompose a TB Hamiltonian into blocks describing parts of the full band structure.

[48] R. McWeeny, *Symmetry: An Introduction to Group Theory and its Applications* (Dover, 2002).

[49] In SLG, the carbon atoms with multiplicity $m = 2$ are characterized by the site symmetry group $\mathcal{G}_W = D_{3h}$, see Table I. Here, likewise, the group of the wave vector at the **K** point is $\mathcal{G}_{\mathbf{K}} = D_{3h}$ and symmetrized plane waves at **K** transform according to the two-dimensional IR Γ_6 of D_{3h}, see Table VII. On the other hand, in BLG, the carbon atoms at positions $\mathbf{R}_j^{d1}, \mathbf{R}_j^{d2}$ have site symmetry $\mathcal{G}_W = C_{3v}$, whereas the symmetrized plane waves at **K** for these positions transform according to the two-dimensional IR Γ_3 of D_3. Neither of the groups C_{3v} and D_3 can be viewed as a subgroup of the other one.

[50] H. Jones, *The Theory of Brillouin Zones and Electronic States in Crystals*, 2nd ed. (North-Holland, Amsterdam, 1975).

[51] In Cornwell's notation [22], different Wyckoff positions each with multiplicity $m = 1$ are positions each forming a Bravais lattice.

[52] L. L. Boyle and J. E. Lawrenson, The origin dependence of Wyckoff site description of a crystal structure, Acta Cryst. A **29**, 353 (1973).

[53] C. Herring, Effect of time-reversal symmetry on energy bands of crystals, Phys. Rev. **52**, 361 (1937).

[54] The classification of representations under time reversal adopted here from Ref. [3] is the most convenient for physical applications, but it differs from that customary in courses on group theory, where real representations are assigned to case (a), complex inequivalent and equivalent representations to cases (b) and (c). The two classifications agree for single-group representations, but cases (a) and (c) must be interchanged for double-group representations.

[55] E. I. Rashba, Symmetry of energy bands in crystals of wurtzite type: I. Symmetry of bands disregarding spin-orbit interaction, Sov. Phys.–Solid State **1**, 368 (1959).

[56] G. F. Koster, J. O. Dimmock, R. G. Wheeler, and H. Statz, *Properties of the Thirty-Two Point Groups* (MIT Press, Cambridge, Massachusetts, 1963).

[57] The symmetry-adapted bases derived here for MoS_2 define unitary transformations for block-diagonalizing a MoS_2 TB Hamiltonian that agree with the unitary transformations discussed in Ref. [30].

[58] T. Hahn, ed., *International Tables for Crystallography*, 5th ed., Vol. A (Springer, Dordrecht, 2005).

[59] L. D. Landau and E. M. Lifshitz, *Theory of Elasticity*, 2nd ed. (Pergamon, New York, 1970).

[60] G.-B. Liu, W.-Y. Shan, Y. Yao, W. Yao, and D. Xiao, Three-band tight-binding model for monolayers of group-VIB transition metal dichalcogenides, Phys. Rev. B **88**, 085433 (2013).